CSTS

Consortium to Study Trends in Seismicity

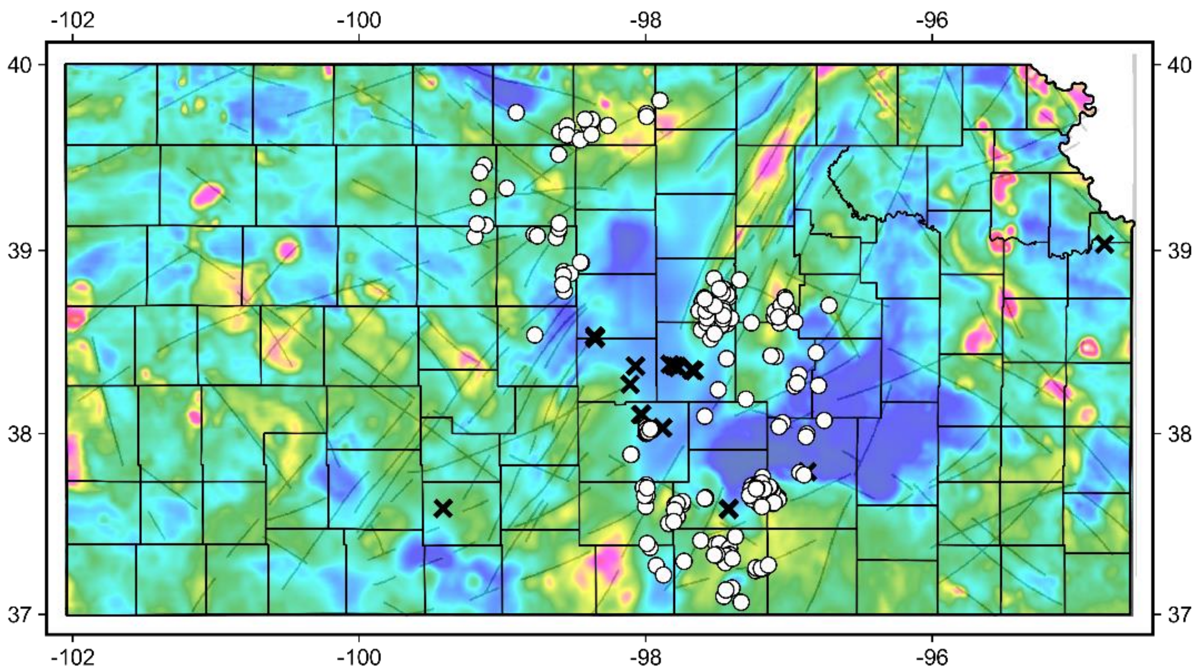

July 1, 2020 – June 30, 2021

Annual Report by
Rex Buchanan, Shelby Peterie, and Rick Miller

Kansas Geological Survey Open-file Report 2022-23

Cover Figure Caption: Earthquakes (white) located using CSTS stations that otherwise would not have been located by any other seismic network. Correlated with structural trends, the earthquakes provide insight into the stress conditions and relative stability of both unmapped faults and faults interpreted from geologic and geophysical datasets.

Kansas Geological Survey
Consortium to Study Trends in Seismicity

2020-2021 Annual Report

NOTICE: This annual report was released in draft form to Consortium members, as well as to the Kansas Department of Health and Environment, on February 7, 2022, and was subject to further review and comment by Consortium members until August 7, 2022. The KGS was then allowed an additional three months to revise the draft report and distribute the final annual report.

CONSORTIUM TO STUDY TRENDS IN SEISMICITY
KANSAS GEOLOGICAL SURVEY
Fourth Quarter / Annual Report
July 1, 2020 – June 30, 2021

INTRODUCTION

The Kansas Geological Survey's Consortium to Study Trends in Seismicity (CSTS) is a public-private project aimed at studying trends in seismicity in Kansas. The Consortium focuses on areas where public and private entities could benefit from high-sensitivity seismic monitoring. Seismicity has increased significantly in Kansas and the midcontinent since 2013, leading to a need to better define and understand earthquake activity, particularly as it relates to subsurface fluid disposal. The CSTS oversees the operation of a seismic network that records and allows accurate location and magnitude estimates of seismicity for felt earthquakes and particularly for microseismic events that are hundreds of times smaller than can be routinely identified with previous regional seismic networks. Understanding current microtrends in seismicity and establishing a data-driven awareness of potential factors affecting seismicity should help with industry response, guide governmental oversight, and inform public opinion.

The CSTS is operated by the Kansas Geological Survey (KGS), a research and service division of the University of Kansas with a long history of studying the state's subsurface and seismic issues. Current members of the CSTS are from the state's Class I disposal well community (Class I wells are used for disposal of municipal and industrial waste and regulated by the Kansas Department of Health and Environment [KDHE]). Membership in the CSTS is voluntary; the CSTS objective is to identify and understand seismicity at magnitudes down to zero in proximity to member facilities. The CSTS works to establish baseline or background seismicity near those facilities, provide a scientific basis for differentiating natural from induced seismicity, and predict future earthquake occurrences. Confidence in distinguishing natural from induced earthquake trends and predicting future occurrences is greatly enhanced through extended monitoring periods with stations near earthquake events.

The following report describes the third year of CSTS activities, including a discussion of membership status; network station installation and operation; earthquakes recorded and identified, and earthquake alerts provided to members; web page development; other activities, especially involving publications, presentations, and meeting attendance; and plans for the coming year. Three quarterly reports were provided to members since the Consortium's annual meeting in August 2020. This current report includes summaries of seismicity and CSTS activities both in the past quarter (April, May, and June of 2021) and for the past year.

STATUS OF MEMBERS

The CSTS was established with a two-tier membership system. For Tier 1 members, the CSTS provides equipment, installation, and monitoring of a seismograph station; maintains a catalog of seismic events, updated weekly, with a goal of providing e-mail alerts within 24 hours or less of any earthquakes greater than magnitude 2 within 30 miles of a facility; provides quarterly reports of monitoring findings; and hosts an annual meeting at which results are discussed and plans formulated for the coming year. Tier 2 members have access to information related to the general information about the seismicity being studied by the CSTS and can attend the annual meeting but do not have the right to vote at that meeting or use the reports while still under confidential status.

The CSTS currently has ten Tier 1 members.

STATUS OF NETWORK

The CSTS seismic network currently consists of 11 stations in Ellsworth, Rice, McPherson, Reno, Kiowa, Sedgwick, Butler, and Johnson counties, Kansas (Figure 1, Appendix A). Waveforms for these stations are available for Tier 1 members on the seismic network page of the CSTS website. For each of those locations, ambient noise tests were completed to establish background noise levels. Those tests identified noise from nearby highways, trains, pumpjacks, and other facilities that might interfere with earthquake analysis. Stations were relocated with a site-specific ambient noise test when initially deployed in places where noise and vibrations interfered with station response characteristics above a predetermined threshold. Many of the existing sites are in cemeteries, on government property, or in other locations where noise levels are measured to be low and are likely to remain low. In all cases, KGS has obtained written agreements with landowners of each station location.

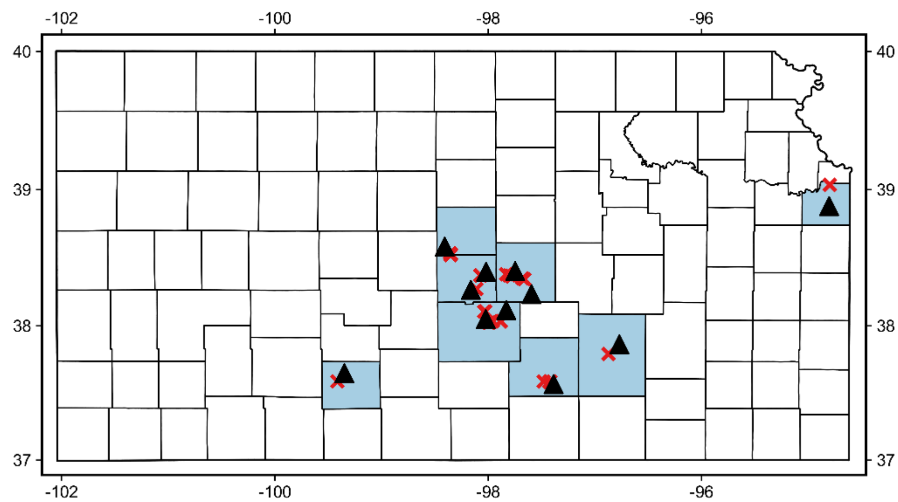

Figure 1. Earthquake stations (black triangles) with member facilities (red X) provide high sensitivity coverage with the potential to identify earthquakes with magnitudes below 0 within 20 miles of each facility.

Each station consists of a seismic sensor that includes a shallowly buried seismometer embedded in a concrete platform atop a gravel layer and a digitizer (Figure 2). Ground motion detected by the seismometer is transmitted back to KGS offices in Lawrence in real time via a cellular modem. That communication system is powered by a solar panel that charges two deep-cycle marine batteries. The footprint for each station is approximately 10 feet by 10 feet. The stations operated over the last year with a better than 98% continuous data stream and within designated operational sensitivity and signal-to-noise ratio.

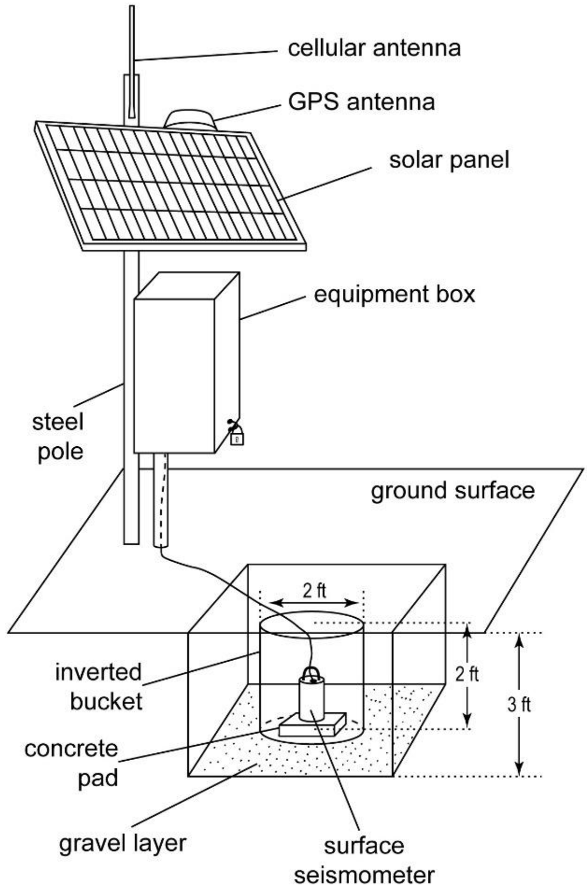

Figure 2. Diagram illustrating a temporary seismic installation.

EARTHQUAKE ALERTS, CATALOG

Earthquakes with magnitudes of 2 or larger represent a threshold above which energy levels provide highly confident automatic analysis for feeds coming from a network as dense as the CSTS network and especially in conjunction with the KGS regional and subregional networks. It is therefore reasonable to provide accurate epicenter locations using automated picking routines for each event down to M 2, with results available within minutes of the fault rupture. KGS staff notify CSTS members of a M 2 or larger earthquake within 30 miles of Tier 1 member wells. There were 95 earthquake alerts from July 2020 through June 2021 (Table 1), a slight reduction relative to the 2019–2020 reporting year. Earthquakes below magnitude 2.5 are generally considered below felt levels. Earthquakes with magnitudes down to 1 can be located with confidence in areas where at least three CSTS stations are within 50 miles of each other.

Table 1. M 2 or larger earthquakes recorded from July 2020 through June 2021 with epicenters located within 30 mi of member wells.

Origin Time (UTC)	Latitude	Longitude	Magnitude	County
2020-07-04 17:27:20	38.7249	-97.5412	2.5	Saline
2020-07-07 09:16:38	38.7144	-97.5134	2.0	Saline
2020-07-16 01:31:11	37.2541	-97.2214	1.9	Sumner
2020-07-16 23:45:48	37.2468	-97.2010	2.3	Sumner
2020-07-19 05:24:19	38.6895	-97.5120	2.1	Saline
2020-08-03 15:32:36	38.0186	-97.9839	2.3	Reno
2020-08-13 13:24:16	37.6194	-96.6716	2.1	Butler
2020-09-09 23:49:22	38.7230	-97.5471	2.0	Saline
2020-09-10 18:16:51	37.6575	-98.0314	2.1	Kingman
2020-09-11 21:37:16	38.7124	-97.5657	2.2	Saline
2020-10-01 17:11:29	37.5184	-97.7878	2.0	Sedgwick
2020-10-09 13:27:23	38.6989	-97.5852	2.1	Saline
2020-10-19 17:48:53	37.5064	-97.8705	2.2	Kingman
2020-10-21 09:25:12	38.0033	-96.8707	2.5	Butler
2020-10-23 00:39:00	38.9132	-98.6139	2.5	Russell
2020-10-24 21:19:00	38.8396	-98.5854	2.2	Russell
2020-10-26 20:47:26	38.6526	-97.4529	2.2	Saline
2020-10-27 15:23:03	37.9958	-96.8950	3.0	Butler
2020-11-02 22:06:30	37.2597	-97.6005	2.0	Sumner
2020-11-05 02:26:56	37.5052	-97.7971	2.4	Sedgwick
2020-11-12 12:45:14	37.6587	-98.0326	2.0	Kingman
2020-11-18 15:50:55	38.6974	-97.5105	2.3	Saline
2020-11-26 22:27:43	37.7128	-97.2134	2.7	Sedgwick
2020-11-27 18:27:41	37.7134	-97.2154	2.6	Sedgwick
2020-11-30 15:11:30	37.7039	-97.2081	2.3	Sedgwick
2020-12-01 19:41:46	37.3844	-97.8087	2.2	Harper
2020-12-02 13:14:16	38.9158	-98.5543	2.2	Russell
2020-12-07 16:55:48	37.2987	-97.4645	2.4	Sumner
2020-12-08 16:54:06	37.7069	-97.2231	3.2	Sedgwick
2020-12-09 14:59:23	37.7061	-97.2123	2.5	Sedgwick
2020-12-10 08:34:32	37.7041	-97.2250	2.9	Sedgwick
2020-12-10 13:36:20	37.7018	-97.2154	2.6	Sedgwick
2020-12-11 08:59:34	38.6717	-97.5409	2.3	Saline
2020-12-12 01:31:21	37.6969	-97.2083	2.0	Sedgwick
2020-12-13 17:26:50	37.6993	-97.2235	2.2	Sedgwick
2020-12-19 17:42:07	37.7088	-97.2164	2.9	Sedgwick
2020-12-19 18:40:50	37.7118	-97.2224	2.9	Sedgwick
2020-12-19 18:47:58	37.7114	-97.2168	3.8	Sedgwick
2020-12-19 19:18:21	37.7060	-97.2063	2.7	Sedgwick
2020-12-19 21:12:04	37.7075	-97.2107	2.3	Sedgwick
2020-12-20 08:20:08	37.7092	-97.2162	2.7	Sedgwick
2020-12-20 22:38:54	37.3102	-97.4677	2.6	Sumner
2020-12-21 07:25:12	37.3100	-97.4612	2.1	Sumner
2020-12-23 09:42:29	37.7052	-97.2113	2.1	Sedgwick
2020-12-28 10:19:54	37.7108	-97.2108	2.7	Sedgwick
2020-12-29 23:57:30	38.7244	-97.5745	2.6	Saline
2020-12-30 11:04:47	37.7005	-97.2126	3.9	Sedgwick
2020-12-30 11:23:16	37.7080	-97.2278	1.9	Sedgwick
2020-12-31 04:52:46	37.7043	-97.2199	2.6	Sedgwick
2020-12-31 18:54:47	37.7005	-97.2085	2.0	Sedgwick
2021-01-04 06:51:50	37.6960	-97.1990	2.2	Sedgwick
2021-01-07 21:12:27	37.4580	-97.7600	2.2	Sumner
2021-01-10 06:52:15	37.3000	-97.4750	3.1	Sumner
2021-01-24 22:55:36	38.6450	-97.4560	2.0	Saline
2021-01-28 10:24:47	38.6900	-97.5980	2.1	Saline
2021-02-09 22:20:19	37.3390	-97.8370	2.1	Harper
2021-02-15 19:02:03	38.0120	-97.9980	2.7	Reno
2021-02-21 11:35:27	38.6690	-97.4590	2.1	Saline
2021-02-24 05:02:02	38.6720	-97.4560	2.1	Saline

Table 1. Continued

Origin Time (UTC)	Latitude	Longitude	Magnitude	County
2021-02-26 02:05:49	37.5010	-97.7970	2.8	Sedgwick
2021-02-26 02:07:48	37.5050	-97.7950	2.2	Sedgwick
2021-02-26 02:19:06	37.4960	-97.8030	2.6	Sedgwick
2021-02-26 16:29:09	37.4990	-97.7970	2.3	Sedgwick
2021-03-14 11:29:40	37.7195	-97.2140	3.5	Sedgwick
2021-03-14 11:31:33	37.7101	-97.2260	3.7	Sedgwick
2021-03-14 12:02:15	37.7218	-97.2214	3.2	Sedgwick
2021-03-14 13:30:48	37.7066	-97.2173	2.2	Sedgwick
2021-03-14 23:08:35	37.7097	-97.2239	3.9	Sedgwick
2021-03-15 05:29:00	37.6970	-97.2420	2.5	Sedgwick
2021-03-15 13:52:31	37.7131	-97.2362	3.4	Sedgwick
2021-03-15 13:59:15	37.7090	-97.2287	3.6	Sedgwick
2021-03-16 21:17:21	37.6960	-97.2310	2.3	Sedgwick
2021-03-17 16:03:06	37.6070	-97.6260	2.0	Sedgwick
2021-03-21 15:00:51	37.7050	-97.2240	2.0	Sedgwick
2021-03-29 03:02:19	37.3060	-97.4630	2.2	Sumner
2021-04-02 05:39:37	37.6191	-97.2076	2.2	Sedgwick
2021-04-10 07:29:50	38.6670	-97.5190	2.2	Saline
2021-04-15 13:30:35	37.4190	-97.3850	2.3	Sumner
2021-04-15 16:42:44	38.6950	-97.5500	2.7	Saline
2021-04-20 12:05:13	38.6660	-97.5540	2.3	Saline
2021-04-26 02:16:20	37.4810	-97.7970	2.0	Sedgwick
2021-05-02 15:42:20	38.6530	-97.4410	2.3	Saline
2021-05-08 00:40:24	38.6660	-97.4470	2.4	Saline
2021-05-11 04:41:25	38.7130	-97.9210	2.0	Saline
2021-05-16 07:24:01	37.7440	-98.9210	2.2	Pratt
2021-05-17 17:43:19	37.5040	-97.7940	2.0	Sedgwick
2021-05-22 20:14:54	38.7060	-97.5580	2.0	Saline
2021-06-03 23:03:50	37.2860	-97.4250	2.0	Sumner
2021-06-10 11:31:13	37.7110	-97.1980	2.3	Sedgwick
2021-06-16 05:29:30	37.6750	-96.7870	2.3	Butler
2021-06-20 10:49:34	38.6320	-97.5750	2.5	Saline
2021-06-23 15:42:58	37.6740	-97.2000	2.3	Sedgwick
2021-06-24 13:18:45	37.4190	-97.7270	2.5	Sumner
2021-06-29 00:23:53	37.4180	-97.7190	2.6	Sumner

End of table

INTERESTING OBSERVATIONS AND SIGNIFICANT TRENDS

Regional Seismicity (M 2 or larger)

During the past year, 286 earthquakes magnitude (M) 2 or larger were recorded in Kansas (Figure 3). The overall earthquake rate continued to decline, and the number of regional-scale events (M 2 or larger) decreased by about 30% relative to the previous year (429 from July 2019 through June 2020). The vast majority of these events occurred either in parts of the state where historic earthquakes occurred along prominent basement structures or where earthquakes were recorded in recent years. Interestingly, seven counties had the first or largest earthquakes ever recorded in that county this year (Figure 3). The most notable earthquake sequences this year occurred near Wichita and included nearly a dozen $M \geq 3$ events, which is unexpected based on recurrence of natural earthquakes in this area.

South-Central Kansas (Sedgwick Basin)

More than a quarter of the regional-scale earthquakes (M 2 or larger) recorded by the KGS network were located in south-central Kansas (Figure 4). However, the rate of earthquakes in this area has dropped dramatically since the KGS network was installed in 2015. In Harper and Sumner counties, 31 M 2 or larger earthquakes were recorded during the past year, which is less than half in the previous reporting period and an overall decrease of more than 95% relative to 2015. Earthquake clusters generally occurred in areas where earthquakes were observed in previous years.

From 2015 to 2018, earthquakes migrated from the highly active zones of seismicity in Harper and Sumner counties progressively farther along structural trends into surrounding counties, including Sedgwick, western Butler, Kingman, and Reno counties. Earthquakes along these trends are most likely induced, triggered as a result of elevated pore pressure that effectively reduced frictional resistance along critically stressed basement faults. Seismicity continues to occur at generally much lower rates within this zone of elevated pressure. Notable sequences of earthquakes near Hutchinson in 2019–2020 and Wichita in 2020–2021 may be related to nearby injection operations.

Pratt Anticline

West of the Sedgwick Basin, elevated pore pressure was likely the cause of a significant increase in seismic activity in Barber, Comanche, and surrounding counties in 2015–2018. Earthquakes have continued to occur near the Pratt anticline since that time but at a much lower rate. Similar to the previous reporting year, only 11 regional-scale earthquakes occurred in this area during the past year (Figure 5). This is noteworthy because 244 M 2 or larger earthquakes were recorded here in 2015–2018, an average of more than 60 events of this size per year. The large reduction in seismicity over the past three years is consistent with stabilizing formation pressures across the region.

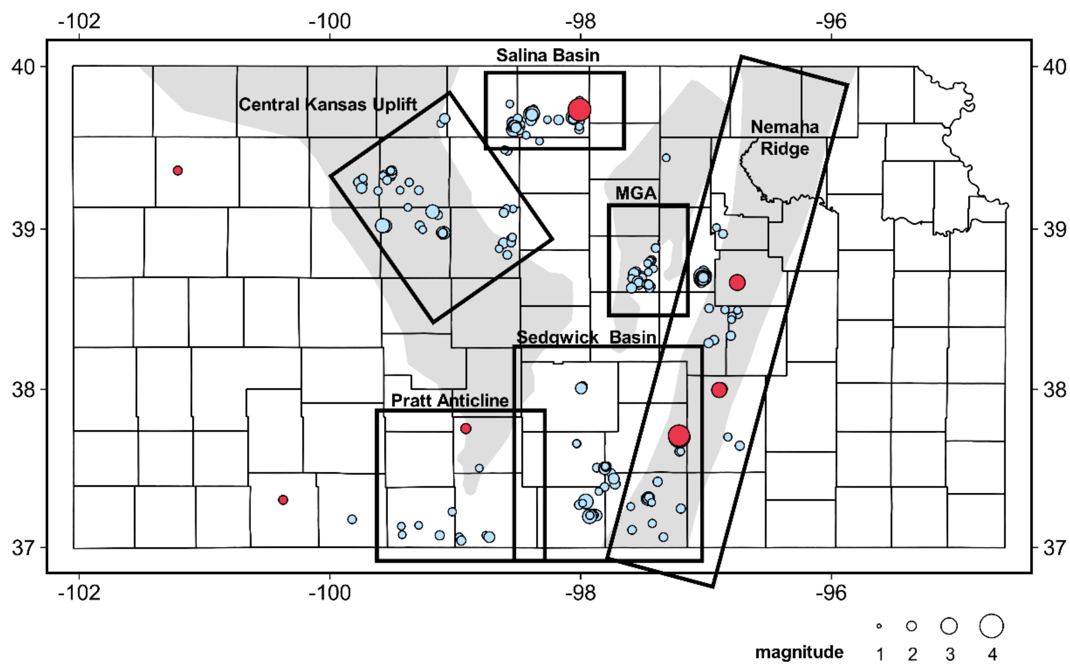

Figure 3. M 2 or larger earthquakes recorded in Kansas by the KGS seismic network from July 2020 through June 2021 (blue) superimposed on the prominent basement structures (gray). Red circles represent the largest (or tie for largest) earthquake ever recorded in a particular county; black boxes indicate areas discussed in the text.

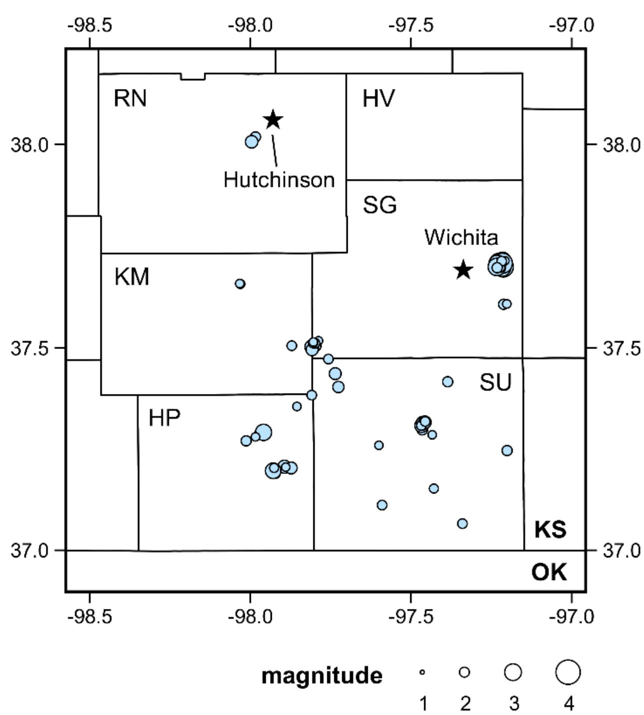

Figure 4. M 2 or larger earthquakes recorded in south-central Kansas from July 2020 through June 2021.

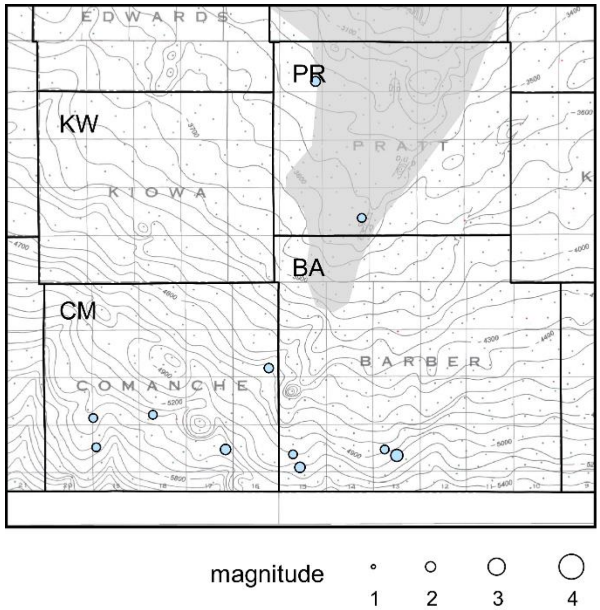

Figure 5. M 2 or larger earthquakes recorded in Kiowa, Pratt, Barber, and Comanche counties July 2020 through June 2021 superimposed on Precambrian structural contours (from Cole, 1976). The interpreted Pratt anticline is shown in gray.

Central Kansas Uplift

Similar to the 2019–2020 reporting year, 50 M 2 or larger earthquakes were recorded in areas affected by the Central Kansas Uplift (Figure 6). The largest event was a M 3.2 north of Ellis near the location of a large cluster of earthquakes that occurred in 2016. This is notable because no M 3 or larger earthquakes had occurred in this area since 2016. Although seismic activity is generally reduced in and around the Central Kansas Uplift, earthquakes persist and the spatial extent of the seismically active area has progressed to greater distances over time, most notably from west to east across Russell County. Although reliable pressure measurements are not available from wells that penetrate the full thickness of the Arbuckle Group (as in central and south-central Kansas), the persistent seismicity and progression of earthquakes is not expected for natural seismicity and, thus, earthquakes in this area may be induced. This region has a history of induced seismicity; earthquakes recorded in Rooks County in the late 1980s strongly correlated with nearby saltwater disposal operations (Armbruster et al., 1989).

North-Central Kansas (Salina Basin)

Eighty-one M 2 or larger earthquakes were recorded in Smith, Jewell, Osborne, and Mitchell counties during the past year (Figure 7). The largest event was a M 4.1 in eastern Jewell County, the largest earthquake ever recorded in the Salina Basin. The number of earthquakes in this area has progressively increased since early 2020 when there was a four-month period from April to August of that year with no recorded earthquakes. Three M 3 or larger earthquakes occurred between 1928 and 2017, averaging one earthquake of this size every 44 years. Since 2017, nearly three dozen M 3 or larger earthquakes occurred in Jewell County every 1–2 months on average. This significant increase in recurrence rate is not expected for

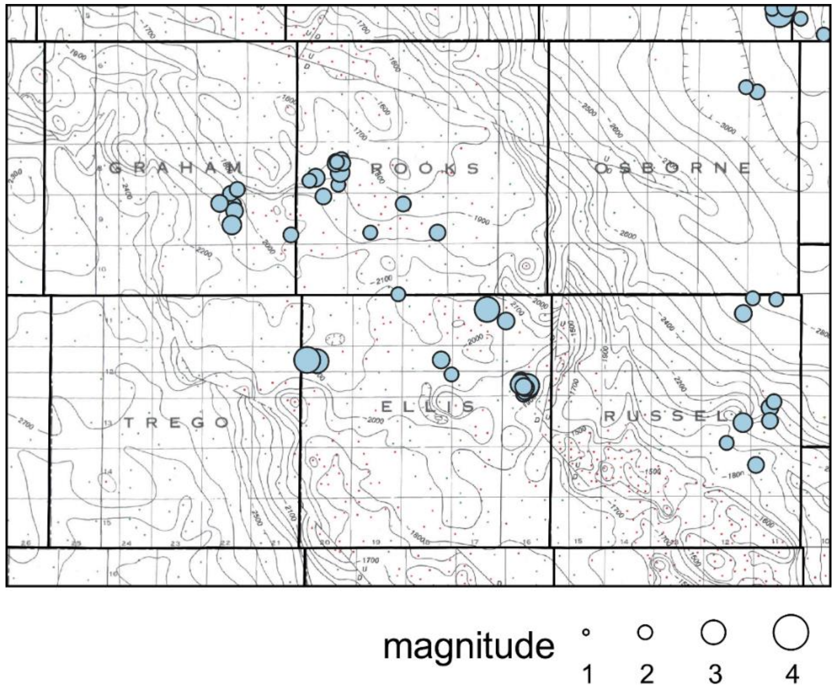

Figure 6. M 2 or larger earthquakes recorded near the Central Kansas Uplift from July 2020 through June 2021.

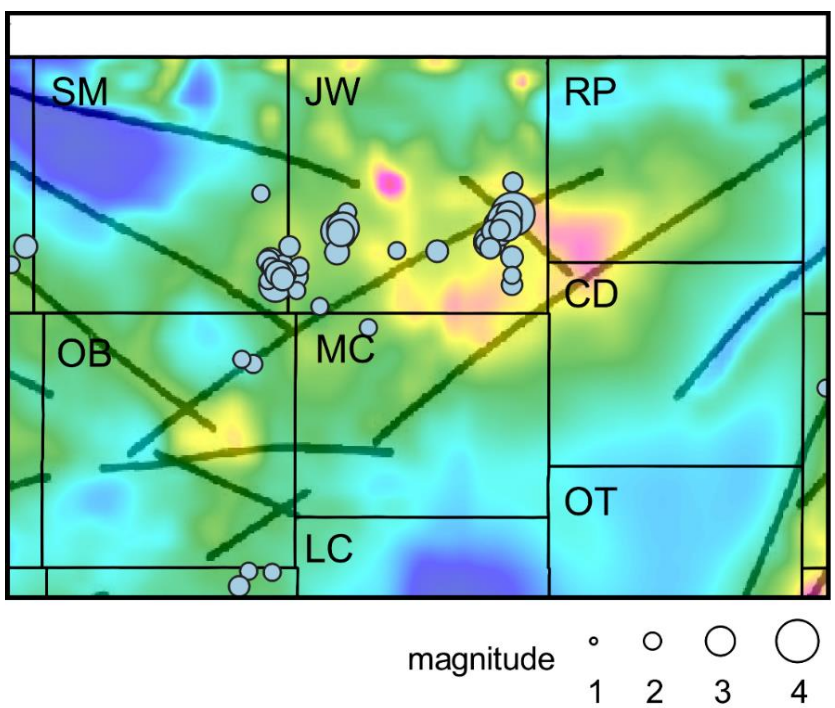

Figure 7. M 2 or larger earthquakes recorded in the Salina Basin from July 2020 through June 2021 superimposed on the aeromagnetic map (Xia et al., 1995a; 1995b) and interpreted magnetic lineaments (Yarger, 1983).

natural earthquakes. At this time, the trigger for these earthquakes remains unclear, but they appear to occur along lineaments interpreted on aeromagnetic data.

Midcontinent Geophysical Anomaly

The Midcontinent Geophysical Anomaly (MGA, the largest positive gravity anomaly in North America) is interpreted to be the result of a thick sequence of mafic igneous rocks that formed during major late Precambrian rifting as part of the Midcontinent Rift System. Two ongoing clusters of earthquakes have been recorded along the southeastern margin of the MGA since the KGS network was installed in 2015. Thirty-seven M 2 or larger earthquakes were recorded in distinct clusters in eastern Saline County (Figure 8). These clusters are discussed in greater detail in the section on local seismicity near McPherson County member wells.

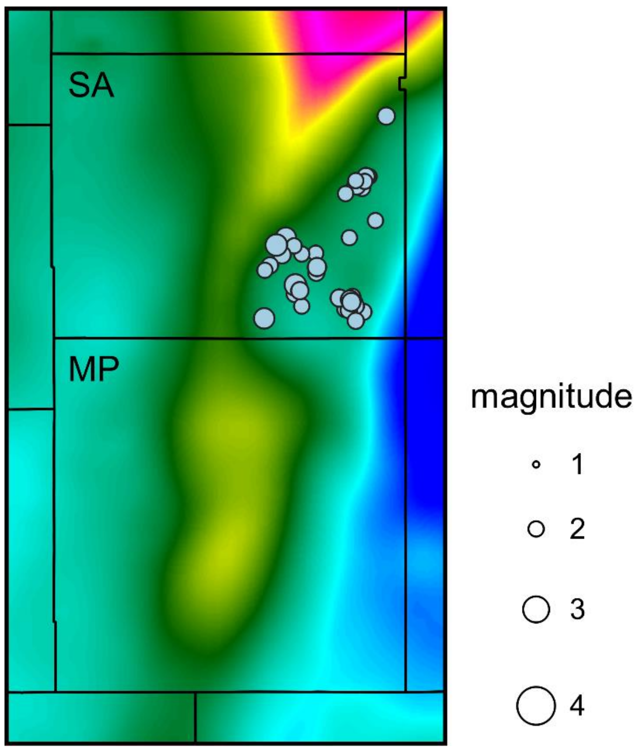

Figure 8. M 2 or larger earthquakes recorded near the Midcontinent Geophysical Anomaly from July 2020 through June 2021 superimposed on the gravity anomaly map of Kansas (Xia et al., 1995a; 1995b).

Nemaha Ridge

The Nemaha Ridge is one of the most prominent crustal features in Kansas, extending across the state with a northeast-southwest orientation. The Nemaha Ridge formed during post-Mississippian uplift of Precambrian-age granite. A system of normal and reverse faults on the eastern margin of the Nemaha Ridge forms the Humboldt Fault Zone. Transform faults with a northwest-southeast trend intersecting the Nemaha Ridge represent a pre-Phanerozoic crustal extension associated with the Midcontinent Rift System. Dozens of historic earthquakes have been felt or recorded along the Nemaha Ridge, including an estimated M 5.2 near Wamego in 1867.

Forty-four M 2 or larger earthquakes were recorded during the reporting period along the Nemaha Ridge ranging from Riley County to Marion County (Figure 9), 25% less than the previous year. Last year, an apparent increase was noted due, at least in part, to aftershocks from M 3.7 events in Chase and Dickinson counties. This year, seismic activity was scattered along the ridge in areas where clusters have previously been observed. The only prominent cluster was in southeast Dickinson, where earthquakes have persisted since late 2018. Six M 3 or larger events occurred this year, the most that has occurred in any one-year period thus far. The rate of M 3 or larger earthquakes is unusual relative to more than a decade of monitoring in the 1970s and 1980s and the primary trigger for these events is unclear at this time, but the increase in seismic activity may represent a natural temporal fluctuation in seismic rate.

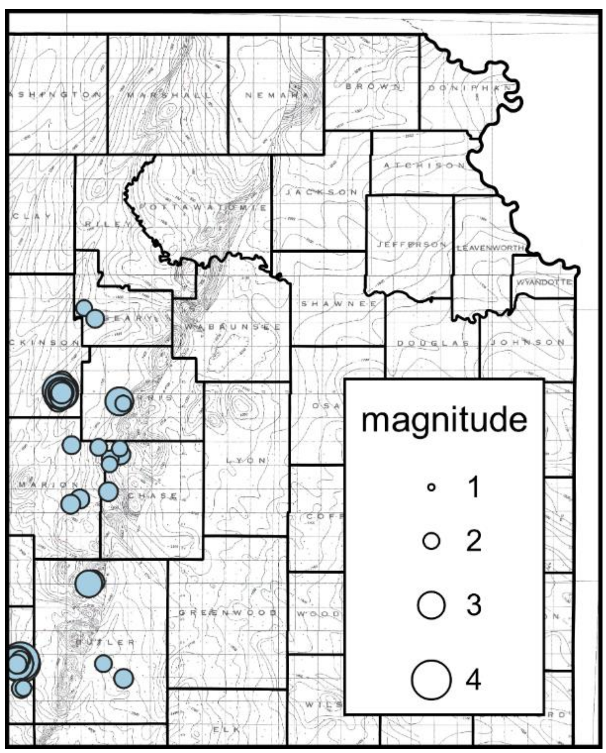

Figure 9. M 2 or larger earthquakes recorded along the Nemaha Ridge from July 2020 through June 2021 superimposed on Precambrian structural contours (from Cole, 1976).

Local Seismicity within 20 mi of Member Wells

Together with regional-scale felt events, analysis of events well below M 2 greatly improves our ability to interpret earthquakes relative to structures and evaluate possible causal factors. Sub M 2 events provide opportunities to forecast once the recursion relationship in specific areas can be accurately calculated for a given pressure regime. During the past year, 881 microearthquakes (M less than 2) were recorded by the KGS seismic network (with enhanced sensitivity and improved location accuracy with the addition of CSTS stations) (Figure 10). Similar to regional-scale earthquakes, the overall number of microearthquakes continued to decline. Microearthquakes make up 75% of the events logged into the earthquake catalog last year. Of the entire catalog at all magnitudes, 283 earthquakes (24%) were mapped within 20 mi of Tier 1 member wells (Appendix B).

Uniquely locating the epicenter of an earthquake requires detecting P- and/or S-waves at three or more stations. Subnetwork events are defined as earthquakes (typically with magnitudes less than M 1) that are recorded only on a single station or at most two stations and, therefore, the epicenter location cannot be determined uniquely. Rather, the epicenter exists somewhere on a circle centered on the seismic station with radius equal to the calculated distance to the earthquake epicenter. The magnitude of a subnetwork event is estimated from the coda, or duration—the time from the first P-wave arrival until the energy is approximately equal to or drops below the noise floor at that time and station (background noise usually based on pre-event noise levels). More than 1,000 subnetwork events were recorded at CSTS stations during this reporting period (Appendix C). Some events may have an anthropogenic origin (for example, underground blasting). However, the majority of these subnetwork events are low-energy microearthquakes that provide valuable insight into the relative stability and stress conditions of faults in proximity to the station (within about 12 mi).

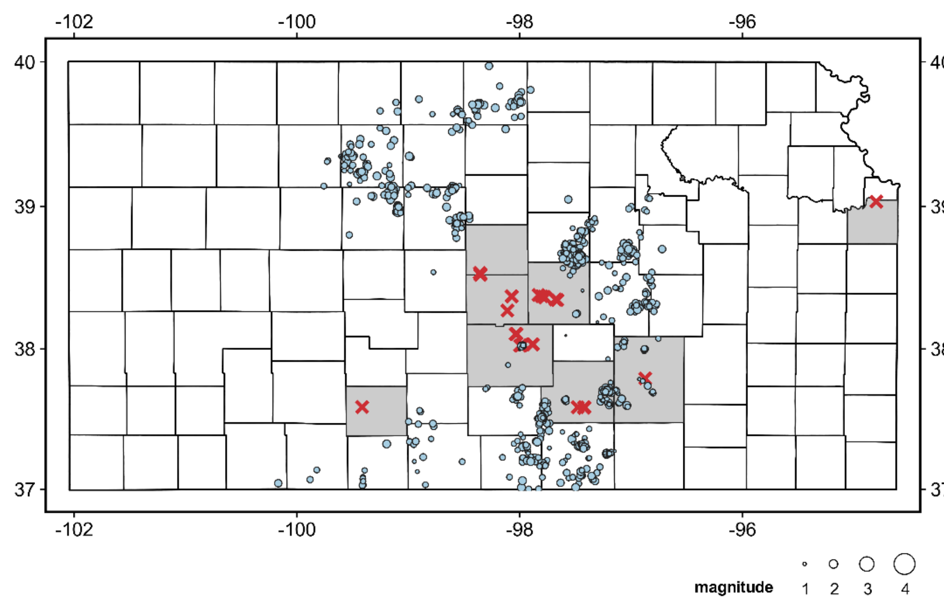

Figure 10. Microearthquakes (M less than 2) recorded in Kansas by the KGS seismic network from July 2020 through June 2021. Gray shading indicates counties with CSTS member wells (red Xs).

In this section, seismicity at all magnitudes (including both uniquely located events and subnetwork events) and relevant basement structures are evaluated in each of the eight counties that have Tier 1 member wells.

Kiowa County

No earthquakes were recorded within 20 miles of the Kiowa County member well and only one subnetwork event was recorded within 12 mi of station KW02 (Figure 11). The nearest uniquely located earthquakes were 22 mi or more away in neighboring Comanche and Pratt counties. These events were sparse, low-magnitude, and the majority occurred at about the same location as a cluster of earthquakes recorded during previous reporting periods. Interestingly, about 30 mi from the Kiowa County well, a M 2.2 earthquake was recorded in northwestern Pratt County more than 10 mi from any previously recorded seismicity. This event likely represents natural movement along faults associated with the Pratt anticline. However, a measured rise in the Arbuckle formation pressure in Kiowa County could suggest pressures may also be rising in surrounding counties, which might have triggered an earthquake on a fault where pore pressure changes had not previously been sufficient. The lack of seismic activity in Kiowa County is consistent with the overall stabilizing of pressures in south-central Kansas, but somewhat surprising giving the measured rise in pressure.

Rice and Ellsworth Counties

No earthquakes were located within 20 mi of the member wells in Rice and Ellsworth counties (Figure 12a) where the network sensitivity would allow events of about M 1.0 and larger to be located with the current network. However, a number of earthquakes were mapped just beyond 20 mi in neighboring counties. A single M 1.3 event was recorded in Barton County. Given its low magnitude and location within the Central Kansas Uplift, it is likely a natural event caused by crustal stresses on faults associated with this structure. Unlike the event in Barton County, the earthquakes in Russell and Lincoln counties appear to follow a trend of seismicity that progressed southeastward from Rooks, Ellis, and Osborne counties unlike any previous progression of earthquakes. Seismicity began in Ellis County in 2016 and has gradually progressed outward. This region has a long history of saltwater disposal, primarily within the Arbuckle Group, and injection volumes are higher here than anywhere else in Kansas. In 2020, the saltwater disposal volume in Ellis County was 95 MMbbl, the most in any single county. For reference, the disposal volume in Ellis County was even greater than Harper County in 2015 (116 and 112 MMbbl, respectively) when disposal volumes and seismicity peaked in south-central Kansas following development of the Mississippian limestone play.

At least some of the fluid injected in the Arbuckle in Ellis County was produced from the Arbuckle, although it is challenging to accurately assess the exact proportion. Using reasonable assumptions and conservative estimates, the net Arbuckle injection volume (injected fluid minus produced water) is +254 MMbbl since the mid-1990s. Given the complex structural and pressure settings within the Arbuckle, the locations of extraction vs. injection, the associated pressure gradients at these locations are crucial considerations for assessing impact on pore pressure and fault stability. The assumption that these processes and forces are balanced requires better data to support, much less defend. The sudden onset of seismicity, extended swarm-like nature of earthquakes, and pattern of progression away from high-volume disposal wells suggests the earthquakes in Ellis and Russell counties may be induced by poroelastic effects resulting from fluid injection.

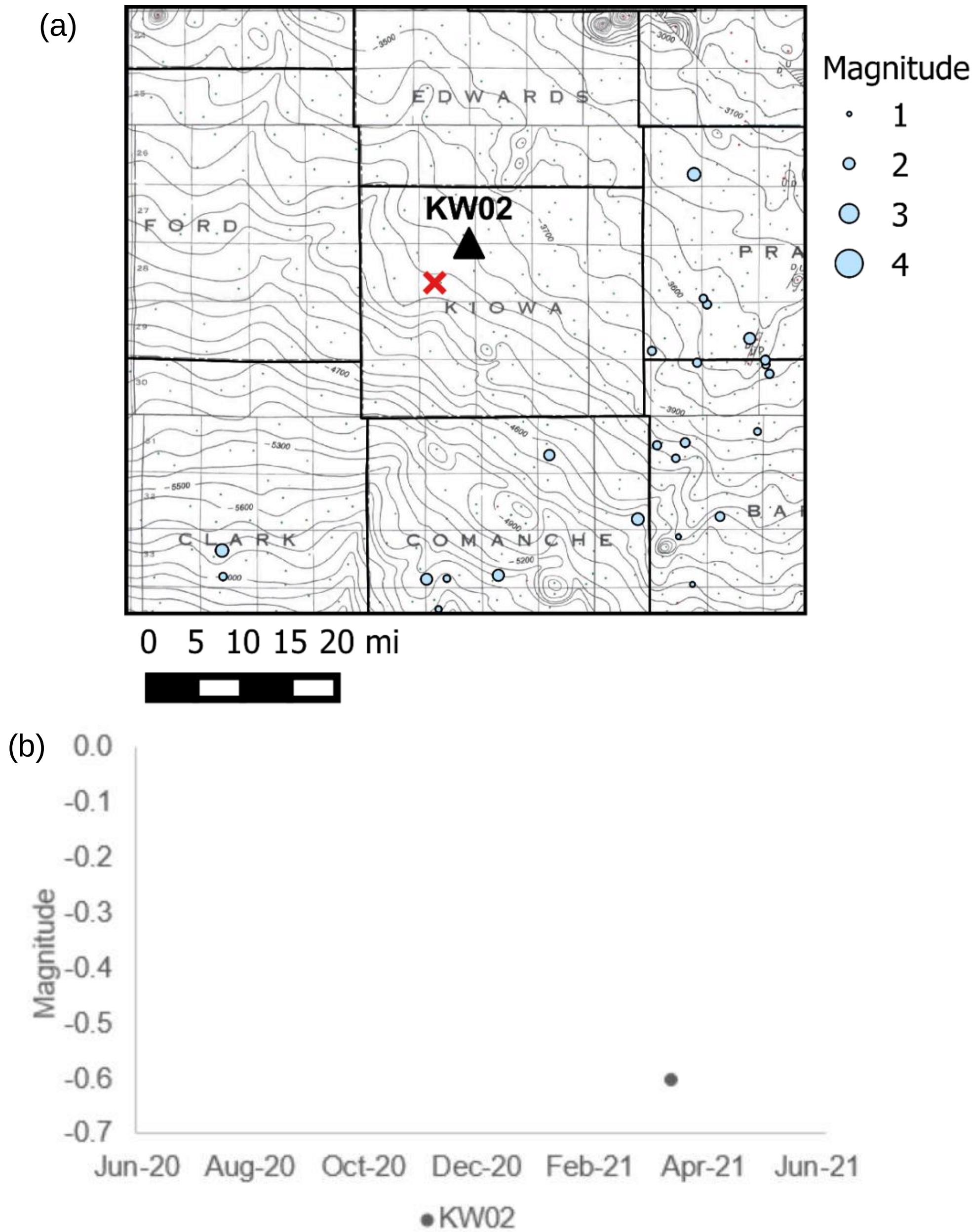

Figure 11. (a) Earthquakes recorded in Kiowa County from July 2020 through June 2021 superimposed on Precambrian structural contours (from Cole, 1976). The red X indicates a CSTS member well, and the black triangle indicates a station in the CSTS network. (b) Scatter plot of subnetwork events recorded within 12 mi of the CSTS station.

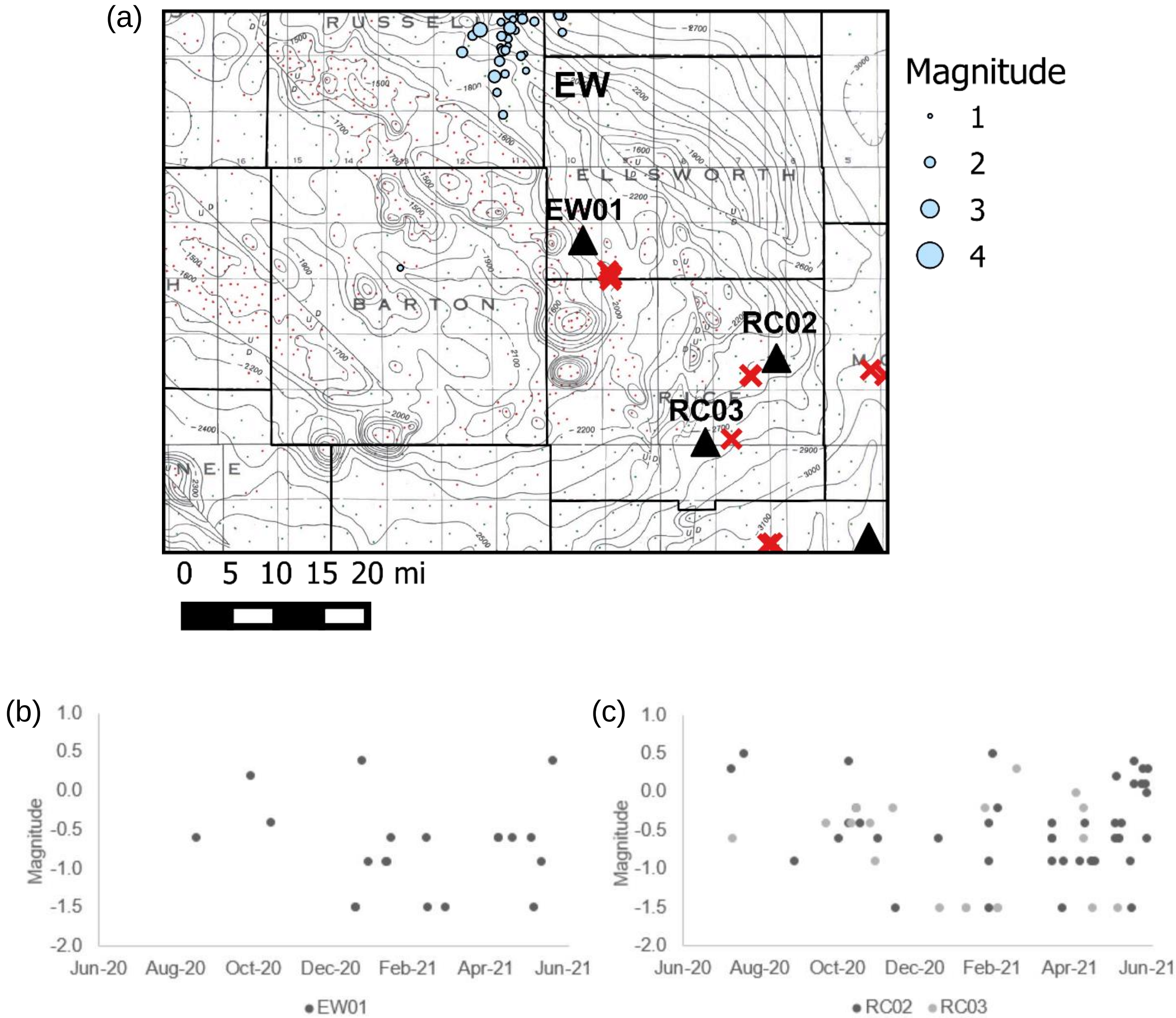

Figure 12. (a) Earthquakes near Rice and Ellsworth counties from July 2020 through June 2021 superimposed on Arbuckle Group structural contours (from Berendsen and Blair, 1986). Red Xs indicate CSTS member wells, and black triangles indicate stations in the CSTS network. Scatter plots of subnetwork events recorded within 12 mi of CSTS stations in (b) Ellsworth County and (c) Rice County.

Station EW01 is located in the southwest corner of Ellsworth County. An average of 5 subnetwork events per year have been detected at EW01 since recording began in 2017. This year, 20 subnetwork events with M ≤ 0.4 were recorded at epicentral distances of 2–8 mi (Figure 12b). Seismic activity had previously been interpreted as representing continued low-energy movement on faults that produced nearby historic earthquakes prior to noted increases in pore pressures in the Arbuckle. It is possible that the increase in subnetwork events this year simply represents a natural fluctuation in earthquake rates. However, the progression of possibly induced earthquakes across neighboring Russell County may indicate that pore pressure changes could be propagating into Ellsworth County and triggering low-magnitude earthquakes.

Station RC02 is located in eastern Rice County near the center of the Geneseo Uplift, an eastern lobe of the Central Kansas Uplift that is bounded by faults mapped on the top of the Arbuckle Group to the north, west, and east (Berendsen and Blair, 1986). An average of 22 subnetwork events per year have been detected at this station since 2017. This year, 45 subnetwork events with magnitudes from M -1.5 to 0.5 were recorded at RC01 at epicentral distances ranging from about 1 to 11 mi away (Figure 12c). These events likely originated from faults bounding the Geneseo Uplift, the predominant basement structure in Rice County. Similar to observations at EW01, an uptick in subnetwork events occurred in the first half of 2021. The cause of the increase is unclear at this time and may simply represent a natural fluctuation in seismicity.

Station RC03 is located in south-central Rice County near the Peace Creek Fault Zone located on the western margin of the Geneseo Uplift. More than 500 subnetwork seismic events were recorded at RC03 with magnitudes ranging from -1.5 to 0.5. The vast majority of these events occur at regular times of day, corresponding to 5 a.m., 1 p.m., and 9 p.m. local time (Figure 13a). This regular timing and clustering at a distance of about 7 mi (Figure 13b) strongly suggest these events have an anthropogenic origin. The amplitude spectrum of small, nearby microearthquakes is typically dominated by higher frequencies. The majority of seismic events near RC03 have relatively large amplitudes toward the low frequency end of the amplitude spectrum (Figure 13c) and are likely underground mining blasts. To discriminate blasts from other subnetwork events, the catalog was filtered to remove events within the time and distance ranges of blasts. The filtered catalog has 19 remaining subnetwork events, which is consistent with previous years (Figure12c).

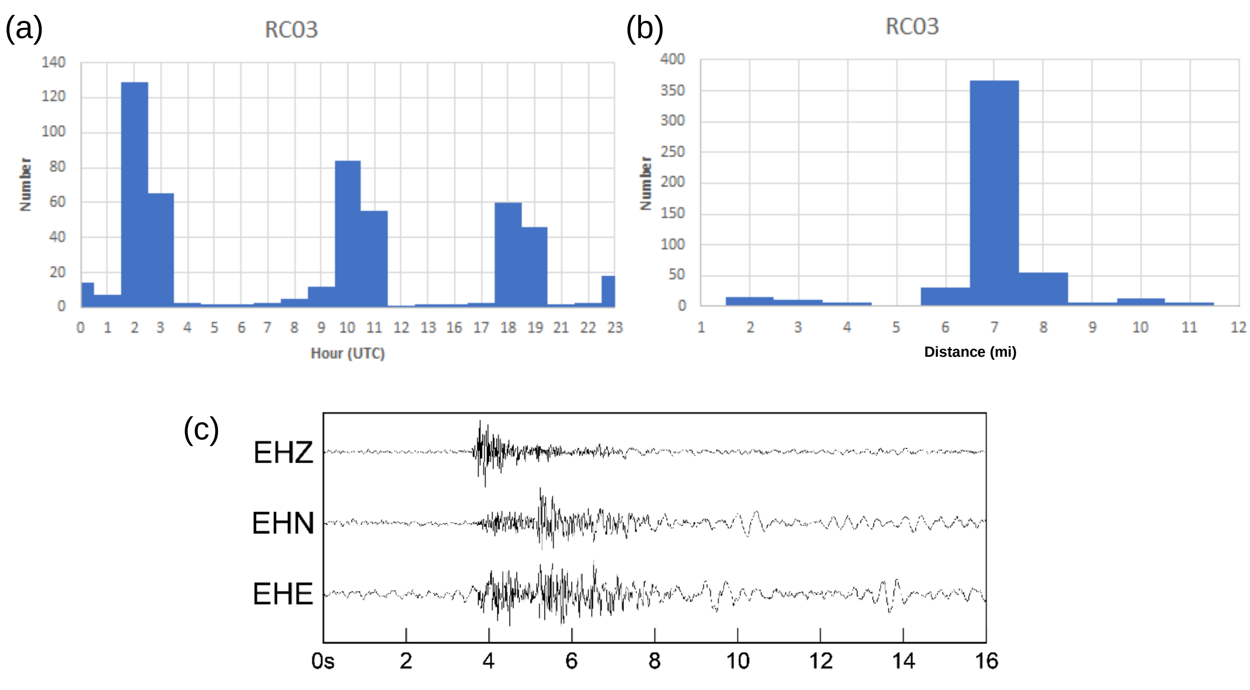

Figure 13. Histogram indicating the (a) time of day (UTC) and (b) epicentral distance of subnetwork events recorded at station RC03. (c) A representative waveform of a subnetwork event recorded at RC03.

McPherson County

Seismic activity within 20 km of member wells in McPherson County was primarily concentrated near the McPherson-Saline border (Figure 14). These events occur near the eastern margin of the Midcontinent Geophysical Anomaly (MGA) along and east of the Salina Fault in Saline County. Seismicity in this area has been ongoing with more than 100 M 2 or larger earthquakes recorded since installation of the KGS seismic network in 2015. Historically, seismicity within 20 mi of McPherson County member wells in this area is extremely sparse and persistent seismicity in this area would not be expected. To date, only a few earthquakes have occurred in McPherson County outside of the cluster at the northern county line. This year, a grouping of three microearthquakes occurred in the southeast corner of the county 11 mi or more from member wells. These events are located in the same area as two events in 2019, indicating the presence of a seismically active structure. Continued monitoring for changes in rate or progression into surrounding areas will be key for assessing the potential influence from any nearby fluid disposal.

Station MP01 is bounded to the west and east by northeast trending faults mapped in Precambrian and/or Arbuckle Group rocks associated with the Midcontinent Rift System. Thirty-seven subnetwork events were recorded at MP01 with magnitudes ranging from -1.5 to 0.4 (Figure 14b). These events occurred at various times of day and most occurred at an epicentral distance of about 5 mi. This distance is consistent with the location of a M 2.6 earthquake that occurred on November 3, 2014 (Figure 14a). The average rate of subnetwork events at MP01 is about a dozen events per year and, therefore, this year's rate is about three times greater than average. Similar to observations elsewhere, it is unclear at this time whether the rate increase represents a natural fluctuation or whether it suggests a local anthropogenic influence. This cluster bears special attention that includes enhanced comparisons between diffusivity, injection rates and volumes, and pressures in member wells.

Forty-seven subnetwork events were recorded at station MP02 with magnitudes ranging from -1.5 to 0.4 (Figure 14b). Although this may seem like a large number, the rate of subnetwork events at MP02 is generally higher than other stations with about two dozen per year. These events occurred at epicentral distances ranging from 1 to 9 mi, averaging 6 mi from the station. MP02 is bounded to the west by a system of faults associated with the Voshell anticline and to the southeast by the Halstead Fault and is surrounded by a number of anticlinal and synclinal structures. The 6 mi average epicentral distance corresponds with the grouping of mapped earthquakes in the southeast corner of the county. Therefore, these events are likely part of the foreshock-aftershock sequences of the larger mapped earthquakes.

Clustering of earthquakes and persistent seismicity can be an indicator that elevated pore pressures are influencing seismicity in McPherson and neighboring Saline counties. With a b-value of 1, this cluster is producing earthquakes with magnitudes consistent with the Gutenberg-Richter relationship, which was formulated based on naturally occurring earthquakes. Several dozen Class II saltwater disposal wells operate in the immediate vicinity of the McPherson-Saline earthquakes, more than 10 of which terminate in the Arbuckle Group. However, these wells are relatively low-rate, with the highest-rate well injecting less than 3,000 bbl/day. Therefore, it is unclear what role nearby disposal may play in the elevated seismic activity.

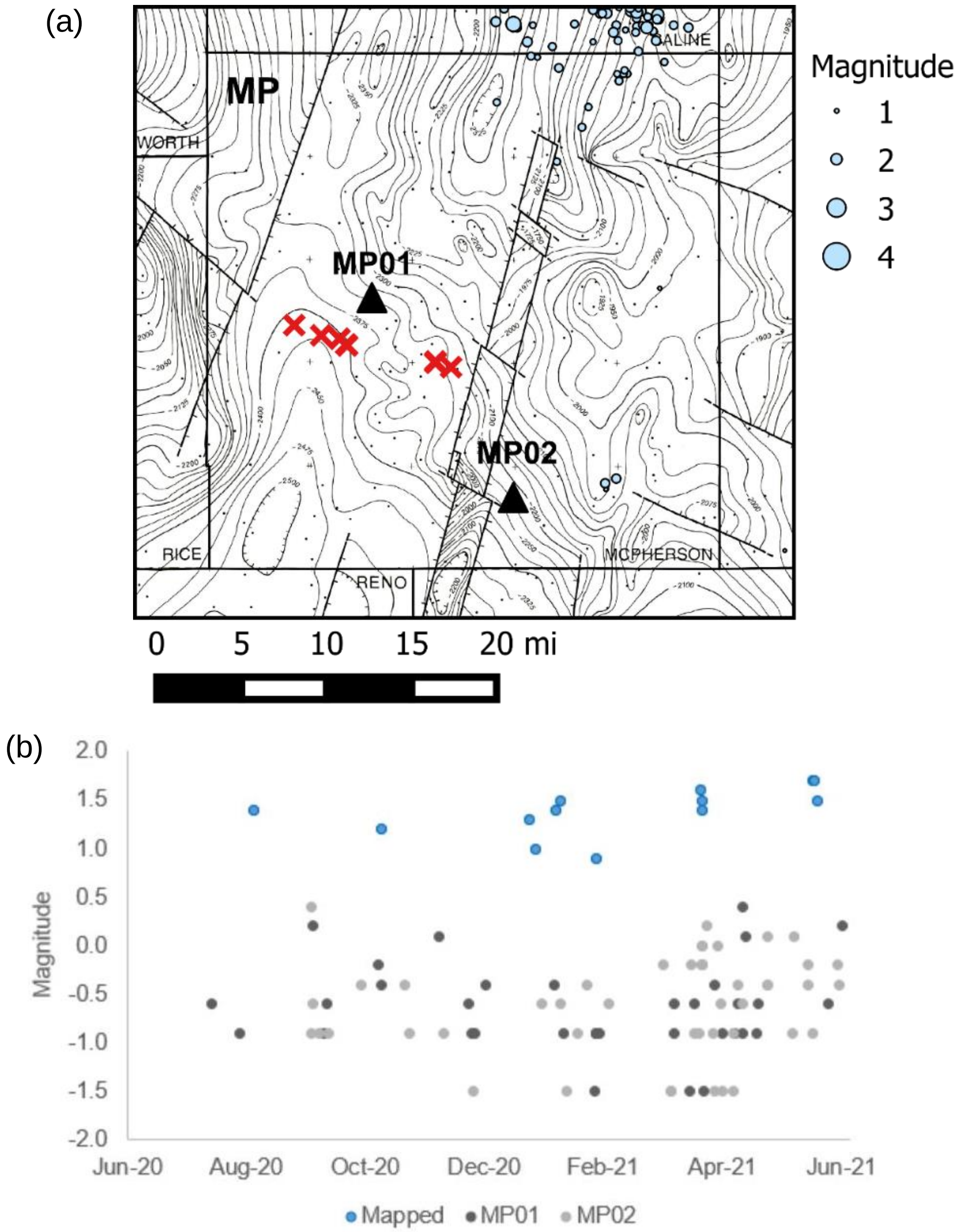

Figure 14. (a) Earthquakes recorded in McPherson County from July 2020 through June 2021 superimposed on Arbuckle Group structural contours (from Berendsen and Blair, 1986). Red Xs indicate CSTS member wells, and black triangles indicate stations in the CSTS network. (b) Scatter plot of earthquakes (blue) recorded within 20 mi of member wells and subnetwork events (gray) recorded within 12 mi of CSTS stations.

Reno County

Only 13 earthquakes were recorded in Reno County during the current reporting period. Two small ($M \leq 1.3$) earthquakes were located near a previously recorded cluster in Arlington, and 11 earthquakes were recorded in the Hutchinson cluster (Figure 15a). This is a remarkable decrease in seismic activity, considering that an order of magnitude more earthquakes (133) were recorded in Reno County during the previous reporting period. The decrease in seismic activity is consistent with stabilizing or possibly decreased pore pressures measured here in 2020. The largest event recorded near Hutchinson this year was a M 2.7 on February 15, 2021. In general, earthquakes did not occur as distinct foreshock-mainshock-aftershock sequences but rather as sparse individual events.

Station RN01 is located 2–3 mi northwest of the Hutchinson earthquakes. One-hundred forty-five subnetwork events were recorded at RN01 with magnitudes ranging from -1.5 to 0.3 (Figure 15b). Like the larger earthquakes mapped near Hutchinson, these events occurred regularly throughout the year but appeared to taper off after the first quarter, gradually decreasing in frequency through the fourth quarter. The estimated epicentral distances of nearly all these events is about 4.8 mi. Although this is slightly larger than the 2.8 mi to the center of the Hutchinson earthquake swarm, these microearthquakes almost certainly originate from the same fault or set of faults. The epicentral distance was calculated assuming a fixed earthquake depth of 3 mi, which is a common assumption used to locate earthquakes in the midcontinental United States. Earthquakes are likely occurring on faults within the shallow Precambrian basement, which is at a depth of about 1 mi in this part of Reno County. Recalculating the epicentral distance using a depth of 1 mi results in an average distance of 3 mi, which is consistent with the location of the swarm of earthquakes located by the KGS regional seismic network. These events provide confidence in the suggestion that the Hutchinson earthquakes are occurring in the shallow basement.

More than 200 subnetwork events were recorded at station RN03. However, similar to events recorded at RC03, the vast majority of these events have timing, distance, and spectral characteristics that strongly suggest underground blasting. Events outside the time and distance ranges of probable blasts were cataloged as probable earthquakes following the same procedure described for station RC03. Sixteen probable earthquakes occurred regularly throughout the year, similar to previous years.

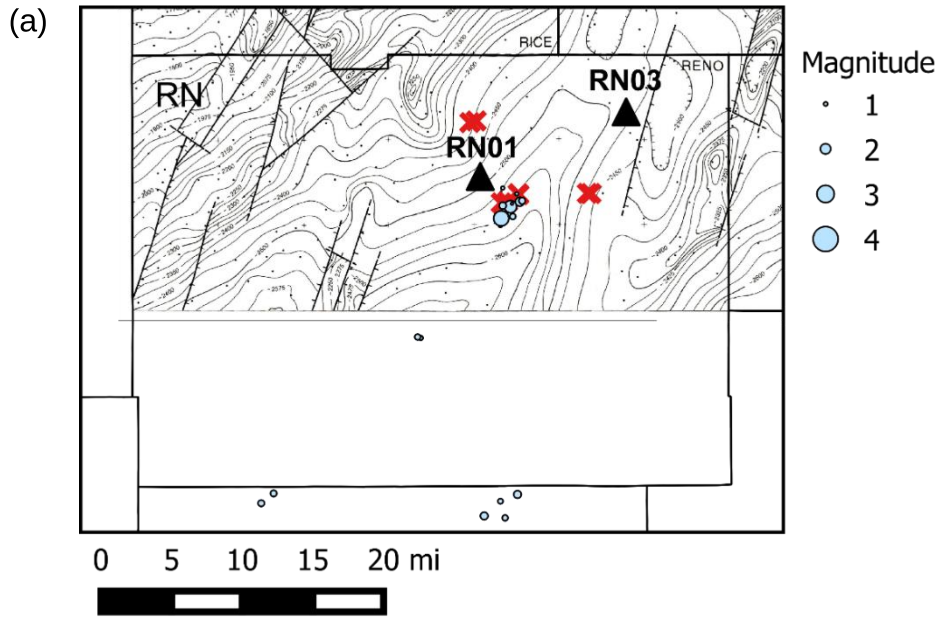

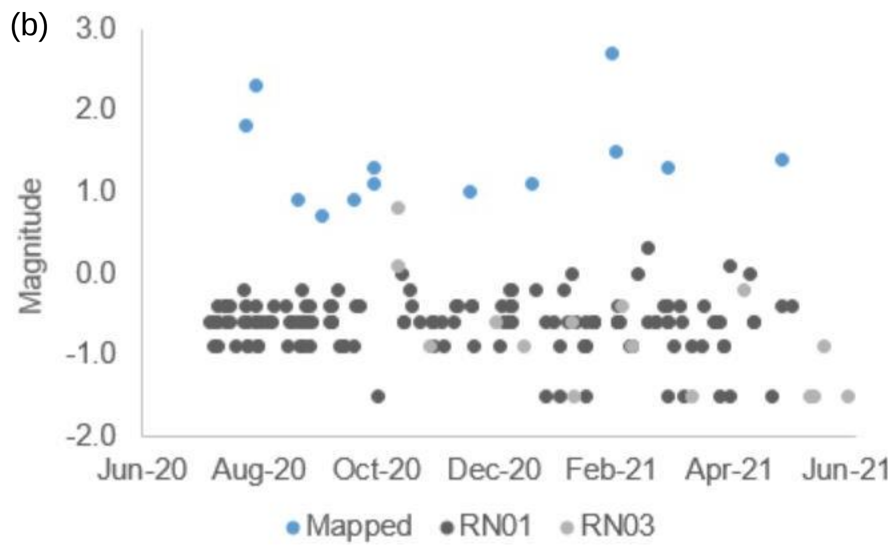

Figure 15. (a) Earthquakes recorded in Reno County from July 2020 through June 2021 superimposed on Arbuckle structural contours (from Berendsen and Blair, 1986). Red Xs indicate CSTS member wells, and black triangles indicate stations in the CSTS network. (b) Scatter plot of earthquakes (blue) recorded within 20 mi of member wells and subnetwork events (gray) recorded within 12 mi of CSTS stations.

Sedgwick County

The most notable earthquakes in Sedgwick County this year were a cluster of nearly 150 earthquakes recorded in east Wichita (Figure 16a), including multiple distinct sequences with 25 M 2 and 11 M 3 earthquakes. The largest earthquakes were M 3.9 events on December 30, 2020, and March 14, 2021. In previous years, only sparse low-magnitude seismicity was recorded in this area, with more prominent clusters farther to the east near Rose Hill and Andover in Butler County. Previous seismicity followed induced trends that progressed to the northeast from Sumner and into Sedgwick and Butler counties. Unlike previous earthquakes near Wichita, the events had an abrupt onset and increasing energy release from November 26 to December 30, 2020 (Figure 16b). This clustering of earthquakes trending in a northwest/southeast direction is distinctive compared to alignments of previously recorded earthquakes within 15 miles of this cluster. Given the stabilizing and possibly decreasing formation pressures in Sedgwick County, earthquakes in this area are not wholly unexpected. However, the sudden increase in seismicity while pressures are beginning to decrease is somewhat surprising and may suggest that local disposal operations could be a contributing factor.

With the exception of Wichita, seismic activity in Sedgwick County was down overall and primarily persisted in previously identified areas in the southern half of the county (Figure 16a). In the Cheney area, only about 30 earthquakes were recorded this year, a decrease of more than 50% relative to the 84 earthquakes recorded here during the previous reporting period. A small cluster of seven microearthquakes occurred in December 2020 and February 2021 just west of Goddard in an area with only a sparse history of seismicity. Given the low magnitudes ($M \leq 1.7$), temporal grouping, and lack of spatiotemporal progression, these events may be natural earthquakes on a fault associated with the nearby Valley Center anticline. Although it is likely these earthquakes have been influenced by regionally elevated formation pressures, they do not appear to be directly related to nearby disposal operations.

Thirty subnetwork events were recorded at station SG02 with magnitudes ranging from -1.5 to 0.3 (Figure 16b). These events occurred at epicentral distances ranging from 3 to 10 mi and do not appear to correlate with any mapped earthquakes. Subnetwork events are likely occurring on faults associated with the Valley Center anticline as a result of elevated formation pressures and the occurrence rate is consistent with past years.

(a)

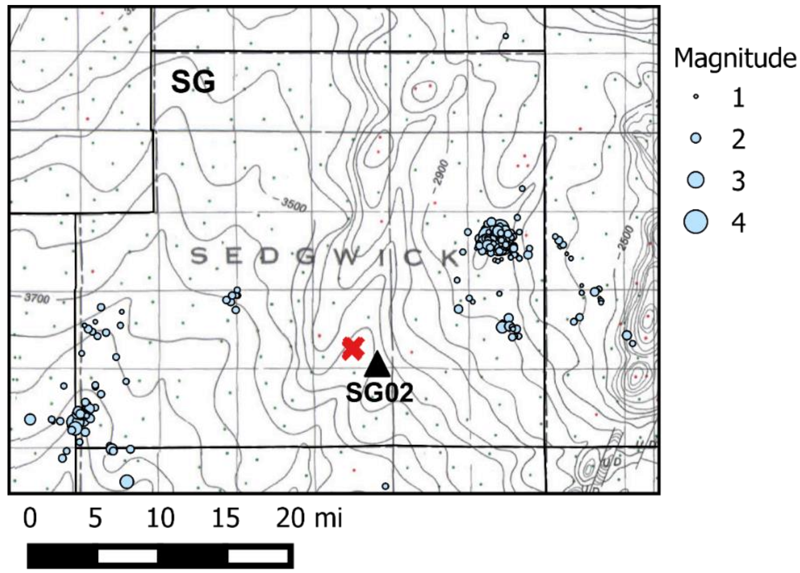

(b)

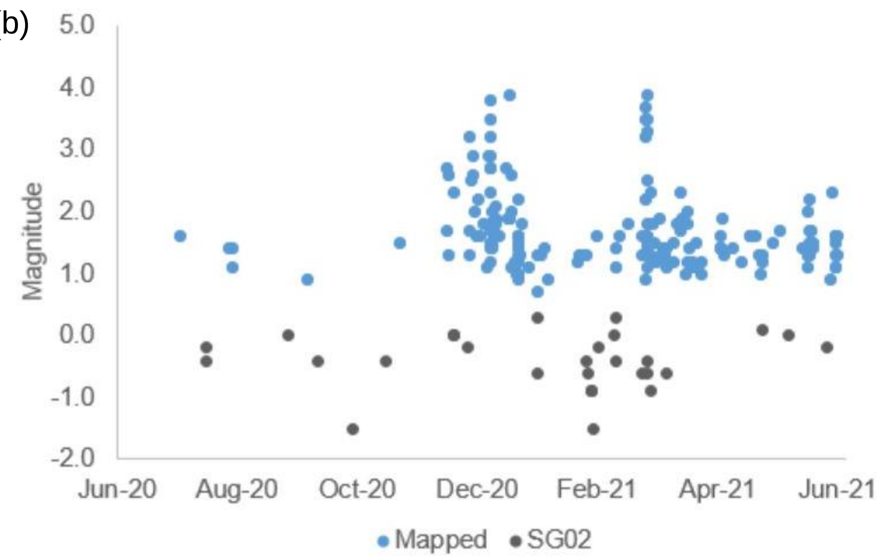

Figure 16. (a) Earthquakes recorded in Sedgwick County from July 2020 through June 2021 superimposed on Arbuckle Group structural contours (from Berendsen and Blair, 1986). The red X indicates a CSTS member well, and the black triangle indicates a station in the CSTS network. (b) Scatter plot of earthquakes (blue) recorded within 20 mi of the member well and subnetwork events (gray) recorded within 12 mi of the CSTS station.

Butler County

Forty-three earthquakes were mapped within 20 mi of the Butler County member well this year. In addition to the earthquakes near the Sedgwick-Butler county line discussed in the previous section, more than a dozen earthquakes occurred in central Butler County (Figure 17). The largest earthquake was a M 3.0 on October 27, 2020, in the north-central part of the county along the crest of the Nemaha Ridge. Several sparse earthquakes occurred in the central part of the county, three of which were within 5 mi of the Butler County member facility. These earthquakes do not follow a definitive spatial or temporal trend, suggesting they are not likely triggered as a result of poroelastic changes driven by either regional or local disposal. These earthquakes are most likely a result of natural crustal stress, but because formation pressures are slightly elevated in Butler County, the influence of elevated pore pressures cannot be confidently ruled out.

Sixteen subnetwork events were recorded at station BU02 with magnitudes between -0.9 and 0.4 at epicentral distances of 2–11 mi. The majority of these events appear to be low-energy foreshocks and aftershocks of the M 3.0 earthquake in north-central Butler County.

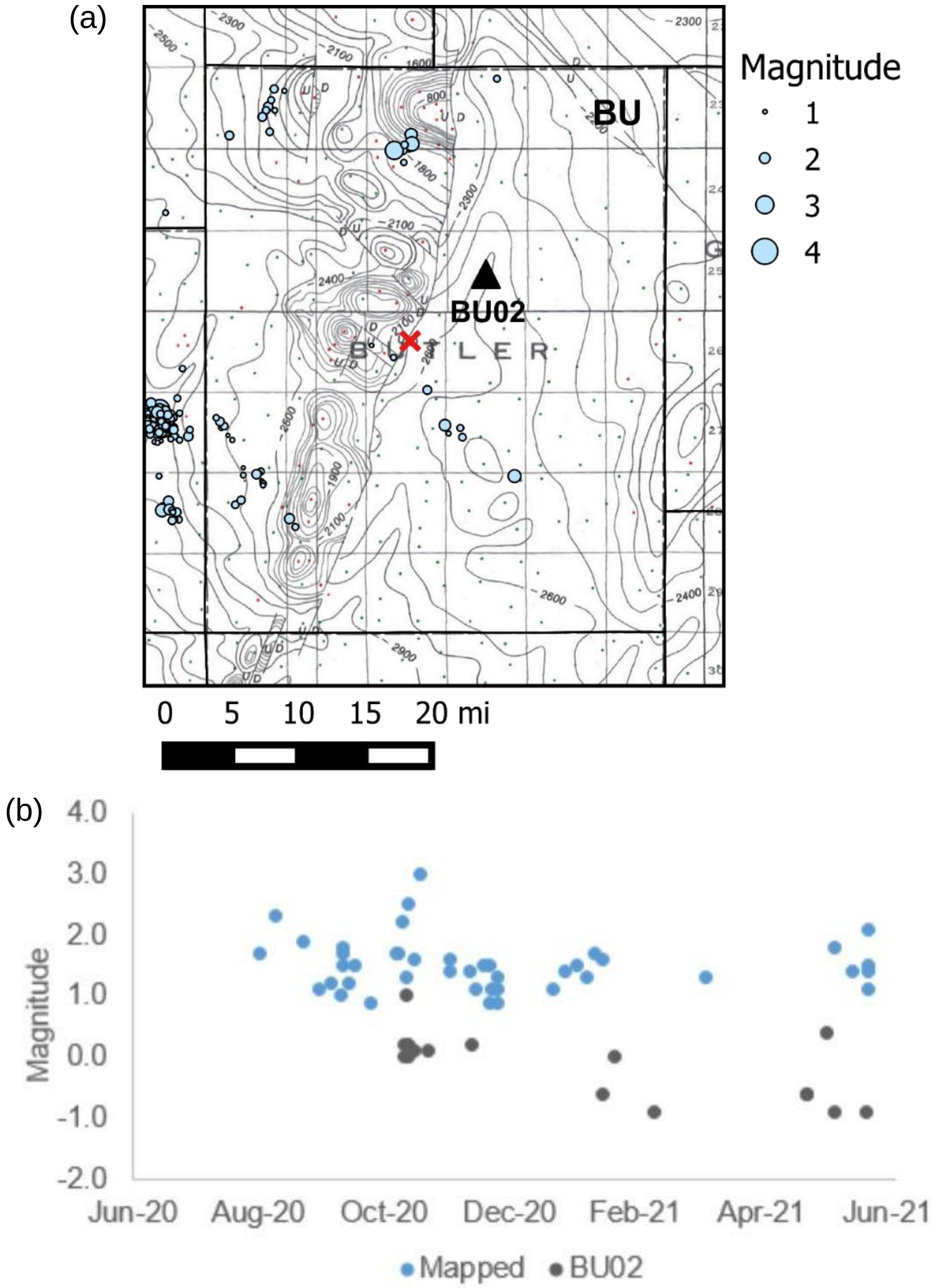

Figure 17. (a) Earthquakes recorded in Butler County from July 2020 through June 2021 superimposed on Arbuckle Group structural contours (from Berendsen and Blair, 1986). The red X indicates a CSTS member well, and the black triangle indicates a station in the CSTS network. (b) Scatter plot of earthquakes (blue) recorded within 20 mi of the member well and subnetwork events (gray) recorded within 12 mi of the CSTS station.

Johnson County

No earthquakes were mapped within 20 mi of the Johnson County member well (Figure 18a). Only four subnetwork events were recorded at station JO01, consistent with previous years (Figure 18b). These observations are unsurprising given the stable tectonic regime and limited number of historic earthquakes recorded in this area.

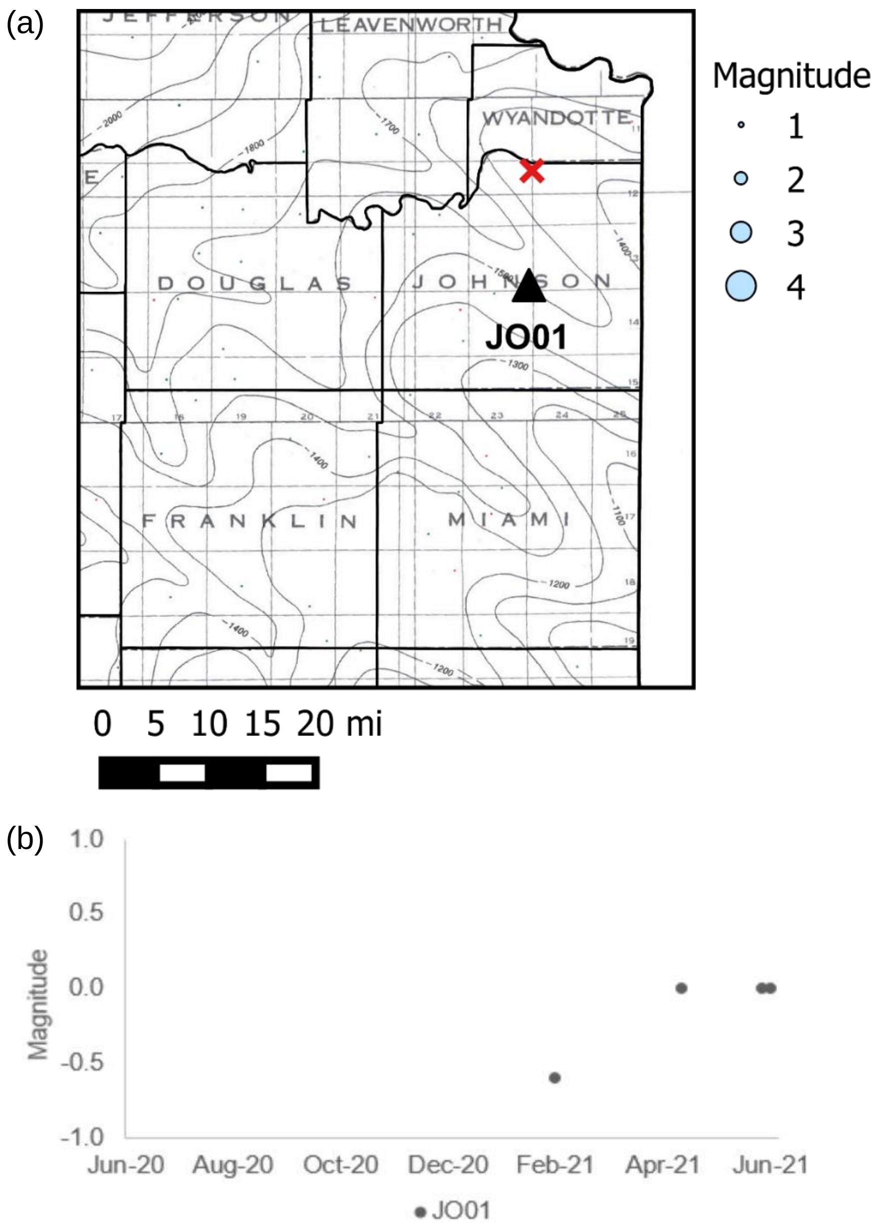

Figure 18. (a) Earthquakes recorded in Johnson County from July 2020 through June 2021 superimposed on Arbuckle Group structural contours (from Berendsen and Blair, 1986). The red X indicates a CSTS member well, and the black triangle indicates a station in the CSTS network. (b) Scatter plot of subnetwork events recorded within 12 mi of the CSTS station.

Felt Clusters and Their Relationship to Consortium Facilities

Felt earthquakes originating from within the Wichita cluster received the most attention from residents and government officials last year in Kansas. Though Wichita has a history of felt earthquakes dating back to 1919 (Figure 19a), only four earthquakes were reported between 1919 and 1948—an average rate of only one felt earthquake every 10 years. A total of 23 earthquakes of this size ($M \geq 2.5$) were recorded beginning in November 2020, representing a significant increase in the earthquake rate. With more than 70 years since the previous felt earthquake in 1948, Wichita could be considered "overdue" for an earthquake of this size by 2020. In fact, based on the Gutenberg-Richter relationship, the probability of a natural earthquake occurring at that time was more than 99.9%. A large number of main shocks are not expected after a long period without an earthquake because earthquakes follow a Poisson distribution and, by their very nature, main shocks occur independently. Therefore, it is surprising that at least five distinct sequences occurred within a four-month interval between November 2020 and March 2021 (Figure 19b). Although it is possible these earthquakes were natural, the probability of each successive main shock is increasingly unlikely (Figure 19c).

As mentioned in the previous section, even in the context of regionally elevated formation pressure, the Wichita earthquakes are somewhat unexpected given the apparent decline in pressure measured in Sedgwick County wells in 2020. With formation pressures being well above historic levels, critically stressed faults will be more sensitive to even small pressure fluctuations from local injection operations. The majority of Arbuckle disposal wells within 15 mi of the Wichita cluster inject at rates of < 5,000 bbl/day, which for single wells is less likely to produce large enough pressure changes to trigger earthquakes. Five wells within 15 mi inject at rates > 5,000 bbl/day: the Adamson 3 SWD about 11 mi from the Wichita cluster and four wells at the Oxy Chem facility about 14 mi away (Figure 20a).

Metered daily disposal volumes were obtained for the Oxy Chem wells, and daily volumes for the Adamson 3 SWD were estimated based on the produced volumes and approximate water cut. The Adamson 3 SWD and Oxy Chem WWDW#8 were both abruptly shut in during the months preceding the Wichita earthquakes (Figure 20b and 20c). Diffusivity is the hydraulic parameter that describes pore pressure diffusion and is related to permeability of the reservoir rock. Given the distance and timing relative to the Wichita earthquakes, the calculated apparent hydraulic diffusivity for the Adamson 3 SWD and Oxy Chem WWDW#8 would be around 1 m^2/s and 3.5 m^2/s, respectively. Both values of apparent diffusivity are reasonable for induced seismicity (Haggenson and Rajaram, 2021). This observation simply indicates that it is physically possible for a pressure pulse resulting from shut-in of either of these wells to have propagated to the epicenters of earthquakes within this cluster at the onset of the seismicity.

It should be clearly noted that there is no direct evidence or correlation between disposal rates in Adamson 3 SWD or Oxy Chem WWDW#8 and the individual earthquake sequences. Furthermore, it is unclear whether the change in pressure from the abrupt shut-ins and start-ups would have been sufficient to trigger earthquakes more than 10 mi from these wells. At Oxy Chem, the wastewater was diverted to other wells at the facility, which may have mitigated any localized pressure changes from shutting in WWDW#8. However, seismicity induced from abrupt changes in disposal volume is well documented and these kinds of abrupt changes in volume should be avoided. Volume changes should be made gradually when possible to avoid sudden pressure changes that might trigger seismicity, especially in areas with elevated formation pressures.

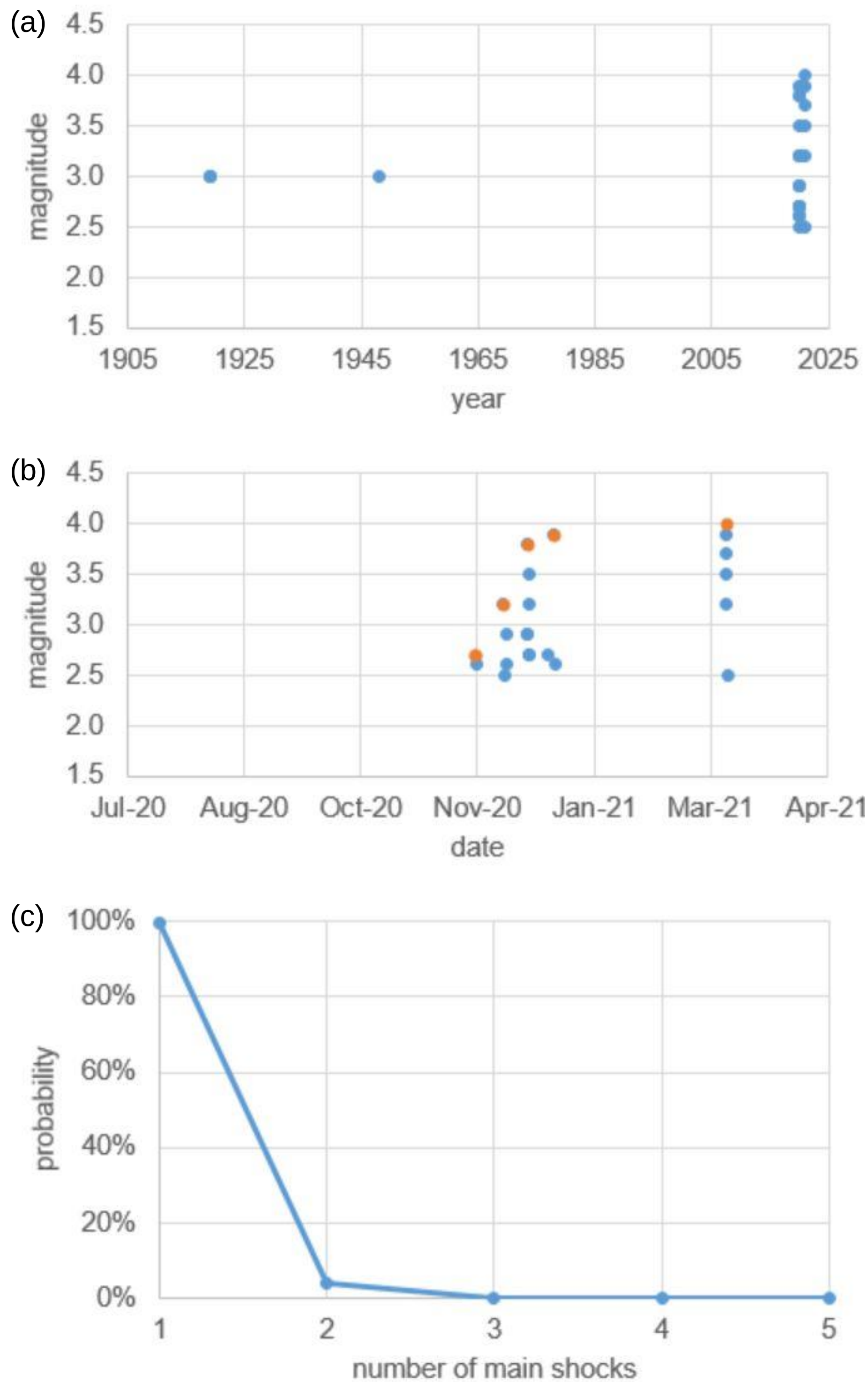

Figure 19. (a) Scatter plot of felt ($M \geq 2.5$) earthquakes in Wichita. (b) Close up of (a) for the 2020–2021 reporting year where orange indicates main shocks. (c) Probability of each of the five main shocks based on the characteristic Poisson distribution of natural earthquakes with a rate of 0.1 earthquakes/year.

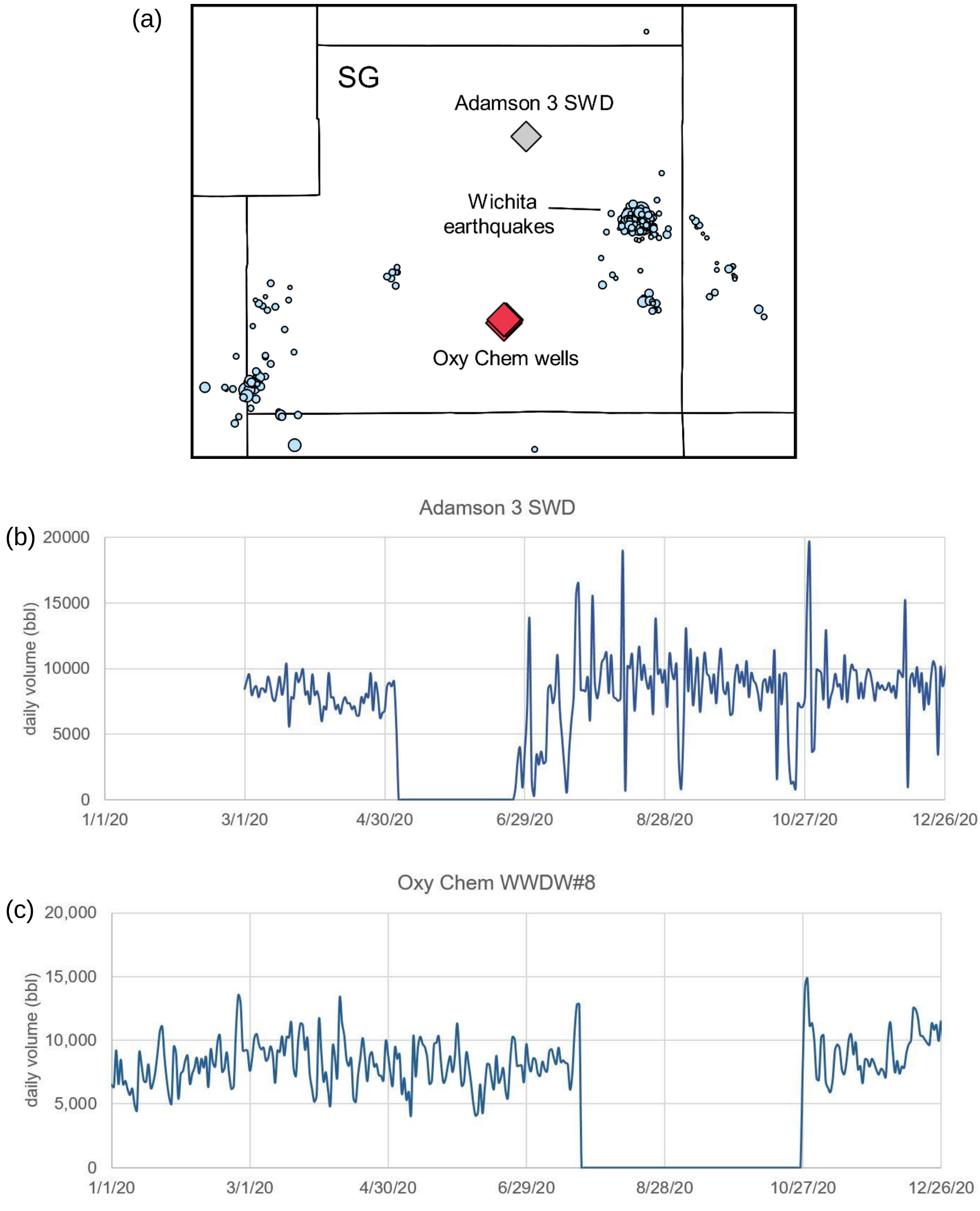

Figure 20. (a) Earthquakes and wells injecting more than 5,000 bbl/day in Sedgwick and Butler counties. (b) Estimated daily injection volumes in the Adamson 3 SWD. (c) Metered daily injection volumes in Oxy Chem WWDW#8.

DISCUSSION

The Arbuckle Group is a deep aquifer that serves as the injection zone for thousands of Underground Injection Control (UIC) wells in Kansas and neighboring Oklahoma. Widespread seismic activity across central Oklahoma and south-central Kansas is primarily attributed to elevated pore pressures along critically stressed faults in the hydraulically connected basement underlying the Arbuckle Group. As injection volumes in south-central Kansas decreased over the past five years, pressures in south-central Kansas began to stabilize in 2016 and the earthquake rate likewise began leveling off (Figures 21 and 22). In 2020 (the most current year with complete pressure data), pore pressures within the Arbuckle Group (and thus, basement) remain elevated at levels above the earthquake-triggering threshold but appear to be gradually declining in some areas while increasing in others (Figure 23). Therefore, earthquakes will likely persist as crustal stresses continue to load near-critical faults properly aligned with the stress field. Furthermore, injection practices that produce even small pressure fluctuations or pulses may contribute to trigger earthquakes on nearby faults, as may have been the case in Wichita.

The rate of earthquakes in general continues to decline and epicenters largely persist in previously identified areas. However, activity appears to have picked up in areas where earthquake rates or sizes are traditionally low/small (e.g., eastern Russell and eastern Sedgwick counties). The monthly number of earthquakes reached an all-time low (since the network was established in 2015) in July 2020, then subtly and gradually increased throughout the reporting year (Figure 24). Additionally, it is notable that seven counties had either the largest magnitude earthquake ever recorded or tied for the largest in that county: Butler, Jewell, Meade, Montgomery, Pratt, Sedgwick, and Thomas (Figure 3). It appears the rate of low-magnitude earthquakes may be increasing statewide with seismicity progressing into areas with little to no historic seismicity.

Seismicity in proximity to CSTS members' facilities is sporadic, with some events sharing commonality with mapped structures and historic earthquakes. Many groups of earthquakes continue to establish and align with structural trends previously unmapped and with no drill or geophysical evidence they existed, except CSTS-identified earthquake epicenters. Although the increase in seismicity across the state can be correlated to increases in observed bottomhole pressures in Class I wells starting about 2013, the current trends in bottomhole pressures only loosely correlate with the significant decrease in earthquake activity. It is likely that with increasing pore pressure, many of the critically stressed faults were triggered, and as the pressure has stabilized above the triggering threshold SWD operations that previously were tolerated by the critically stressed faults will now trigger their movement.

Earthquake hotspots that have minimal to no "significant" localized injection and that are not located coincident with historical areas of seismicity (Saline, Jewell, Dickinson, and Chase counties) defy a first-order explanation. Understanding the location of the foci of the earthquakes and the possible triggering mechanisms provides some insights and options worth considering. Fluid injected into the Arbuckle dissipates both horizontally into the Arbuckle Group along high permeability layers and vertically into basement rocks through faults and fractures. Basement rock is for the most part granite and has zero permeability within the rock matrix. Permeability in granite comes from fractures (faults or stress fractures). Basement faults and fractures provide extremely anisotropic diffusivity. These high velocity fluid pathways could easily transport large volumes of fluid across long distances much quicker than estimated when compared to the spherical divergence that would be appropriate for most sedimentary reservoirs.

Basement lineaments interpreted on potential fields data in Phillips, Smith, Jewell, Republic, Cloud, Mitchell, Osborne, and Rooks counties in the north-central part of the state and Saline, Dickinson, McPherson, Morris, Marion, and Chase counties in central Kansas provide an intriguing potential pathway for very constrained fluid movement in basement rocks. Temporal progression of earthquakes that appear coincident with and aligned with these lineaments could be suggestive of pressure migration across areas of the state without significant injection into deep Paleozoic rocks. These fluid pathways might transport enough fluid to increase pore pressure beyond triggering thresholds. This suggestion is purely speculative since no drill data exist to confirm or refute such an interpretation.

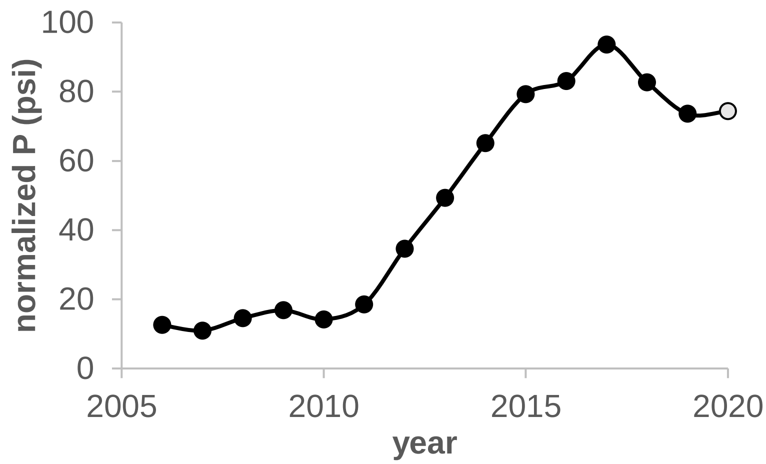

Figure 21. Arbuckle Group pore pressure reported for the Class I facility in Harper County.

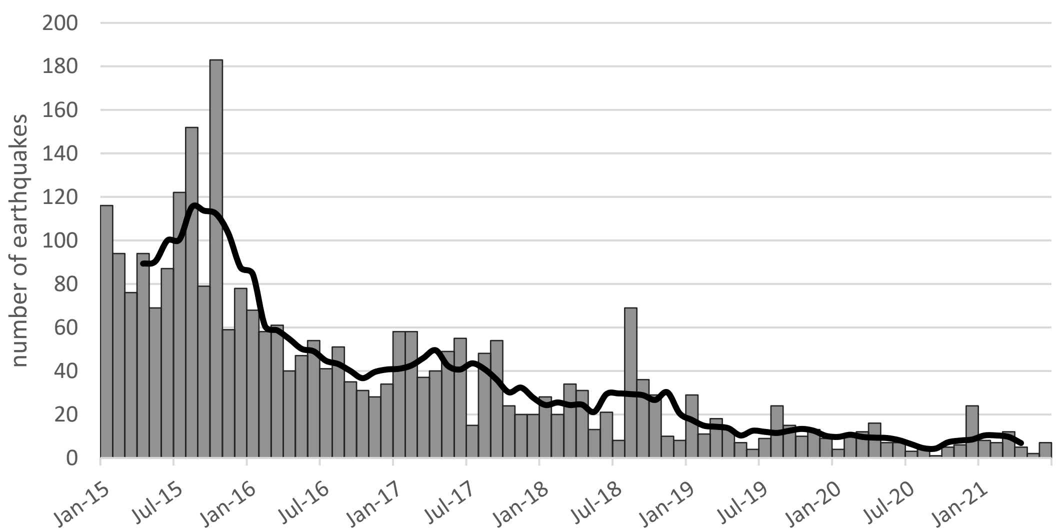

Figure 22. Monthly number of earthquakes M 2 or larger in south-central Kansas.

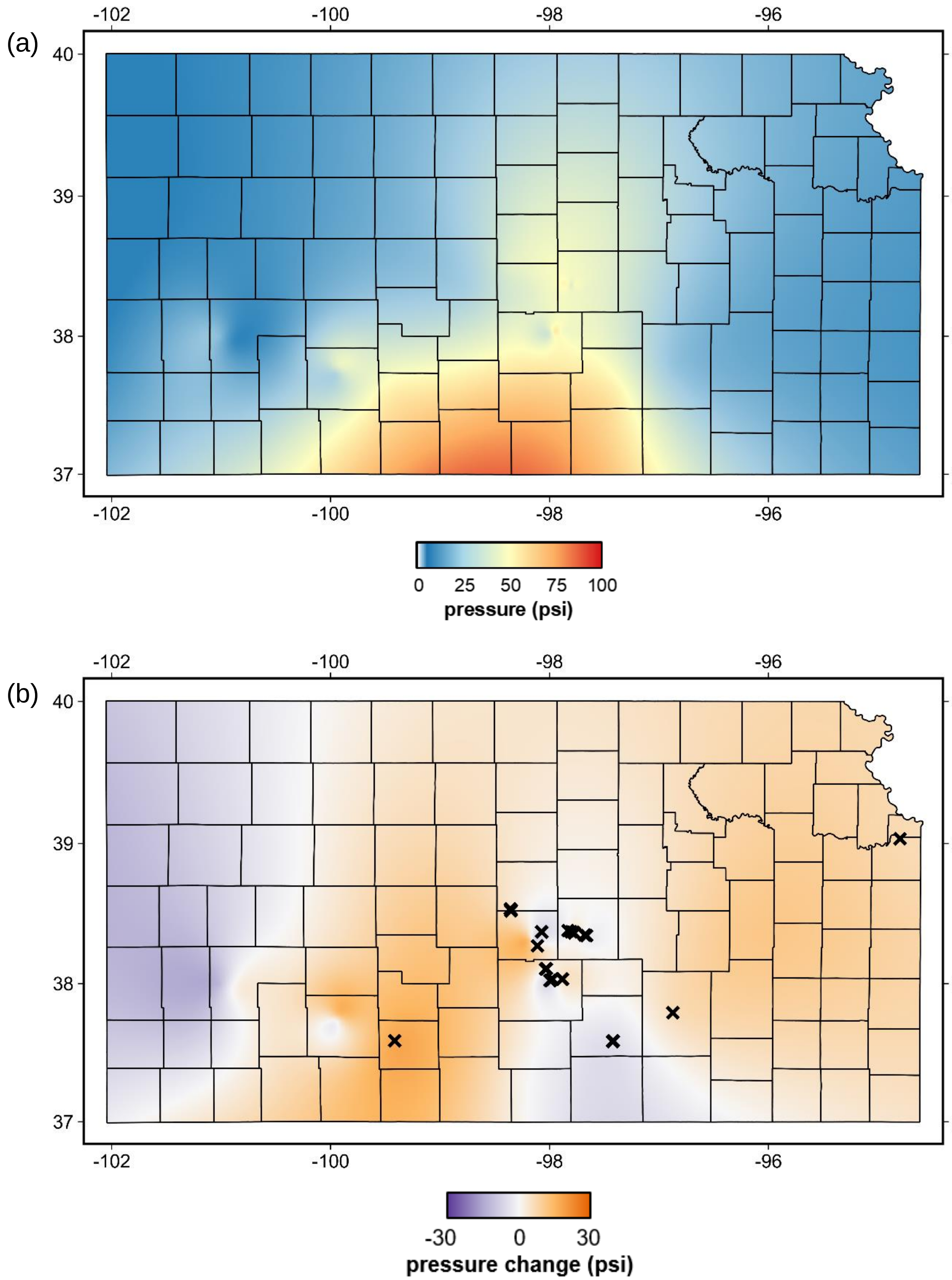

Figure 23. (a) Change in Arbuckle Group pore pressure in 2020 (relative to baseline pressures reported in 2002, or first reported year thereafter). (b) Change in Arbuckle Group pore pressure from 2019 to 2020. Black Xs indicate Tier 1 member wells.

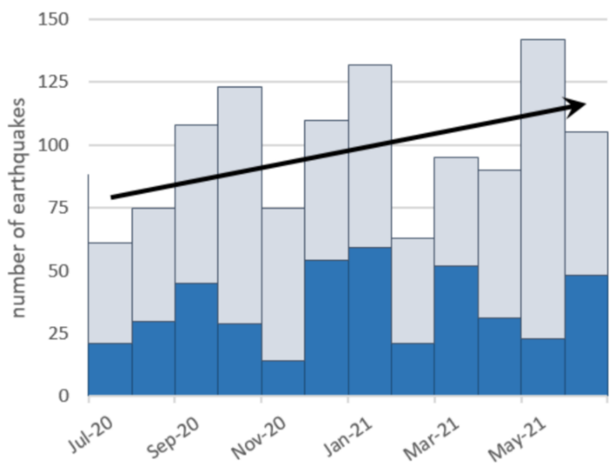

Figure 24. Monthly number of earthquakes of all magnitudes in south-central Kansas (blue) and elsewhere in the state (gray).

WEBSITE CONTENT

The CSTS website (http://www.kgs.ku.edu/Geophysics/CSTS/index.html) is operated by the KGS. It includes links to information about meetings, publications, network updates, and seismic updates (for Tier 1 members) and information about the seismic network for Tier 2 members. It includes semiannual newsletters about earthquake activity, along with access to a comprehensive catalog of events, including time, location, magnitude, and the Seismic Action Score (based on evaluation criteria developed by the state's Induced Seismicity Task Force) for each event. The website also includes a series of pictures and accounts of the installation process and gives a feel for the environment and footprint of each CSTS station. Currently at least one station has been installed within 20 miles of every Tier 1 member's well (Figure 1, Appendix A). A short discussion and set of pictures are posted on the website documenting the installation process.

Beginning this year, the Publications section of the website includes a detailed overview of recent publications that may be relevant to Consortium members (https://www.kgs.ku.edu/Geophysics/CSTS/Group/recent_lit.html, Appendix D). For each paper, we provide three key points highlighting the primary findings, a summary (paraphrased from the published abstract, in most cases), and link to the full paper on the publisher's website. This section of the website will continue to be updated as new relevant papers are published. In time, we hope to provide detailed overviews for past induced seismicity publications as well.

OTHER ACTIVITIES

The 2021 annual meeting was held virtually on August 5. The agenda is shown below and a video of the meeting is available on the CSTS web page.

CONSORTIUM TO STUDY TRENDS IN SEISMICITY
Virtual Annual Meeting Agenda – August 5, 2021

9:30 a.m.	Welcome and Introductions — *Rex Buchanan*, Kansas Geological Survey (KGS)
9:45 a.m.	A Year of Seismicity Monitoring, Trends, and Observations — *Shelby Peterie*, KGS
10:15 a.m.	Produced Water and Induced Seismicity Programs at the Ground Water Protection Council — *Dan Yates*, Ground Water Protection Council
10:45 a.m.	Regulatory, Legislative, and Industry Aspects of Seismicity — *Rick Miller*, KGS
11:15 a.m.	KGS Earthquake Mapper and Alert Access — *Shelby Peterie*, KGS
11:30 a.m.	Consortium Future Activities, Discussion — All

PLANS

With more than three years of recording on all stations, preliminary searches for associations between subnetwork seismicity and operations at each site is an exercise that was started last year and will continue with the increased number of events to work with. We are looking at injection practices and seismicity at the M 0.0 to 2.0 levels within 10 miles of each facility to ensure our general observations are in fact substantiated with actual well-specific operations and will continue that practice. We acknowledge that it was premature to begin looking at correlations or response characteristics at individual facilities, but some systematic or baseline relationships might begin to emerge at some point. We started that process a bit early just to ensure we have the opportunity to observe any correlations as they begin to become statistically defensible. We are likely still a few years ahead of having enough data for this kind of detailed investigation.

As the statewide network has expanded over the last year, the infill station near Salina is providing improved location accuracy as well as representing another station that is helping with event triangulation for earthquakes currently too small to be detected on three or more stations.

Preliminary investigations into the potential of incorporating products of the Arbuckle working group with seismic monitoring products (locations, waveforms, depths, distributions—spatial and temporal, etc.) should eventually begin to expand the scope of the CSTS and increase the significance and first-order use of CSTS products into a wide range of member needs.

CONCLUSION

This year's trends in seismicity, as they relate to CSTS facilities, are generally consistent with observations reported over the year prior. The relationship between the price of oil and Class II injection volumes is becoming well established, and the temporally staggered correlations between the volumes of produced water disposed of in the Arbuckle and seismicity have been observed to track in a reasonably consistent fashion since 2013. Monitoring seismic activity during this time of reduced disposal volumes and earthquake numbers and sizes is critical and will play a vital role in establishing natural recursion numbers for micro levels and the associated development of expectations for distinguishing natural from induced seismicity.

Natural recursion relationships and earthquake characteristics are most accurately quantified and statistically consistent when studied and averaged over long periods of time. Relying on small sample sizes (less than several years to a decade) for statistical analysis of temporally variable events will likely alias the results and minimize confidence in any future attempts to categorize triggering mechanisms.

Three M 4+ events within the Hutchinson cluster occurred during this reporting period. Those events and the fluid injection records have provided significant insights into the recursion relationship and possible cause and effect associated with large injection rate changes in temporally relevant periods. Highly variable sequences of earthquakes associated with these main shocks are likely indicative of a highly dynamic stress field.

Seismicity in proximity to CSTS members' facilities is sporadic, with some events sharing commonality with mapped structures and historic earthquakes. Many groups of earthquakes continue to establish and align with structural trends previously unmapped and with no previous evidence they existed, except CSTS-identified earthquake epicenters.

REFERENCES

Armbruster, J.G., D.W. Steeples, and L. Seeber, 1989, The 1989 earthquake sequence near Palco, Kansas: A possible example of induced seismicity (abstract): *Seismological Research Letters*, v. 60, no. 4, p. 141.

Berendsen, P., and K.P. Blair, 1986, Subsurface structural maps over the central North American rift system (CNARS), central Kansas, with discussion: Kansas Geological Survey, Subsurface Geology Series 8, 16 p.

Cole, V.B., 1976, Configuration of the top of the Precambrian rocks in Kansas: Kansas Geological Survey, Map M-7, scale 1:500,000.

Haggenson, R., and H. Rajaram, 2021, Seismic diffusivity and the influence of heterogeneity on injection-induced seismicity: *Journal of Geophysical Research: Solid Earth*, 126, e2021JB021768.

Healy, J.H., W.W. Rubey, D.T. Griggs, and C.B. Raleigh, 1968, The Denver earthquakes: *Science*, v. 161, no. 3848, p. 27.

Xia, J., R.D. Miller, and D.W. Steeples, 1995a, Aeromagnetic map of Kansas, reduced to a horizontal plane and reduced to the pole: Kansas Geological Survey, Map Series M-41D.

Xia, J., R.D. Miller, D.W. Steeples, and D. Adkins-Heljeson, 1995b, Residual Bouguer gravity map of Kansas, the second order regional trend removed: Kansas Geological Survey, Map Series M-41E.

Yarger, H.L., 1983, Regional interpretation of Kansas aeromagnetic data: Kansas Geological Survey, Geophysics Series 1, p. 1–35.

[This page is intentionally blank.]

Appendix A: CSTS Station Locations, Pictures, and Descriptions

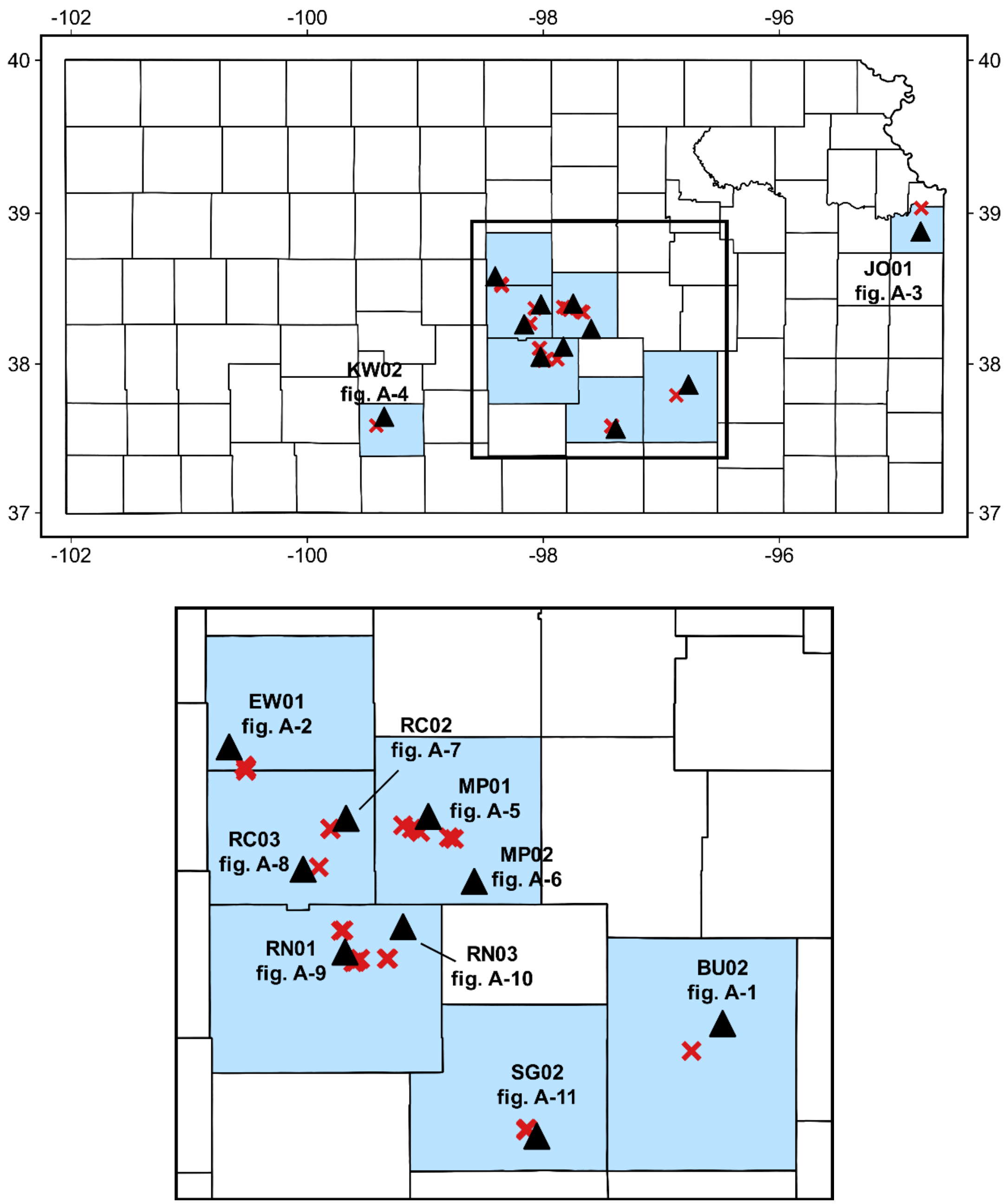

Figure A-0. Base map for pictures of equipment configuration at each station included in this appendix. The top figure is a map of Kansas, and the bottom figure is an enlargement of the black box in the upper figure. Black triangles are earthquake stations and red Xs are members' injection facility locations.

Figure A-1. BU02 is located in the El Dorado State Park in northern Butler County. This station is in a pasture near El Dorado Lake about 4 mi from Interstate 35.

Figure A-2. EW01 is located in southwestern Ellsworth County near the city of Holyrood. The station is in a cemetery about 1 mi from Kansas Highway 156.

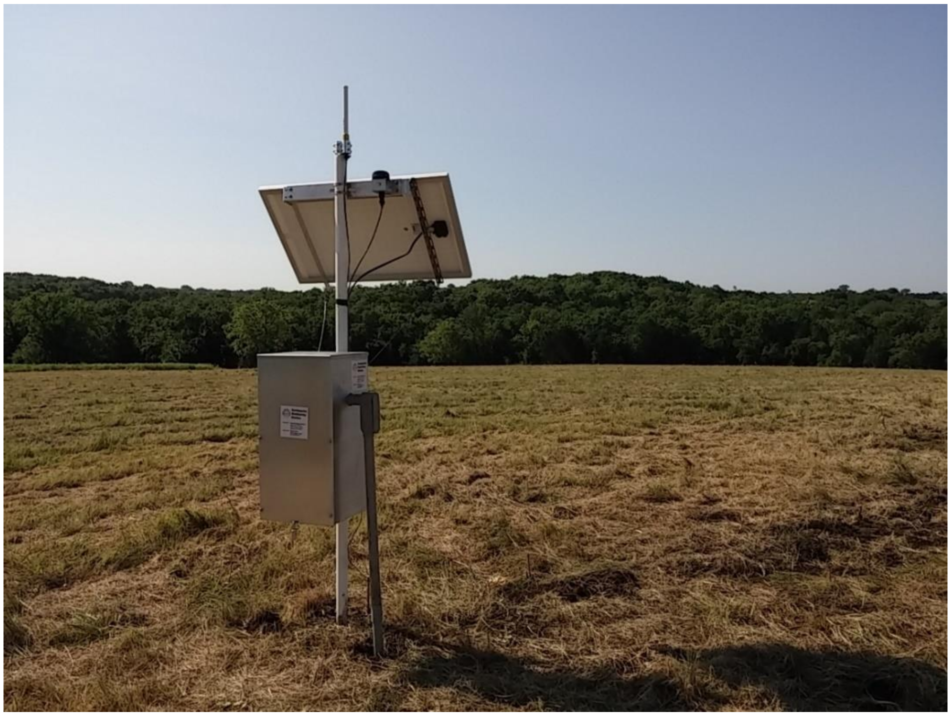

Figure A-3. JO01 is located on the grounds of the Olathe Prairie Center in Johnson County about 4 mi west of Kansas Highway 10. There is light traffic around the station, and two rock quarries are within about 5 mi of the station.

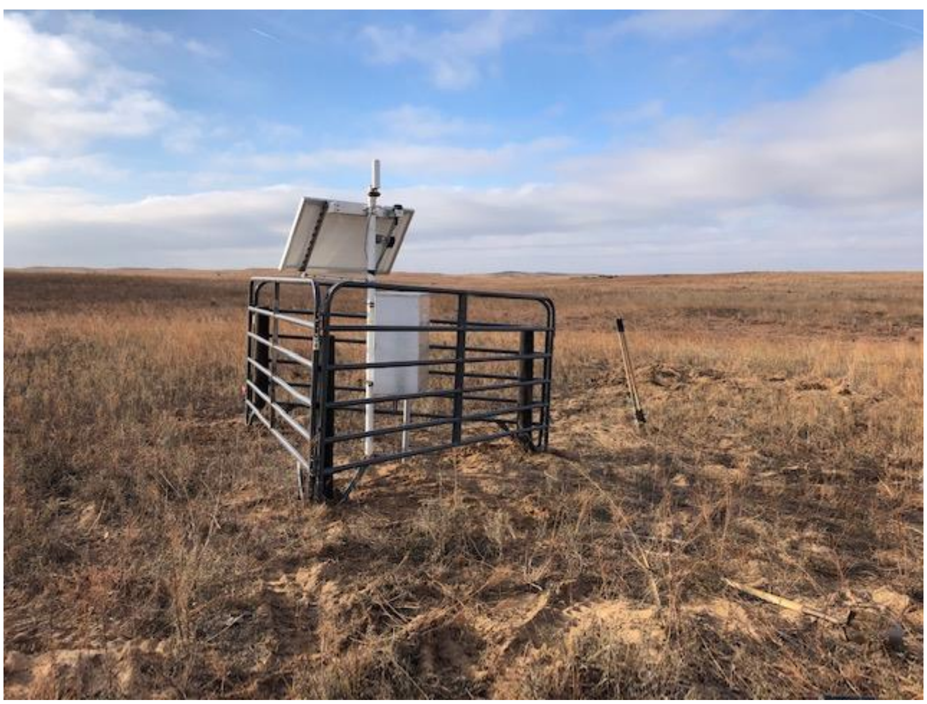

Figure A-4. KW02 is located in northern Kiowa County in a pasture located between Mullinville and Greensburg more than 1 mi from the railroad and highway.

Figure A-5. MP01 is located in the McPherson Valley Wetlands Wildlife Area in McPherson County. The station is northwest of Conway about 2 mi from US Highway 56.

Figure A-6. MP02 is located in south-central McPherson County southeast of McPherson. The station is in a pasture on the grounds of a local church about 3 mi from Interstate 135.

Figure A-7. RC02 is located in eastern Rice County near the city of Little River. This station is installed in a pasture more than 1 mi from US Highway 56 and Kansas Highway 46.

Figure A-8. RC03 is located in Rice County between Lyons and Sterling. This station is installed in a pasture about 2 mi from Kansas Highway 96 and is near a small landing strip.

Figure A-9. RN01 is located in Reno County west of Hutchinson. This station is installed in a cemetery about 2 mi from Kansas Highway 14.

Figure A-10. RN03 is located in Reno County northeast of Hutchinson in Sand Hills State Park. It is installed about 2.5 mi from Kansas Highway 61.

Figure A-11. SG02 is located in Sedgwick County south of Wichita. This station is on the grounds of a local church about 3 mi from Interstate 35 and US Highway 81 and 2 mi from two sets of railroad tracks to the west and east.

[This page is intentionally blank.]

Appendix B: CSTS Earthquake Catalog 7/1/2020 – 6/30/2021

This catalog includes all earthquakes that were uniquely located and within 20 miles of a CSTS member facility.

Origin Time (UTC)	Latitude	Longitude	Magnitude
2020-07-04 23:07	37.6020	-97.7650	1.6
2020-07-29 06:08	38.0240	-97.9720	1.8
2020-07-31 10:07	37.5480	-97.7370	1.4
2020-08-02 19:06	37.6100	-97.7450	1.4
2020-08-02 20:41	37.6250	-97.7430	1.1
2020-08-03 15:32	38.0190	-97.9840	2.3
2020-08-09 06:55	38.5680	-97.6120	1.4
2020-08-13 13:24	37.6450	-96.7310	2.3
2020-08-26 21:03	38.0380	-97.9940	0.9
2020-08-28 15:51	37.5990	-97.0380	1.9
2020-09-08 13:34	38.0220	-97.9820	0.7
2020-09-10 20:30	37.5420	-97.7800	1.4
2020-09-12 09:56	37.6140	-97.2120	0.9
2020-09-15 11:26	37.3030	-97.4190	1.2
2020-09-16 13:11	37.7860	-96.9260	1.0
2020-09-21 07:53	37.6460	-97.1010	1.2
2020-09-22 01:13	37.3590	-97.5310	1.9
2020-09-22 02:59	37.3980	-97.4940	1.2
2020-09-22 03:01	37.3890	-97.5080	1.1
2020-09-22 11:27	37.3940	-97.4860	1.2
2020-09-23 14:56	38.0160	-97.0650	1.5
2020-09-26 09:59	38.0320	-97.9760	0.9
2020-10-01 17:10	37.5437	-97.7803	1.5
2020-10-02 04:26	37.6538	-97.1013	0.9
2020-10-07 08:00	37.8852	-98.0999	1.1
2020-10-07 09:49	37.8858	-98.1039	1.3
2020-10-10 22:39	37.3310	-97.4160	1.5
2020-10-13 21:10	38.6149	-97.5522	1.5
2020-10-14 06:22	37.3670	-97.4158	1.3
2020-10-15 04:51	37.7379	-96.8500	1.7
2020-10-16 20:06	37.9988	-96.8748	1.7
2020-10-18 04:04	38.6061	-97.5684	1.2
2020-10-18 14:37	38.0128	-96.8725	2.2
2020-10-20 08:21	37.9831	-96.8817	1.3
2020-10-21 09:25	38.0033	-96.8707	2.5
2020-10-21 20:51	37.3205	-97.4455	1.6
2020-10-25 02:13	37.9956	-96.8829	1.6
2020-10-27 15:23	37.9958	-96.8950	3.0
2020-11-01 02:13	37.5748	-97.7508	1.5
2020-11-22 01:29	37.6503	-97.0769	1.4
2020-11-25 06:19	37.6968	-97.1307	1.1
2020-11-26 22:27	37.7128	-97.2134	2.7
2020-11-26 22:43	37.6922	-97.2112	1.7
2020-11-27 11:48	37.6977	-97.1950	1.3
2020-11-27 18:27	37.7134	-97.2154	2.6
2020-11-29 05:36	38.0000	-97.9973	1.0
2020-11-30 01:52	37.6990	-97.1273	1.5
2020-11-30 15:11	37.7039	-97.2081	2.3
2020-12-02 05:09	37.6888	-97.1221	0.9
2020-12-03 01:11	38.0021	-96.8812	1.5
2020-12-03 17:35	37.6478	-97.0786	1.1
2020-12-06 08:54	37.6404	-97.0763	0.9
2020-12-06 08:55	37.6373	-97.0741	1.3
2020-12-06 08:57	37.6354	-97.0743	1.1
2020-12-07 16:55	37.2987	-97.4645	2.4
2020-12-08 12:03	37.6363	-97.5906	1.7
2020-12-08 16:50	37.6431	-97.5812	1.3
2020-12-08 16:54	37.7069	-97.2231	3.2
2020-12-09 14:59	37.7061	-97.2123	2.5

Origin Time (UTC)	Latitude	Longitude	Magnitude
2020-12-10 08:34	37.7041	-97.2250	2.9
2020-12-10 13:36	37.7018	-97.2154	2.6
2020-12-12 01:31	37.6969	-97.2083	2.0
2020-12-12 11:13	37.6272	-97.5837	1.6
2020-12-13 17:26	37.6993	-97.2235	2.2
2020-12-14 22:43	37.6378	-97.5974	1.6
2020-12-16 17:09	37.6276	-97.2725	1.8
2020-12-18 11:28	37.7048	-97.2092	1.1
2020-12-19 17:42	37.7088	-97.2164	2.9
2020-12-19 18:40	37.7118	-97.2224	2.9
2020-12-19 18:47	37.7114	-97.2168	3.8
2020-12-19 18:52	37.7104	-97.2132	3.5
2020-12-19 19:18	37.7060	-97.2063	2.7
2020-12-19 21:12	37.7075	-97.2107	2.3
2020-12-20 02:39	37.7080	-97.2129	3.2
2020-12-20 07:08	37.6991	-97.2177	1.8
2020-12-20 08:20	37.7092	-97.2162	2.7
2020-12-20 08:39	37.7029	-97.2096	1.7
2020-12-20 09:49	37.7047	-97.2051	1.5
2020-12-20 15:04	37.6489	-97.5817	1.4
2020-12-20 16:39	37.6861	-97.1995	1.2
2020-12-20 21:20	37.6984	-97.2047	2.0
2020-12-20 22:38	37.3102	-97.4677	2.6
2020-12-20 23:23	37.6919	-97.1969	1.5
2020-12-21 04:38	37.7074	-97.1965	1.4
2020-12-21 07:25	37.3100	-97.4612	2.1
2020-12-21 21:29	37.6998	-97.2185	1.7
2020-12-22 14:41	37.6984	-97.2112	1.8
2020-12-22 18:18	37.7076	-97.2095	1.9
2020-12-23 09:42	37.7052	-97.2113	2.1
2020-12-24 09:20	37.4725	-97.7314	1.7
2020-12-25 04:24	37.7129	-97.2121	1.6
2020-12-28 10:19	37.7108	-97.2108	2.7
2020-12-29 05:14	37.7064	-97.2056	1.9
2020-12-30 06:14	38.0942	-97.5849	0.6
2020-12-30 11:04	37.7005	-97.2126	3.9
2020-12-30 11:23	37.7080	-97.2278	1.9
2020-12-30 14:47	37.6969	-97.2086	1.9
2020-12-31 04:52	37.7043	-97.2199	2.6
2020-12-31 07:53	37.7104	-97.2103	1.1
2020-12-31 18:54	37.7005	-97.2085	2.0
2021-01-01 22:36	37.6950	-97.2010	1.1
2021-01-02 09:53	37.7060	-97.2100	1.2
2021-01-02 23:12	38.0060	-97.9930	1.1
2021-01-03 09:35	37.7190	-97.2220	1.0
2021-01-04 03:09	37.6990	-97.2050	1.0
2021-01-04 03:55	37.6840	-97.1160	1.1
2021-01-04 03:58	37.6830	-97.2130	0.9
2021-01-04 04:38	37.6880	-97.1920	1.0
2021-01-04 05:45	37.7060	-97.2200	1.2
2021-01-04 05:52	37.7020	-97.2090	1.4
2021-01-04 06:51	37.7050	-97.2140	2.2
2021-01-04 06:56	37.7020	-97.2160	1.6
2021-01-04 07:04	37.7050	-97.2250	1.5
2021-01-04 07:17	37.6980	-97.2120	1.3
2021-01-04 07:48	37.7010	-97.2140	1.6
2021-01-05 12:53	37.7610	-97.1840	1.3
2021-01-06 03:00	37.7100	-97.1990	1.8
2021-01-06 09:57	38.5920	-97.4820	1.3

Appendix B. Continued

Origin Time (UTC)	Latitude	Longitude	Magnitude
2021-01-08 00:50	37.3180	-97.4750	1.5
2021-01-09 10:10	37.3250	-97.4380	1.5
2021-01-09 13:50	37.7030	-97.2140	1.1
2021-01-10 03:29	38.2410	-97.4940	1.0
2021-01-10 05:07	37.3070	-97.4750	1.8
2021-01-10 06:52	37.3090	-97.4670	2.9
2021-01-10 07:06	37.3280	-97.4350	1.3
2021-01-10 07:07	37.3210	-97.4480	1.5
2021-01-10 11:28	37.3330	-97.4160	1.4
2021-01-10 11:34	37.3180	-97.4480	1.4
2021-01-10 16:32	37.3290	-97.4230	1.5
2021-01-10 22:53	37.3160	-97.4640	2.7
2021-01-11 08:29	37.3110	-97.4640	2.4
2021-01-11 08:36	37.3360	-97.4200	1.5
2021-01-11 11:33	37.3240	-97.4430	1.4
2021-01-11 18:52	37.3300	-97.4100	1.6
2021-01-11 20:23	37.3170	-97.4570	2.7
2021-01-12 02:33	37.3090	-97.4680	2.2
2021-01-12 03:31	37.3210	-97.4560	1.7
2021-01-12 04:06	37.3110	-97.4650	1.7
2021-01-12 08:11	37.3170	-97.4510	1.4
2021-01-14 22:21	37.7110	-97.2310	1.3
2021-01-14 22:23	37.7060	-97.2220	0.7
2021-01-16 07:27	37.7160	-97.2220	1.3
2021-01-16 20:34	37.6140	-97.1120	1.5
2021-01-17 04:38	37.4710	-97.7550	1.7
2021-01-18 22:20	37.6980	-97.1960	1.4
2021-01-20 05:29	37.6930	-97.2010	0.9
2021-01-21 01:16	38.5640	-97.5130	1.4
2021-01-21 20:45	37.7730	-96.8960	1.3
2021-01-23 09:31	38.5860	-97.4800	1.5
2021-01-24 09:47	37.3220	-97.4430	1.8
2021-01-25 19:06	37.7040	-97.1330	1.7
2021-01-29 10:29	37.3260	-97.4400	1.6
2021-01-30 01:33	37.6190	-97.1040	1.6
2021-02-05 11:52	37.7100	-97.2170	1.2
2021-02-06 00:58	37.6430	-97.5830	1.3
2021-02-09 03:01	37.7150	-97.2280	1.3
2021-02-10 08:24	37.7070	-97.1980	1.3
2021-02-12 02:54	38.4110	-97.4360	0.9
2021-02-15 19:02	38.0070	-97.9960	2.7
2021-02-15 20:57	37.7030	-97.2090	1.6
2021-02-18 14:18	38.0200	-97.9940	1.5
2021-02-25 20:54	37.6400	-97.2580	1.4
2021-02-26 04:49	37.6360	-97.2530	1.1
2021-02-28 09:20	37.6430	-97.5890	1.6
2021-03-04 12:22	37.7150	-97.2250	1.8
2021-03-11 23:31	37.5340	-97.7720	1.6
2021-03-12 04:48	37.7130	-97.1880	1.3
2021-03-14 11:29	37.6980	-97.2170	3.5
2021-03-14 11:31	37.7100	-97.2270	3.7
2021-03-14 12:02	37.7170	-97.2150	3.2
2021-03-14 12:30	37.6950	-97.2480	0.9
2021-03-14 13:30	37.7150	-97.2340	2.2
2021-03-14 23:08	37.7090	-97.2160	3.9
2021-03-14 23:17	37.7110	-97.2000	1.5
2021-03-15 03:01	37.7060	-97.2440	1.8
2021-03-15 05:29	37.7120	-97.2310	2.5
2021-03-15 08:05	37.6880	-97.1950	1.4
2021-03-15 09:39	37.6140	-97.7800	1.1
2021-03-15 09:50	37.6300	-97.7720	1.6
2021-03-15 11:28	37.7210	-97.2270	1.3

Origin Time (UTC)	Latitude	Longitude	Magnitude
2021-03-15 13:52	37.7090	-97.2320	3.3
2021-03-15 13:59	37.7000	-97.2330	3.5
2021-03-16 06:32	37.7150	-97.2180	1.8
2021-03-16 13:30	37.7060	-97.2310	1.3
2021-03-16 19:27	37.7070	-97.2180	1.3
2021-03-16 21:17	37.6990	-97.2240	2.3
2021-03-17 16:03	37.7020	-97.2110	1.8
2021-03-17 23:06	37.7040	-97.2210	1.8
2021-03-19 04:16	38.0090	-97.9810	1.3
2021-03-19 05:38	37.7220	-97.2330	1.5
2021-03-20 02:38	37.7040	-97.2380	1.2
2021-03-21 15:00	37.7240	-97.2270	1.9
2021-03-22 06:04	37.6980	-97.2440	1.3
2021-03-23 13:09	37.7050	-97.2150	1.4
2021-03-23 16:40	37.7120	-97.2190	1.4
2021-03-24 03:58	37.7080	-97.1380	1.3
2021-03-24 14:35	37.6960	-97.2260	1.3
2021-03-25 16:26	37.7000	-97.2280	1.1
2021-03-25 16:31	37.6850	-97.2000	1.2
2021-03-25 19:49	37.6940	-97.2280	1.4
2021-03-28 22:01	37.7170	-97.2260	1.2
2021-03-29 03:02	37.3190	-97.4560	2.2
2021-03-29 03:20	37.5980	-97.7770	1.5
2021-03-29 03:57	37.3190	-97.4440	1.2
2021-03-30 17:38	37.6880	-97.1760	1.8
2021-04-02 05:39	37.6080	-97.2120	2.3
2021-04-02 08:25	37.6060	-97.1920	1.7
2021-04-02 17:16	37.6180	-97.2030	1.9
2021-04-05 02:08	37.7110	-97.2200	1.0
2021-04-05 16:26	37.6090	-97.2020	2.0
2021-04-05 17:10	37.6450	-97.2160	1.2
2021-04-05 17:24	37.7050	-97.2260	1.8
2021-04-07 06:06	37.7120	-97.2230	1.4
2021-04-08 06:55	37.7130	-97.2310	1.2
2021-04-08 06:57	37.6990	-97.2300	1.1
2021-04-10 05:26	38.5970	-97.5450	1.6
2021-04-10 15:17	37.7130	-97.2600	1.5
2021-04-11 01:11	38.6070	-97.5750	1.5
2021-04-11 10:41	38.5180	-97.5470	1.4
2021-04-12 09:17	37.4320	-97.3750	1.4
2021-04-13 06:03	37.7000	-97.2320	1.0
2021-04-13 16:11	37.7070	-97.2100	1.2
2021-04-14 07:38	38.6190	-97.5790	1.8
2021-04-15 13:30	37.4170	-97.3860	2.3
2021-04-23 17:33	37.5980	-97.1890	1.4
2021-04-23 17:35	37.5980	-97.1950	1.4
2021-04-23 18:27	37.6080	-97.1980	1.4
2021-04-23 18:44	37.5970	-97.1980	1.6
2021-04-25 03:46	37.7060	-97.2340	1.9
2021-04-25 12:52	37.7000	-97.2130	1.3
2021-04-30 07:19	37.7010	-97.2260	1.4
2021-05-01 03:53	37.3020	-97.4000	1.6
2021-05-05 08:46	37.6980	-97.1950	1.2
2021-05-09 22:51	37.7020	-97.2310	1.6
2021-05-09 23:04	37.6920	-97.2160	1.6
2021-05-12 17:08	37.7120	-97.2000	1.6
2021-05-14 02:19	37.6950	-97.1980	1.3
2021-05-15 03:34	37.7070	-97.2340	1.0
2021-05-16 05:25	37.6840	-97.1880	1.3
2021-05-16 09:21	37.6060	-97.1970	1.2
2021-05-21 00:23	38.0250	-97.9690	1.4
2021-05-22 03:10	37.7040	-97.2321	1.5

Appendix B. Continued

Origin Time (UTC)	Latitude	Longitude	Magnitude
2021-05-26 05:57	37.7110	-97.2130	1.7
2021-05-30 00:38	37.6470	-97.0830	1.8
2021-06-02 09:01	37.3060	-97.4180	1.7
2021-06-02 09:13	37.3100	-97.3950	0.9
2021-06-07 02:34	37.7080	-97.1960	1.4
2021-06-07 20:23	37.5900	-97.0300	1.4
2021-06-10 02:54	37.7040	-97.2130	1.4
2021-06-10 04:16	37.6950	-97.2070	1.1
2021-06-10 07:03	37.7150	-97.2080	2.0
2021-06-10 07:43	37.7000	-97.2040	1.3
2021-06-10 09:35	37.7070	-97.1990	1.3
2021-06-10 11:02	37.7200	-97.2150	1.3
2021-06-10 11:31	37.7140	-97.2180	2.2
2021-06-10 12:20	37.7290	-97.1910	1.4
2021-06-10 12:41	37.6950	-97.1740	1.4
2021-06-10 14:21	37.7110	-97.2040	1.7
2021-06-10 15:59	37.6970	-97.2050	1.3
2021-06-10 16:08	38.2500	-97.4830	1.7
2021-06-11 01:10	37.6990	-97.2070	1.5
2021-06-11 02:42	38.2460	-97.4950	1.7
2021-06-11 19:10	37.6950	-97.1960	1.7
2021-06-12 15:33	37.7120	-97.2140	1.5
2021-06-12 23:02	38.5470	-97.5200	1.5
2021-06-13 03:31	37.6910	-97.2670	1.4
2021-06-16 04:54	37.3320	-97.5030	1.0
2021-06-16 05:00	37.6870	-96.8020	1.5
2021-06-16 05:04	37.6910	-96.8210	1.1
2021-06-16 05:06	37.3300	-97.5210	1.0
2021-06-16 05:29	37.7000	-96.8260	2.1
2021-06-16 07:59	37.6970	-96.8050	1.4
2021-06-22 11:55	37.7010	-97.2280	0.9
2021-06-23 15:43	37.6980	-97.2320	2.3
2021-06-25 11:11	37.6820	-97.2220	1.1
2021-06-25 11:13	37.6810	-97.2180	1.1
2021-06-25 11:15	37.6920	-97.2400	1.6
2021-06-25 11:20	37.6980	-97.2440	1.6
2021-06-25 12:02	37.6900	-97.2280	1.5
2021-06-25 13:02	37.6600	-97.2750	1.3
2021-06-25 13:10	37.7000	-97.2240	1.3
2021-06-25 13:14	37.6960	-97.2290	1.6
2021-06-29 10:45	37.4100	-97.6160	1.2

End of table

[This page is intentionally blank.]

Appendix C: Subnetwork Events Catalog

Subnetwork events recorded from July 1, 2020, to June 30, 2021, with epicentral distance within 12 miles of member wells. Epicentral distance is the estimated distance from the earthquake epicenter to the seismic station where it was recorded.

Station	Origin Time (UTC)	Distance (mi)	Magnitude
BU02	2020-10-19 05:03:54	11.1	0.2
BU02	2020-10-20 02:58:46	10.8	0.0
BU02	2020-10-20 08:21:27	10.9	1.0
BU02	2020-10-21 11:28:43	11.1	0.2
BU02	2020-10-21 22:27:11	10.2	0.0
BU02	2020-10-24 17:26:19	10.6	0.1
BU02	2020-11-01 09:40:58	11.2	0.1
BU02	2020-11-23 13:25:40	11.4	0.2
BU02	2021-01-30 12:00:32	4.7	-0.6
BU02	2021-02-05 12:14:33	11.0	0.0
BU02	2021-02-25 17:31:06	3.8	-0.9
BU02	2021-05-15 06:47:09	2.5	-0.6
BU02	2021-05-15 08:06:37	3.8	-0.6
BU02	2021-05-25 19:01:00	10.2	0.4
BU02	2021-05-30 07:47:42	2.4	-0.9
BU02	2021-06-15 01:38:34	2.7	-0.9
EW01	2020-08-22 10:47:59	2.8	-0.6
EW01	2020-10-07 05:53:00	11.4	0.2
EW01	2020-10-23 11:17:10	7.7	-0.4
EW01	2021-01-02 19:28:58	2.5	-1.5
EW01	2021-01-02 20:35:32	2.9	-1.5
EW01	2021-01-08 09:40:26	7.3	0.4
EW01	2021-01-12 20:51:25	4.3	-0.9
EW01	2021-01-27 17:28:15	3.5	-0.9
EW01	2021-01-29 16:51:17	2.6	-0.9
EW01	2021-02-01 12:32:49	5.7	-0.6
EW01	2021-03-02 16:28:24	4.2	-0.6
EW01	2021-03-04 16:29:53	2.9	-1.5
EW01	2021-03-18 17:14:39	2.7	-1.5
EW01	2021-05-02 04:03:49	8.4	-0.6
EW01	2021-05-02 17:16:28	4.6	-0.6
EW01	2021-05-14 09:58:15	6.9	-0.6
EW01	2021-05-30 12:36:31	4.4	-0.6
EW01	2021-06-01 13:36:56	2.4	-1.5
EW01	2021-06-08 01:24:54	2.6	-0.9
EW01	2021-06-17 03:33:16	9.1	0.4
JO01	2021-02-15 10:02:21	4.2	-0.6
JO01	2021-05-03 01:19:15	3.6	0.0
JO01	2021-06-20 22:50:42	4.4	0.0
JO01	2021-06-25 22:52:34	6.1	0.0
KE01	2020-07-30 06:32:23	2.9	-1.5
KE01	2020-07-30 06:35:27	2.7	-0.9
KW02	2021-04-03 02:15:14	4.7	-0.6
MP01	2020-07-17 02:38:03	2.3	-0.6
MP01	2020-08-01 04:50:10	6.1	-0.9
MP01	2020-09-10 15:06:19	9.7	0.2
MP01	2020-09-16 11:25:16	4.4	-0.9
MP01	2020-09-18 00:44:29	6.1	-0.6
MP01	2020-10-15 23:40:00	8.8	-0.2
MP01	2020-10-18 00:06:47	4.0	-0.4
MP01	2020-11-17 23:12:32	8.1	0.1
MP01	2020-12-04 08:30:02	2.9	-0.6
MP01	2020-12-06 05:02:38	3.2	-0.9
MP01	2020-12-08 01:21:28	1.9	-0.9
MP01	2020-12-14 01:41:04	3.9	-0.4
MP01	2021-01-20 00:27:21	6.1	-0.4
MP01	2021-01-25 13:08:40	3.5	-0.9
MP01	2021-02-11 04:00:55	3.0	-1.5
MP01	2021-02-12 06:22:22	3.3	-0.9
MP01	2021-02-12 10:30:49	3.4	-0.9
MP01	2021-02-12 10:42:10	3.1	-0.9
MP01	2021-02-12 12:34:03	3.3	-0.9
MP01	2021-02-13 01:12:19	2.1	-0.9
MP01	2021-02-14 00:48:01	2.3	-0.9
MP01	2021-03-26 16:48:50	6.9	-0.6
MP01	2021-03-27 06:34:34	4.7	-0.9
MP01	2021-04-04 01:12:04	1.4	-1.5
MP01	2021-04-07 06:01:00	5.6	-0.6
MP01	2021-04-11 14:24:52	2.0	-1.5
MP01	2021-04-18 00:25:42	9.3	-0.4
MP01	2021-04-22 00:05:24	2.4	-0.9
MP01	2021-04-28 18:24:58	4.2	-0.9
MP01	2021-05-01 01:43:35	3.2	-0.6
MP01	2021-05-03 01:35:26	1.8	-0.9
MP01	2021-05-03 02:39:57	7.8	0.4
MP01	2021-05-04 15:47:03	5.6	0.1
MP01	2021-05-11 08:44:23	2.1	-0.9
MP01	2021-05-11 15:44:29	5.3	-0.6
MP01	2021-06-19 06:04:33	7.2	-0.6
MP01	2021-06-26 19:05:15	11.4	0.2
MP02	2020-09-09 07:56:59	10.7	0.4
MP02	2020-09-09 14:22:12	3.0	-0.9
MP02	2020-09-10 09:52:11	3.9	-0.6
MP02	2020-09-13 21:05:36	2.5	-0.9
MP02	2020-09-18 22:02:02	5.5	-0.9
MP02	2020-10-06 16:14:51	5.5	-0.4
MP02	2020-10-30 08:19:14	7.0	-0.4
MP02	2020-11-02 07:03:25	4.3	-0.9
MP02	2020-11-21 00:04:51	4.1	-0.9
MP02	2020-12-06 21:23:25	1.8	-1.5
MP02	2021-01-13 08:58:33	2.6	-0.6
MP02	2021-01-23 20:09:54	7.9	-0.6
MP02	2021-01-27 10:48:49	2.4	-1.5
MP02	2021-02-01 21:57:11	4.2	-0.9
MP02	2021-02-07 08:37:55	5.6	-0.4
MP02	2021-02-19 09:08:10	4.0	-0.6
MP02	2021-03-21 02:22:29	6.1	-0.2
MP02	2021-03-25 11:11:01	1.9	-1.5
MP02	2021-03-25 11:12:18	2.5	-1.5
MP02	2021-04-04 20:12:04	9.0	-0.2
MP02	2021-04-07 06:04:41	3.6	-0.9
MP02	2021-04-09 04:50:49	2.4	-0.9
MP02	2021-04-11 08:48:47	8.9	0.0
MP02	2021-04-11 08:55:26	12.0	0.0
MP02	2021-04-11 08:55:41	10.2	-0.2
MP02	2021-04-11 08:57:17	8.7	-0.2
MP02	2021-04-11 09:04:37	9.3	-0.2
MP02	2021-04-14 00:54:41	8.6	0.2
MP02	2021-04-17 01:15:21	3.9	-0.9
MP02	2021-04-17 22:52:25	3.1	-1.5

Appendix C. Continued

Station	Origin Time (UTC)	Distance (mi)	Magnitude
MP02	2021-04-20 00:40:36	7.9	0.0
MP02	2021-04-21 06:33:49	8.2	-0.6
MP02	2021-04-22 08:00:36	2.2	-1.5
MP02	2021-04-28 05:04:09	5.5	-0.9
MP02	2021-04-28 13:39:07	1.2	-1.5
MP02	2021-04-30 21:46:29	10.1	-0.4
MP02	2021-05-03 15:23:23	6.5	-0.6
MP02	2021-05-16 16:42:00	4.4	-0.4
MP02	2021-05-17 02:28:47	10.8	0.1
MP02	2021-05-17 04:06:44	8.9	-0.4
MP02	2021-05-30 16:30:16	2.6	-0.9
MP02	2021-05-31 05:35:54	3.9	0.1
MP02	2021-06-08 02:27:02	4.8	-0.2
MP02	2021-06-08 04:21:52	10.1	-0.4
MP02	2021-06-10 13:30:10	2.4	-0.9
MP02	2021-06-24 10:28:34	3.7	-0.2
MP02	2021-06-25 08:05:04	2.9	-0.4
RC02	2020-07-12 02:17:40	3.6	0.3
RC02	2020-07-22 10:20:34	5.0	0.5
RC02	2020-09-03 02:20:09	4.3	-0.9
RC02	2020-10-10 07:13:03	2.3	-0.6
RC02	2020-10-17 22:55:47	6.8	0.4
RC02	2020-10-18 00:53:06	4.9	-0.4
RC02	2020-10-24 11:39:10	6.7	-0.2
RC02	2020-10-27 16:23:03	4.6	-0.4
RC02	2020-11-12 00:29:38	5.1	-0.6
RC02	2020-11-26 22:00:47	1.4	-1.5
RC02	2021-01-01 21:37:45	4.4	-0.6
RC02	2021-02-12 23:20:10	1.9	-0.9
RC02	2021-02-12 23:35:18	2.2	-1.5
RC02	2021-02-13 01:00:26	2.8	-0.4
RC02	2021-02-16 06:40:45	10.7	0.5
RC02	2021-02-20 13:06:21	3.3	-0.2
RC02	2021-04-07 05:23:18	1.4	-0.9
RC02	2021-04-07 05:35:54	4.2	-0.6
RC02	2021-04-07 05:36:37	4.6	-0.4
RC02	2021-04-07 05:37:43	4.1	-0.6
RC02	2021-04-15 07:24:07	2.5	-1.5
RC02	2021-04-16 05:53:27	1.6	-0.9
RC02	2021-04-30 09:40:09	2.7	-0.9
RC02	2021-05-05 05:28:54	7.1	-0.4
RC02	2021-05-10 09:49:47	2.9	-0.9
RC02	2021-05-11 06:36:43	4.9	-0.9
RC02	2021-05-13 09:48:17	3.9	-0.9
RC02	2021-05-30 05:17:50	9.2	-0.4
RC02	2021-05-30 15:16:48	3.6	-0.6
RC02	2021-05-30 15:16:48	3.6	-0.4
RC02	2021-05-30 15:16:48	3.3	-0.4
RC02	2021-05-31 07:02:44	8.6	0.2
RC02	2021-06-01 22:03:01	4.1	-0.6
RC02	2021-06-01 23:06:18	6.0	-0.6
RC02	2021-06-04 17:23:09	6.7	-0.4
RC02	2021-06-12 03:37:10	3.3	-0.9
RC02	2021-06-12 12:50:00	3.0	-1.5
RC02	2021-06-15 14:43:18	5.9	0.1
RC02	2021-06-15 15:01:36	9.5	0.4
RC02	2021-06-21 07:11:40	10.2	0.1
RC02	2021-06-22 12:45:43	6.1	0.3
RC02	2021-06-24 09:21:12	4.6	0.1
RC02	2021-06-25 06:29:38	3.0	-0.6

Station	Origin Time (UTC)	Distance (mi)	Magnitude
RC02	2021-06-26 03:52:08	3.0	0.0
RC02	2021-06-26 19:35:35	9.5	0.3
RC03	2020-07-09 10:28:24	6.9	-0.4
RC03	2020-07-11 02:20:08	6.9	-0.4
RC03	2020-07-11 02:20:28	7.5	0.0
RC03	2020-07-11 02:20:58	7.2	0.0
RC03	2020-07-11 02:21:21	7.2	-0.2
RC03	2020-07-12 17:43:33	4.4	-0.6
RC03	2020-07-13 04:24:24	3.3	-0.6
RC03	2020-07-13 04:24:24	3.6	-0.6
RC03	2020-07-13 18:21:45	7.7	0.0
RC03	2020-07-15 02:01:56	7.3	-0.4
RC03	2020-07-15 02:02:32	7.4	-0.2
RC03	2020-07-15 02:03:15	7.4	-0.2
RC03	2020-07-15 02:03:51	7.2	-0.4
RC03	2020-07-15 08:25:06	3.3	-0.9
RC03	2020-07-17 18:20:30	7.4	-0.4
RC03	2020-07-17 18:20:45	7.0	-0.2
RC03	2020-07-17 18:22:20	5.1	-0.4
RC03	2020-07-20 23:07:29	7.7	-0.2
RC03	2020-07-22 10:18:34	7.5	-0.2
RC03	2020-07-23 10:24:03	5.2	-0.2
RC03	2020-07-23 10:25:16	8.7	0.9
RC03	2020-07-24 10:28:47	7.4	-0.4
RC03	2020-07-25 02:10:27	6.7	-0.2
RC03	2020-07-25 02:11:42	7.1	-0.2
RC03	2020-07-25 02:12:52	7.2	-0.2
RC03	2020-07-28 02:22:57	7.2	-0.2
RC03	2020-07-28 02:23:46	7.0	-0.2
RC03	2020-07-28 18:22:52	7.2	0.0
RC03	2020-07-28 18:23:41	5.5	-0.4
RC03	2020-07-29 02:23:37	7.3	-0.2
RC03	2020-07-29 02:24:24	7.6	-0.2
RC03	2020-07-29 02:25:12	7.2	-0.4
RC03	2020-07-29 02:25:50	7.3	-0.4
RC03	2020-07-30 10:10:49	6.9	-0.2
RC03	2020-07-31 02:21:52	6.9	-0.2
RC03	2020-07-31 02:22:34	7.6	-0.2
RC03	2020-07-31 18:15:55	7.3	-0.4
RC03	2020-07-31 18:16:42	5.7	-0.4
RC03	2020-08-01 03:40:44	2.5	-0.9
RC03	2020-08-03 18:12:44	7.2	-0.2
RC03	2020-08-03 18:15:26	7.2	0.2
RC03	2020-08-05 10:23:32	7.5	-0.4
RC03	2020-08-05 10:24:29	7.0	-0.2
RC03	2020-08-06 02:10:15	7.5	-0.2
RC03	2020-08-07 02:13:11	6.8	-0.4
RC03	2020-08-07 02:22:41	7.2	-0.4
RC03	2020-08-07 02:22:58	7.2	-0.4
RC03	2020-08-12 10:27:03	7.0	-0.4
RC03	2020-08-13 02:20:58	7.1	-0.2
RC03	2020-08-13 18:24:02	7.4	-0.4
RC03	2020-08-13 18:24:45	6.9	-0.2
RC03	2020-08-13 18:25:30	7.0	-0.2
RC03	2020-08-14 10:24:43	7.2	-0.4
RC03	2020-08-14 10:25:10	7.6	-0.2
RC03	2020-08-14 18:21:21	9.5	-0.4
RC03	2020-08-19 02:22:02	8.7	-0.2
RC03	2020-08-19 02:22:38	7.8	-0.4
RC03	2020-08-19 02:25:05	7.1	-0.4

Appendix C. Continued

Station	Origin Time (UTC)	Distance (mi)	Magnitude
RC03	2020-08-20 00:54:42	7.1	-0.4
RC03	2020-08-20 00:55:35	6.9	-0.2
RC03	2020-08-22 02:20:24	6.9	-0.4
RC03	2020-08-22 02:21:04	7.4	-0.2
RC03	2020-08-22 02:21:51	7.5	0.0
RC03	2020-09-25 02:22:36	7.6	-0.4
RC03	2020-09-25 02:23:39	6.7	-0.2
RC03	2020-09-26 04:02:45	7.0	-0.2
RC03	2020-09-28 10:11:43	6.8	-0.2
RC03	2020-09-29 10:20:24	9.3	-0.2
RC03	2020-09-29 10:21:11	7.3	-0.4
RC03	2020-09-29 16:38:16	7.2	-0.4
RC03	2020-09-30 02:24:04	7.3	-0.2
RC03	2020-09-30 18:21:59	6.6	-0.4
RC03	2020-09-30 18:23:03	6.9	-0.4
RC03	2020-10-02 02:25:53	7.2	0.1
RC03	2020-10-02 02:26:43	7.4	0.0
RC03	2020-10-02 18:20:56	7.2	-0.4
RC03	2020-10-05 18:12:18	6.8	-0.4
RC03	2020-10-06 02:23:34	7.0	0.1
RC03	2020-10-06 02:24:21	7.8	0.0
RC03	2020-10-06 10:10:04	7.3	-0.2
RC03	2020-10-06 10:13:19	6.6	-0.2
RC03	2020-10-07 10:22:40	6.9	0.0
RC03	2020-10-07 18:02:51	7.1	-0.2
RC03	2020-10-07 18:03:39	7.3	-0.4
RC03	2020-10-07 18:05:03	7.4	-0.2
RC03	2020-10-09 02:22:12	6.9	-0.4
RC03	2020-10-09 02:23:02	7.2	-0.2
RC03	2020-10-10 02:17:28	7.0	-0.4
RC03	2020-10-10 02:19:12	7.0	-0.4
RC03	2020-10-10 02:20:09	7.0	-0.4
RC03	2020-10-11 00:32:14	7.3	-0.4
RC03	2020-10-11 02:20:23	7.0	-0.2
RC03	2020-10-11 02:23:44	6.4	-0.4
RC03	2020-10-12 18:27:50	6.9	-0.4
RC03	2020-10-12 18:29:52	6.9	-0.2
RC03	2020-10-12 18:30:45	7.5	-0.4
RC03	2020-10-13 10:24:40	7.1	-0.2
RC03	2020-10-13 10:25:01	6.8	-0.4
RC03	2020-10-13 18:08:26	10.9	-0.2
RC03	2020-10-13 18:10:02	7.0	-0.2
RC03	2020-10-13 18:26:58	7.1	-0.2
RC03	2020-10-13 18:26:58	6.9	-0.2
RC03	2020-10-13 23:34:56	2.0	-1.5
RC03	2020-10-13 23:35:39	2.1	-0.9
RC03	2020-10-13 23:38:02	2.1	-1.5
RC03	2020-10-13 23:39:56	2.9	-1.5
RC03	2020-10-14 10:19:17	6.9	-0.4
RC03	2020-10-14 10:20:28	7.2	-0.4
RC03	2020-10-16 02:31:27	7.1	-0.4
RC03	2020-10-16 18:28:57	6.5	-0.2
RC03	2020-10-16 18:29:56	7.2	-0.2
RC03	2020-10-19 18:26:51	7.0	-0.2
RC03	2020-10-19 18:28:05	6.7	-0.4
RC03	2020-10-19 23:14:23	6.9	0.0
RC03	2020-10-20 10:04:27	6.9	0.2
RC03	2020-10-20 17:44:57	6.8	-0.4
RC03	2020-10-21 02:23:28	6.7	-0.2
RC03	2020-10-21 23:26:33	7.1	-0.2

Station	Origin Time (UTC)	Distance (mi)	Magnitude
RC03	2020-10-21 23:27:05	7.1	-0.4
RC03	2020-10-23 09:56:22	6.7	-0.4
RC03	2020-10-23 10:13:26	6.9	-0.4
RC03	2020-10-23 10:15:05	6.6	-0.4
RC03	2020-10-23 18:20:07	6.6	-0.4
RC03	2020-10-23 23:52:26	6.9	-0.2
RC03	2020-10-24 21:30:02	7.2	-0.2
RC03	2020-10-25 01:31:00	7.4	-0.2
RC03	2020-10-27 02:12:16	7.2	-0.4
RC03	2020-10-27 02:16:06	7.2	-0.4
RC03	2020-10-27 02:16:51	6.6	-0.4
RC03	2020-10-27 08:22:20	7.3	-0.4
RC03	2020-10-27 09:45:37	6.4	-0.4
RC03	2020-10-28 02:21:35	7.1	-0.2
RC03	2020-10-28 02:33:39	6.9	0.4
RC03	2020-10-29 02:20:53	6.9	-0.2
RC03	2020-10-29 02:21:39	6.3	-0.2
RC03	2020-10-29 09:36:35	7.2	-0.4
RC03	2020-10-29 10:11:17	7.4	-0.4
RC03	2020-10-30 09:15:23	7.1	0.0
RC03	2020-11-02 11:19:45	6.6	0.1
RC03	2020-11-02 11:20:21	7.1	-0.2
RC03	2020-11-02 19:07:28	7.0	0.0
RC03	2020-11-02 19:08:28	6.8	-0.2
RC03	2020-11-03 11:21:41	6.9	-0.4
RC03	2020-11-03 11:22:12	6.9	-0.4
RC03	2020-11-03 11:24:14	7.2	-0.4
RC03	2020-11-04 10:45:46	7.0	-0.2
RC03	2020-11-04 11:21:01	7.2	-0.2
RC03	2020-11-04 11:21:01	6.9	-0.4
RC03	2020-11-04 11:21:28	6.7	-0.4
RC03	2020-11-04 11:23:28	7.3	-0.6
RC03	2020-11-04 23:38:59	1.7	-1.5
RC03	2020-11-05 02:26:42	10.4	0.0
RC03	2020-11-05 16:13:16	6.6	-0.4
RC03	2020-11-05 19:09:52	6.9	-0.4
RC03	2020-11-05 19:10:34	7.1	-0.4
RC03	2020-11-06 03:12:00	6.9	-0.4
RC03	2020-11-06 03:12:27	6.8	-0.4
RC03	2020-11-07 03:25:18	6.9	-0.4
RC03	2020-11-07 03:25:25	6.3	-0.4
RC03	2020-11-09 10:37:01	7.0	-0.4
RC03	2020-11-09 10:37:55	6.6	-0.4
RC03	2020-11-10 03:22:58	7.0	-0.4
RC03	2020-11-10 03:24:33	6.6	-0.4
RC03	2020-11-10 05:16:25	2.1	-0.9
RC03	2020-11-10 19:13:55	7.3	-0.6
RC03	2020-11-12 11:14:07	10.6	-0.2
RC03	2020-11-13 11:15:55	7.5	-0.4
RC03	2020-11-13 19:14:40	7.2	-0.4
RC03	2020-11-14 09:48:51	9.7	-0.2
RC03	2020-11-14 11:26:56	7.1	-0.4
RC03	2020-11-14 11:27:12	7.2	-0.6
RC03	2020-11-19 10:44:14	2.5	-0.9
RC03	2020-11-19 10:44:45	6.9	-0.2
RC03	2020-11-19 19:22:30	6.8	-0.2
RC03	2020-11-19 19:23:18	6.8	-0.2
RC03	2020-11-19 23:40:56	1.8	-1.5
RC03	2020-11-19 23:41:16	1.5	-1.5
RC03	2020-11-19 23:41:55	1.4	-1.5

Appendix C. Continued

Station	Origin Time (UTC)	Distance (mi)	Magnitude
RC03	2020-11-19 23:42:44	1.4	-0.9
RC03	2020-11-20 11:18:53	5.9	-0.4
RC03	2020-11-21 03:19:40	7.4	-0.4
RC03	2020-11-24 07:49:37	2.6	-0.2
RC03	2020-11-25 11:13:17	7.0	-0.4
RC03	2020-11-26 00:21:29	7.0	-0.2
RC03	2020-11-30 19:18:39	6.9	-0.4
RC03	2020-11-30 19:19:29	7.0	-0.2
RC03	2020-12-01 19:25:46	7.3	-0.4
RC03	2020-12-01 19:26:35	7.4	-0.4
RC03	2020-12-02 03:04:46	7.2	-0.2
RC03	2020-12-02 03:05:39	6.9	-0.4
RC03	2020-12-03 19:31:13	7.0	-0.4
RC03	2020-12-04 03:23:54	6.9	-0.4
RC03	2020-12-04 03:24:21	6.8	-0.4
RC03	2020-12-04 03:25:33	6.8	-0.4
RC03	2020-12-04 11:22:27	6.9	-0.4
RC03	2020-12-04 11:23:14	6.8	0.0
RC03	2020-12-04 11:24:54	6.3	-0.4
RC03	2020-12-05 10:00:01	7.1	-0.4
RC03	2020-12-05 10:00:41	7.1	-0.2
RC03	2020-12-05 10:01:20	6.8	-0.2
RC03	2020-12-07 19:29:59	6.6	-0.4
RC03	2020-12-11 08:03:29	6.7	-0.4
RC03	2020-12-11 11:09:54	6.6	-0.4
RC03	2020-12-11 11:10:34	7.3	-0.2
RC03	2020-12-14 11:11:50	7.0	-0.2
RC03	2020-12-14 11:12:15	7.2	-0.4
RC03	2020-12-15 08:14:21	6.8	-0.2
RC03	2020-12-15 11:07:13	6.5	-0.2
RC03	2020-12-16 03:23:59	6.9	-0.2
RC03	2020-12-16 19:33:43	7.3	-0.2
RC03	2020-12-16 19:34:44	7.2	0.0
RC03	2020-12-17 03:20:43	6.5	-0.4
RC03	2020-12-17 03:21:17	7.2	-0.2
RC03	2020-12-17 03:22:07	7.4	-0.4
RC03	2020-12-17 19:28:55	6.5	-0.4
RC03	2020-12-17 19:29:28	6.5	-0.2
RC03	2020-12-18 03:20:12	6.8	0.0
RC03	2020-12-21 11:12:05	6.9	-0.2
RC03	2020-12-22 03:30:05	6.7	-0.2
RC03	2020-12-22 03:31:07	6.8	-0.4
RC03	2020-12-22 09:54:55	7.0	-0.4
RC03	2020-12-23 03:17:34	7.0	-0.2
RC03	2020-12-31 03:21:45	6.5	-0.2
RC03	2020-12-31 03:22:20	7.4	0.0
RC03	2021-01-02 21:19:49	1.9	-1.5
RC03	2021-01-05 03:22:12	11.3	0.2
RC03	2021-01-05 10:59:52	6.5	0.2
RC03	2021-01-06 03:10:33	9.6	0.0
RC03	2021-01-06 11:07:12	6.9	-0.2
RC03	2021-01-06 11:07:46	6.6	0.1
RC03	2021-01-07 03:12:09	6.7	-0.4
RC03	2021-01-07 03:13:05	10.4	0.0
RC03	2021-01-07 19:24:19	6.7	0.0
RC03	2021-01-11 08:54:18	7.2	0.8
RC03	2021-01-12 18:56:43	7.7	0.0
RC03	2021-01-12 19:25:50	7.3	-0.4
RC03	2021-01-13 11:13:43	6.4	-0.4
RC03	2021-01-13 11:14:02	7.1	-0.2

Station	Origin Time (UTC)	Distance (mi)	Magnitude
RC03	2021-01-14 03:20:57	6.9	-0.4
RC03	2021-01-14 03:21:24	7.0	-0.4
RC03	2021-01-18 11:28:10	6.5	-0.4
RC03	2021-01-18 11:28:26	6.9	-0.4
RC03	2021-01-19 19:31:02	6.4	0.0
RC03	2021-01-19 19:31:37	6.5	-0.4
RC03	2021-01-19 19:32:25	6.8	-0.4
RC03	2021-01-19 19:34:06	7.1	-0.2
RC03	2021-01-21 02:58:22	7.1	-0.4
RC03	2021-01-21 02:58:37	6.8	-0.6
RC03	2021-01-21 03:00:20	6.1	-0.2
RC03	2021-01-22 03:08:13	7.1	-0.4
RC03	2021-01-22 03:09:00	6.8	-0.4
RC03	2021-01-22 03:10:24	7.0	-0.4
RC03	2021-01-22 03:11:07	7.2	-0.2
RC03	2021-01-22 11:11:25	7.8	0.0
RC03	2021-01-22 11:12:03	11.6	0.0
RC03	2021-01-23 03:01:55	7.0	-0.4
RC03	2021-01-24 18:02:21	2.4	-1.5
RC03	2021-01-24 22:50:48	1.7	-1.5
RC03	2021-01-24 22:51:45	2.4	-1.5
RC03	2021-01-25 01:35:34	4.3	-0.6
RC03	2021-01-25 19:31:01	7.0	-0.4
RC03	2021-01-25 19:31:39	7.5	-0.2
RC03	2021-01-26 19:28:02	7.2	-0.4
RC03	2021-01-26 19:29:19	6.9	-0.2
RC03	2021-01-26 19:30:33	7.3	-0.2
RC03	2021-01-27 11:21:11	6.1	-0.6
RC03	2021-01-27 11:21:28	7.5	-0.4
RC03	2021-01-27 23:21:55	2.2	-1.5
RC03	2021-01-27 23:23:43	2.2	-0.9
RC03	2021-01-27 23:31:02	2.5	-1.5
RC03	2021-01-28 03:25:43	6.8	-0.4
RC03	2021-01-28 03:26:05	6.5	-0.4
RC03	2021-01-28 03:28:46	7.0	-0.4
RC03	2021-01-29 03:15:50	6.4	-0.4
RC03	2021-01-29 03:16:19	7.7	0.0
RC03	2021-01-30 02:57:57	7.0	0.0
RC03	2021-01-30 02:58:54	6.5	-0.4
RC03	2021-02-01 11:26:42	7.1	0.0
RC03	2021-02-01 19:29:13	9.4	0.0
RC03	2021-02-02 11:23:06	6.8	-0.6
RC03	2021-02-02 19:25:34	6.9	-0.4
RC03	2021-02-02 19:26:16	6.3	-0.4
RC03	2021-02-03 03:26:04	7.2	0.0
RC03	2021-02-03 03:31:56	7.1	0.2
RC03	2021-02-03 19:13:18	7.1	-0.4
RC03	2021-02-03 19:14:19	6.6	-0.4
RC03	2021-02-05 03:22:05	7.6	-0.4
RC03	2021-02-05 11:13:58	5.8	-0.6
RC03	2021-02-05 11:14:32	7.2	-0.4
RC03	2021-02-10 01:38:45	10.1	-0.2
RC03	2021-02-10 01:38:46	8.7	-0.2
RC03	2021-02-10 07:45:51	7.2	-0.2
RC03	2021-02-10 19:31:16	6.6	-0.4
RC03	2021-02-10 19:32:20	6.8	-0.4
RC03	2021-02-12 02:32:10	7.0	-0.2
RC03	2021-02-12 02:33:01	6.4	0.1
RC03	2021-02-18 11:06:41	6.7	-0.4
RC03	2021-02-19 02:54:05	7.0	-0.2

Appendix C. Continued

Station	Origin Time (UTC)	Distance (mi)	Magnitude
RC03	2021-02-19 02:56:38	10.1	-0.2
RC03	2021-02-19 02:57:10	10.9	0.0
RC03	2021-02-20 03:12:09	6.0	-0.4
RC03	2021-02-20 09:22:32	2.3	-1.5
RC03	2021-02-20 12:35:57	1.9	-1.5
RC03	2021-02-20 13:21:39	3.2	-1.5
RC03	2021-02-23 03:28:08	7.5	0.1
RC03	2021-02-24 03:22:58	7.2	-0.2
RC03	2021-02-24 03:23:43	10.2	0.0
RC03	2021-02-24 19:32:00	7.3	-0.2
RC03	2021-02-24 19:32:50	7.1	-0.6
RC03	2021-02-24 19:36:01	6.6	-0.9
RC03	2021-02-25 11:03:38	10.6	-0.2
RC03	2021-02-25 11:04:01	7.0	-0.4
RC03	2021-02-25 11:20:12	6.8	-0.2
RC03	2021-02-25 11:20:32	6.7	-0.2
RC03	2021-02-26 01:11:11	6.7	-0.2
RC03	2021-02-26 01:11:55	7.6	0.1
RC03	2021-02-27 03:16:33	6.9	-0.2
RC03	2021-02-27 03:17:51	6.8	-0.4
RC03	2021-03-01 11:09:07	10.2	0.0
RC03	2021-03-01 11:16:18	7.7	-0.4
RC03	2021-03-01 11:16:56	6.6	-0.4
RC03	2021-03-02 02:42:44	6.9	-0.4
RC03	2021-03-02 03:23:40	7.5	0.0
RC03	2021-03-02 03:24:06	7.4	-0.4
RC03	2021-03-03 11:24:53	6.3	-0.6
RC03	2021-03-03 11:26:01	6.6	-0.2
RC03	2021-03-04 00:11:13	7.1	-0.4
RC03	2021-03-04 03:17:35	11.9	-0.2
RC03	2021-03-04 03:18:16	6.9	-0.4
RC03	2021-03-05 03:24:00	6.9	-0.4
RC03	2021-03-05 03:24:29	7.1	-0.4
RC03	2021-03-05 03:25:15	7.4	-0.4
RC03	2021-03-05 11:22:38	6.9	-0.6
RC03	2021-03-05 11:22:58	7.1	-0.6
RC03	2021-03-05 11:23:20	7.1	-0.4
RC03	2021-03-06 01:29:52	10.6	-0.4
RC03	2021-03-06 03:23:21	7.4	0.1
RC03	2021-03-08 06:57:53	7.5	0.3
RC03	2021-03-08 11:17:40	7.7	-0.2
RC03	2021-03-08 11:18:08	7.1	-0.4
RC03	2021-03-08 19:25:22	6.9	-0.2
RC03	2021-03-08 19:28:30	6.6	-0.2
RC03	2021-03-08 19:29:27	7.2	-0.4
RC03	2021-03-09 11:22:44	6.7	-0.4
RC03	2021-03-09 19:17:56	6.5	-0.4
RC03	2021-03-10 03:26:00	6.9	-0.2
RC03	2021-03-10 03:28:33	7.0	-0.4
RC03	2021-03-10 11:18:45	7.3	-0.4
RC03	2021-03-10 11:22:00	7.0	-0.2
RC03	2021-03-10 19:35:24	7.2	-0.4
RC03	2021-03-11 03:08:29	7.1	-0.4
RC03	2021-03-11 03:09:16	7.4	-0.2
RC03	2021-03-12 10:50:10	4.1	-0.9
RC03	2021-03-12 10:59:50	3.8	-0.9
RC03	2021-03-12 19:33:26	6.6	-0.6
RC03	2021-03-13 03:29:42	6.6	-0.2
RC03	2021-03-13 03:31:22	6.4	0.0
RC03	2021-03-15 09:38:01	7.0	0.0

Station	Origin Time (UTC)	Distance (mi)	Magnitude
RC03	2021-03-15 18:29:23	10.1	-0.2
RC03	2021-03-16 10:07:21	7.9	-0.2
RC03	2021-03-16 10:08:16	7.3	-0.2
RC03	2021-03-16 10:08:51	7.5	-0.2
RC03	2021-03-16 10:12:03	7.0	0.0
RC03	2021-03-16 18:33:35	9.6	-0.2
RC03	2021-03-16 18:34:33	6.4	-0.6
RC03	2021-03-17 10:08:38	6.7	-0.6
RC03	2021-03-17 10:09:28	7.2	-0.4
RC03	2021-03-18 00:11:36	7.3	-0.4
RC03	2021-03-19 02:24:25	8.1	0.0
RC03	2021-03-19 02:25:11	7.2	-0.2
RC03	2021-03-20 02:00:39	6.8	-0.4
RC03	2021-03-20 02:02:37	6.8	-0.2
RC03	2021-03-22 09:45:02	6.8	-0.2
RC03	2021-03-22 10:21:17	7.1	-0.2
RC03	2021-03-25 00:45:04	7.3	-0.6
RC03	2021-03-25 00:45:07	6.3	-0.6
RC03	2021-03-26 00:12:34	6.7	0.0
RC03	2021-03-26 00:13:30	7.3	-0.2
RC03	2021-03-26 02:24:05	6.9	-0.4
RC03	2021-03-27 00:13:08	6.6	-0.4
RC03	2021-03-27 00:13:42	6.5	-0.6
RC03	2021-03-31 02:21:56	7.0	0.0
RC03	2021-03-31 02:22:40	7.2	-0.2
RC03	2021-03-31 18:15:43	7.3	-0.4
RC03	2021-03-31 18:17:32	7.6	0.0
RC03	2021-04-06 10:30:53	6.8	-0.4
RC03	2021-04-06 18:22:01	7.0	-0.4
RC03	2021-04-06 18:22:58	6.8	-0.4
RC03	2021-04-06 18:23:37	7.4	-0.4
RC03	2021-04-07 10:13:33	7.0	-0.6
RC03	2021-04-07 10:14:03	7.0	-0.2
RC03	2021-04-09 00:36:15	7.8	-0.2
RC03	2021-04-09 03:43:25	7.7	-0.4
RC03	2021-04-09 10:20:32	7.1	-0.2
RC03	2021-04-09 10:21:08	7.0	-0.4
RC03	2021-04-13 02:24:51	7.3	0.0
RC03	2021-04-13 18:28:57	7.3	0.4
RC03	2021-04-14 19:45:23	7.1	-0.2
RC03	2021-04-15 02:23:53	6.5	0.6
RC03	2021-04-15 02:27:23	7.4	-0.6
RC03	2021-04-15 10:06:29	7.8	-0.2
RC03	2021-04-16 02:20:30	7.2	-0.4
RC03	2021-04-16 02:21:21	6.9	-0.2
RC03	2021-04-16 02:23:08	6.6	0.0
RC03	2021-04-16 18:17:47	6.8	-0.6
RC03	2021-04-16 18:18:20	5.9	-0.4
RC03	2021-04-16 18:27:03	7.4	-0.4
RC03	2021-04-19 10:09:01	7.2	-0.2
RC03	2021-04-19 10:10:31	7.2	-0.4
RC03	2021-04-20 02:15:35	6.8	-0.4
RC03	2021-04-20 10:19:16	5.7	-0.4
RC03	2021-04-20 10:19:36	6.8	-0.2
RC03	2021-04-21 02:11:47	6.5	-0.4
RC03	2021-04-21 02:12:27	7.4	0.0
RC03	2021-04-21 02:22:15	6.6	-0.4
RC03	2021-04-21 02:22:57	7.0	-0.4
RC03	2021-04-22 02:13:07	7.2	-0.4
RC03	2021-04-22 02:13:56	7.7	-0.2

Appendix C. Continued

Station	Origin Time (UTC)	Distance (mi)	Magnitude
RC03	2021-04-22 02:18:04	7.2	-0.4
RC03	2021-04-22 02:18:04	7.1	-0.2
RC03	2021-04-22 02:18:48	7.0	-0.4
RC03	2021-04-22 02:18:48	7.6	-0.2
RC03	2021-04-22 02:18:48	7.1	-0.2
RC03	2021-04-22 02:18:48	6.7	-0.6
RC03	2021-04-22 18:21:21	6.7	-0.4
RC03	2021-04-22 18:22:57	6.2	-0.4
RC03	2021-04-22 18:23:48	6.5	-0.4
RC03	2021-04-22 18:24:29	7.5	-0.2
RC03	2021-04-23 10:01:14	6.5	-0.4
RC03	2021-04-23 10:01:41	6.4	-0.4
RC03	2021-04-23 10:18:35	7.6	-0.4
RC03	2021-04-23 10:19:00	6.9	-0.4
RC03	2021-04-26 10:18:25	7.4	-0.4
RC03	2021-04-26 10:18:59	7.2	-0.2
RC03	2021-04-26 10:19:36	7.1	-0.2
RC03	2021-04-27 07:01:45	9.0	0.0
RC03	2021-04-27 10:18:34	6.8	-0.4
RC03	2021-04-27 10:19:07	7.9	-0.2
RC03	2021-04-27 10:20:28	6.9	-0.4
RC03	2021-04-27 18:32:17	7.6	-0.6
RC03	2021-04-27 18:33:14	6.9	-0.4
RC03	2021-04-28 10:19:07	6.9	-0.2
RC03	2021-04-29 02:13:34	6.8	0.0
RC03	2021-04-29 02:14:25	7.2	-0.4
RC03	2021-04-29 02:22:27	7.8	0.0
RC03	2021-05-01 02:24:41	6.9	0.0
RC03	2021-05-01 02:25:27	6.8	-0.4
RC03	2021-05-01 02:25:58	7.2	-0.2
RC03	2021-05-02 02:01:27	6.7	-0.2
RC03	2021-05-03 05:27:05	5.2	-0.6
RC03	2021-05-03 22:39:39	7.3	-0.2
RC03	2021-05-04 02:15:11	6.8	-0.4
RC03	2021-05-04 02:16:03	6.7	-0.4
RC03	2021-05-04 02:16:49	6.8	-0.2
RC03	2021-05-05 02:20:05	6.8	0.2
RC03	2021-05-05 10:25:10	6.7	-0.2
RC03	2021-05-05 10:25:39	7.4	-0.4
RC03	2021-05-10 17:48:12	7.3	0.2
RC03	2021-05-11 13:28:15	2.0	-1.5
RC03	2021-05-12 18:18:26	6.9	-0.2
RC03	2021-05-14 02:14:26	6.7	-0.4
RC03	2021-05-14 02:15:25	6.9	-0.4
RC03	2021-05-14 09:47:43	4.3	-1.5
RC03	2021-05-15 04:08:27	2.9	-0.9
RC03	2021-05-18 02:21:34	7.2	0.0
RC03	2021-05-18 02:22:11	6.3	-0.2
RC03	2021-05-18 18:27:00	6.9	-0.2
RC03	2021-05-19 10:19:21	6.9	-0.2
RC03	2021-05-19 10:19:55	7.3	-0.2
RC03	2021-05-20 02:21:08	6.9	-0.2
RC03	2021-05-20 02:22:09	6.9	-0.2
RC03	2021-05-20 10:12:35	7.0	-0.4
RC03	2021-05-20 10:12:54	7.6	-0.4
RC03	2021-05-20 10:13:15	7.8	-0.2
RC03	2021-05-21 02:34:16	7.6	0.0
RC03	2021-05-21 02:35:25	7.6	0.2
RC03	2021-05-21 02:38:56	7.1	0.0
RC03	2021-05-22 02:06:42	6.9	-0.4

Station	Origin Time (UTC)	Distance (mi)	Magnitude
RC03	2021-05-22 02:07:32	7.6	-0.2
RC03	2021-05-22 09:22:28	7.2	-0.2
RC03	2021-05-22 09:23:57	7.4	-0.2
RC03	2021-05-25 10:06:23	6.4	-0.4
RC03	2021-05-26 02:20:43	7.4	-0.2
RC03	2021-05-26 02:21:39	8.2	0.1
RC03	2021-05-26 02:22:27	7.9	-0.2
RC03	2021-05-26 10:21:55	6.6	-0.4
RC03	2021-05-26 10:22:23	6.2	-0.4
RC03	2021-05-27 10:13:33	6.8	-0.6
RC03	2021-05-27 10:14:02	6.7	-0.4
RC03	2021-05-27 10:14:24	6.3	-0.2
RC03	2021-05-28 18:11:46	7.3	0.0
RC03	2021-05-29 02:06:04	7.8	-0.4
RC03	2021-06-01 06:49:04	2.7	-1.5
RC03	2021-06-02 10:15:07	6.6	-0.2
RC03	2021-06-02 10:15:50	7.3	-0.2
RC03	2021-06-02 18:25:03	6.3	-0.2
RC03	2021-06-03 00:38:15	7.1	-0.2
RC03	2021-06-03 02:17:13	8.4	-0.2
RC03	2021-06-03 02:17:59	8.2	-0.2
RC03	2021-06-03 02:18:29	6.8	-0.2
RC03	2021-06-08 02:22:16	7.0	-0.2
RC03	2021-06-08 10:13:39	6.8	-0.4
RC03	2021-06-08 10:14:09	6.6	-0.2
RC03	2021-06-10 02:19:40	7.3	-0.2
RC03	2021-06-10 02:20:34	6.9	-0.2
RC03	2021-06-10 18:24:56	8.1	-0.2
RC03	2021-06-11 02:21:24	7.0	-0.2
RC03	2021-06-11 10:22:58	7.6	-0.4
RC03	2021-06-12 02:12:24	7.4	-0.2
RC03	2021-06-12 02:16:51	6.4	-0.4
RC03	2021-06-15 18:24:48	6.9	0.7
RC03	2021-06-15 18:30:30	7.7	-0.2
RC03	2021-06-16 02:24:54	6.7	-0.2
RC03	2021-06-16 02:29:58	7.0	0.0
RC03	2021-06-16 10:19:59	7.4	-0.2
RC03	2021-06-17 02:23:55	6.9	0.0
RC03	2021-06-17 02:24:49	7.6	-0.4
RC03	2021-06-17 02:28:40	7.9	0.3
RC03	2021-06-17 10:18:36	7.9	0.6
RC03	2021-06-17 18:22:54	7.4	-0.6
RC03	2021-06-18 02:21:14	7.0	-0.2
RC03	2021-06-18 02:21:52	7.2	-0.4
RC03	2021-06-19 23:41:36	3.2	-1.5
RC03	2021-06-21 03:39:58	4.1	0.1
RC03	2021-06-26 02:30:50	10.4	0.2
RN01	2020-07-09 02:48:51	5.0	-0.6
RN01	2020-07-10 23:31:11	5.2	-0.6
RN01	2020-07-11 06:45:45	4.6	-0.9
RN01	2020-07-12 19:17:12	2.7	-0.9
RN01	2020-07-12 20:53:15	5.5	-0.6
RN01	2020-07-13 15:01:04	5.0	-0.4
RN01	2020-07-18 01:34:29	4.8	-0.4
RN01	2020-07-18 01:35:32	4.8	-0.4
RN01	2020-07-18 01:35:45	4.7	-0.6
RN01	2020-07-18 03:11:51	4.8	-0.4
RN01	2020-07-19 16:09:11	4.7	-0.4
RN01	2020-07-19 16:16:07	4.6	-0.6
RN01	2020-07-23 02:48:54	3.6	-0.9

Appendix C. Continued

Station	Origin Time (UTC)	Distance (mi)	Magnitude
RN01	2020-07-27 22:46:42	5.0	-0.2
RN01	2020-07-28 00:19:51	6.4	-0.6
RN01	2020-07-29 06:14:57	7.2	-0.4
RN01	2020-07-29 07:50:51	5.0	-0.9
RN01	2020-07-30 03:58:16	5.0	-0.9
RN01	2020-07-30 04:06:50	5.3	-0.6
RN01	2020-08-03 15:37:52	5.0	-0.6
RN01	2020-08-03 19:40:32	5.4	-0.4
RN01	2020-08-03 19:49:50	5.1	-0.6
RN01	2020-08-04 02:24:36	4.6	-0.9
RN01	2020-08-04 07:05:24	5.2	-0.9
RN01	2020-08-07 02:50:17	4.5	-0.6
RN01	2020-08-10 02:22:25	4.8	-0.6
RN01	2020-08-10 02:22:25	5.0	-0.6
RN01	2020-08-12 08:49:48	4.3	-0.6
RN01	2020-08-13 04:43:28	5.0	-0.4
RN01	2020-08-19 10:18:04	5.2	-0.4
RN01	2020-08-20 12:14:07	5.3	-0.9
RN01	2020-08-22 12:18:56	4.5	-0.6
RN01	2020-08-22 18:03:39	4.6	-0.6
RN01	2020-08-27 00:41:54	5.7	-0.6
RN01	2020-08-27 03:46:09	5.1	-0.9
RN01	2020-08-28 22:57:10	4.7	-0.2
RN01	2020-08-29 06:41:05	4.4	-0.9
RN01	2020-08-29 09:22:10	4.8	-0.6
RN01	2020-08-30 02:50:29	5.9	-0.6
RN01	2020-08-30 23:05:17	4.6	-0.4
RN01	2020-08-31 17:19:44	5.0	-0.6
RN01	2020-09-02 13:51:50	5.2	-0.9
RN01	2020-09-02 13:52:28	5.2	-0.4
RN01	2020-09-03 15:19:14	4.9	-0.6
RN01	2020-09-13 03:39:24	4.6	-0.4
RN01	2020-09-13 08:10:07	4.4	-0.6
RN01	2020-09-14 08:02:43	5.2	-0.6
RN01	2020-09-14 13:14:35	4.7	-0.4
RN01	2020-09-14 13:18:39	4.5	-0.6
RN01	2020-09-17 14:37:59	4.7	-0.2
RN01	2020-09-18 06:11:39	4.3	-0.9
RN01	2020-09-20 11:50:44	4.2	-0.9
RN01	2020-09-20 12:18:38	4.6	-0.9
RN01	2020-09-26 12:53:37	4.4	-0.9
RN01	2020-09-27 05:46:44	4.7	-0.4
RN01	2020-09-27 05:46:44	4.4	-0.6
RN01	2020-09-27 05:46:44	4.6	-0.6
RN01	2020-09-30 03:46:48	4.6	-0.4
RN01	2020-10-09 10:10:40	1.6	-1.5
RN01	2020-10-23 06:55:24	5.0	0.0
RN01	2020-10-23 18:02:10	4.9	-0.6
RN01	2020-10-24 11:08:21	5.1	-0.6
RN01	2020-10-27 09:09:13	5.0	-0.2
RN01	2020-10-28 03:20:13	5.4	-0.4
RN01	2020-11-02 07:40:50	5.1	-0.6
RN01	2020-11-02 07:40:50	5.0	-0.4
RN01	2020-11-08 02:26:07	4.7	-0.6
RN01	2020-11-09 14:13:17	5.1	-0.6
RN01	2020-11-09 14:50:08	5.3	-0.9
RN01	2020-11-13 21:39:41	4.5	-0.6
RN01	2020-11-15 13:21:12	4.7	-0.9
RN01	2020-11-20 17:15:59	4.5	-0.6
RN01	2020-11-21 18:28:08	4.9	-0.4

Station	Origin Time (UTC)	Distance (mi)	Magnitude
RN01	2020-11-22 14:17:11	4.7	-0.4
RN01	2020-11-30 08:27:46	4.9	-0.4
RN01	2020-11-30 08:29:36	4.9	-0.4
RN01	2020-12-01 11:26:22	5.1	-0.9
RN01	2020-12-16 17:04:16	2.1	-0.9
RN01	2020-12-17 08:40:13	4.6	-0.4
RN01	2020-12-17 08:40:13	4.6	-0.6
RN01	2020-12-18 09:12:24	5.2	-0.6
RN01	2020-12-21 09:26:54	4.9	-0.6
RN01	2020-12-21 09:26:59	4.9	-0.6
RN01	2020-12-21 11:08:16	4.8	-0.4
RN01	2020-12-21 11:09:15	5.2	-0.6
RN01	2020-12-21 12:01:26	4.4	-0.2
RN01	2020-12-22 08:06:14	5.2	-0.2
RN01	2020-12-22 08:16:23	4.5	-0.4
RN01	2020-12-22 10:46:34	5.2	-0.6
RN01	2021-01-05 07:06:20	11.0	-0.2
RN01	2021-01-10 09:40:30	6.3	-0.6
RN01	2021-01-10 13:37:50	1.4	-1.5
RN01	2021-01-14 15:40:37	2.0	-0.6
RN01	2021-01-18 00:44:19	2.2	-1.5
RN01	2021-01-18 01:26:44	4.6	-0.9
RN01	2021-01-21 01:23:05	8.9	-0.2
RN01	2021-01-23 05:12:20	5.2	-0.6
RN01	2021-01-25 02:32:00	4.9	-0.6
RN01	2021-01-25 07:54:13	5.3	0.0
RN01	2021-01-25 21:00:28	4.6	-0.6
RN01	2021-01-27 09:00:38	4.8	-0.6
RN01	2021-02-01 03:17:35	4.0	-0.9
RN01	2021-02-02 00:52:54	4.9	-0.6
RN01	2021-02-02 02:27:18	2.0	-1.5
RN01	2021-02-02 02:27:28	2.5	-0.9
RN01	2021-02-02 02:28:15	3.4	-0.9
RN01	2021-02-05 23:40:57	5.3	-0.6
RN01	2021-02-05 23:43:12	4.6	-0.6
RN01	2021-02-05 23:43:55	4.5	-0.6
RN01	2021-02-05 23:45:25	4.5	-0.6
RN01	2021-02-19 08:51:10	4.5	-0.6
RN01	2021-02-19 12:55:17	5.7	-0.4
RN01	2021-02-19 14:22:16	5.8	-0.6
RN01	2021-02-19 14:49:03	5.5	-0.6
RN01	2021-02-19 17:10:23	5.6	-0.6
RN01	2021-02-21 03:01:21	4.9	-0.6
RN01	2021-02-25 23:56:21	2.7	-0.9
RN01	2021-02-27 04:03:27	4.9	-0.9
RN01	2021-02-27 08:04:25	4.8	-0.9
RN01	2021-03-02 03:18:47	9.1	0.0
RN01	2021-03-08 11:30:07	6.1	-0.6
RN01	2021-03-08 12:45:40	10.0	0.3
RN01	2021-03-12 01:36:54	4.1	-0.6
RN01	2021-03-12 22:30:57	4.8	-0.6
RN01	2021-03-16 15:40:35	6.1	-0.4
RN01	2021-03-19 02:40:47	4.9	-0.4
RN01	2021-03-19 04:25:12	4.5	-0.6
RN01	2021-03-19 04:52:46	5.0	-0.6
RN01	2021-03-19 13:58:36	2.5	-1.5
RN01	2021-03-22 10:39:08	2.8	-0.9
RN01	2021-03-25 23:49:20	4.3	-0.4
RN01	2021-03-26 09:55:38	5.0	-0.6
RN01	2021-03-28 03:16:59	1.5	-1.5

Appendix C. Continued

Station	Origin Time (UTC)	Distance (mi)	Magnitude
RN01	2021-04-01 11:52:43	2.3	-0.9
RN01	2021-04-07 07:18:24	4.1	-0.9
RN01	2021-04-08 02:23:21	9.7	-0.4
RN01	2021-04-13 09:16:25	5.7	-0.6
RN01	2021-04-14 03:40:15	6.6	-0.6
RN01	2021-04-17 02:21:00	8.7	-0.6
RN01	2021-04-17 06:13:10	2.5	-1.5
RN01	2021-04-18 21:50:34	4.5	-0.9
RN01	2021-04-18 21:50:38	4.4	-0.9
RN01	2021-04-22 08:48:37	3.3	-1.5
RN01	2021-04-22 11:10:58	11.7	0.1
RN01	2021-05-03 04:41:53	10.6	0.0
RN01	2021-05-05 09:13:10	5.1	-0.6
RN01	2021-05-06 05:23:12	5.6	-0.6
RN01	2021-05-15 05:53:59	2.2	-1.5
RN01	2021-05-15 05:53:59	2.4	-1.5
RN01	2021-05-21 02:06:58	4.8	-0.4
RN01	2021-05-26 14:49:57	4.7	-0.4
RN03	2020-08-14 05:20:55	8.4	-0.2
RN03	2020-08-18 05:40:02	8.6	-0.2
RN03	2020-08-18 05:40:42	8.9	-0.2
RN03	2020-08-25 05:24:50	10.2	-0.2
RN03	2020-08-25 05:27:44	8.0	-0.4
RN03	2020-08-25 05:28:42	8.8	-0.2
RN03	2020-08-31 00:20:59	2.9	-0.9
RN03	2020-09-01 05:12:04	11.3	-0.2
RN03	2020-09-01 05:13:36	8.5	-0.4
RN03	2020-09-01 05:14:53	8.4	-0.4
RN03	2020-09-01 05:16:19	8.4	-0.4
RN03	2020-09-01 05:18:54	8.9	-0.4
RN03	2020-09-01 05:20:42	9.7	-0.4
RN03	2020-09-02 05:36:37	8.8	-0.2
RN03	2020-09-03 05:43:26	11.1	0.1
RN03	2020-09-03 05:44:49	10.7	0.0
RN03	2020-09-03 05:46:06	10.9	-0.2
RN03	2020-09-03 05:47:19	8.5	0.0
RN03	2020-09-03 05:48:49	9.2	-0.2
RN03	2020-09-11 05:37:58	9.3	-0.4
RN03	2020-09-11 05:39:05	11.7	0.0
RN03	2020-09-11 05:40:15	9.8	-0.2
RN03	2020-09-11 05:41:10	8.9	-0.2
RN03	2020-09-16 05:34:36	9.4	-0.2
RN03	2020-09-16 05:35:45	10.2	-0.2
RN03	2020-09-16 05:36:29	9.2	-0.2
RN03	2020-09-16 05:39:25	8.5	-0.2
RN03	2020-09-16 05:40:31	8.0	-0.2
RN03	2020-09-16 05:41:24	8.9	-0.2
RN03	2020-09-17 05:25:13	8.4	-0.2
RN03	2020-09-17 05:26:30	8.4	0.0
RN03	2020-09-17 05:27:38	9.7	-0.4
RN03	2020-09-17 05:28:26	8.0	0.2
RN03	2020-09-17 05:29:47	8.9	-0.2
RN03	2020-09-17 05:30:57	9.9	-0.2
RN03	2020-09-18 05:42:26	8.7	0.0
RN03	2020-09-18 05:45:03	8.0	0.0
RN03	2020-09-18 05:46:51	8.2	-0.4
RN03	2020-09-18 05:47:46	9.4	-0.2
RN03	2020-09-19 05:20:37	8.4	-0.2
RN03	2020-09-23 05:32:55	9.0	0.0
RN03	2020-09-29 05:15:11	8.1	-0.4

Station	Origin Time (UTC)	Distance (mi)	Magnitude
RN03	2020-09-29 05:17:47	8.9	-0.2
RN03	2020-09-29 05:19:02	9.6	-0.2
RN03	2020-09-29 05:22:07	9.1	0.0
RN03	2020-09-29 05:23:05	9.8	-0.2
RN03	2020-10-02 04:46:12	11.8	-0.2
RN03	2020-10-02 04:47:27	8.8	0.3
RN03	2020-10-02 04:48:42	11.9	0.1
RN03	2020-10-02 04:52:38	9.3	-0.2
RN03	2020-10-20 22:44:13	10.0	0.1
RN03	2020-10-20 22:47:31	8.7	0.8
RN03	2020-10-24 07:15:25	1.7	-1.5
RN03	2020-10-27 05:53:22	10.1	-0.2
RN03	2020-10-27 05:54:58	11.1	-0.2
RN03	2020-10-27 05:56:06	9.1	-0.2
RN03	2020-11-07 00:28:43	4.3	-0.9
RN03	2020-11-11 06:35:59	7.8	-0.2
RN03	2020-11-11 06:38:10	7.8	-0.4
RN03	2020-11-11 06:39:36	8.5	-0.4
RN03	2020-11-11 06:40:23	8.4	-0.2
RN03	2020-11-11 06:41:58	8.6	-0.2
RN03	2020-11-17 06:17:38	9.4	-0.4
RN03	2020-11-17 06:18:47	8.6	-0.4
RN03	2020-11-20 07:04:16	8.1	-0.2
RN03	2020-11-21 06:25:08	7.7	-0.4
RN03	2020-11-21 06:25:29	8.3	-0.2
RN03	2020-11-21 06:28:38	10.1	-0.2
RN03	2020-11-21 06:29:35	8.1	-0.4
RN03	2020-11-23 08:38:38	2.7	-0.9
RN03	2020-11-28 06:20:00	8.4	-0.2
RN03	2020-11-28 06:21:02	8.3	-0.4
RN03	2020-11-28 06:22:55	8.5	-0.2
RN03	2020-11-30 09:38:53	3.8	-0.9
RN03	2020-12-04 06:55:56	9.4	-0.2
RN03	2020-12-04 06:59:24	8.0	-0.2
RN03	2020-12-04 07:00:45	8.7	-0.2
RN03	2020-12-04 07:04:33	9.0	-0.2
RN03	2020-12-04 07:05:36	8.3	-0.2
RN03	2020-12-05 05:47:08	8.7	-0.4
RN03	2020-12-05 05:49:51	11.6	-0.2
RN03	2020-12-05 05:50:55	9.3	-0.2
RN03	2020-12-11 07:53:46	8.2	-0.2
RN03	2020-12-11 07:54:31	9.1	-0.2
RN03	2020-12-11 07:55:41	7.5	-0.2
RN03	2020-12-13 06:16:41	8.6	-0.2
RN03	2020-12-13 06:18:47	8.8	-0.2
RN03	2020-12-13 06:20:01	8.6	-0.2
RN03	2020-12-14 12:02:27	5.7	-0.6
RN03	2020-12-15 06:46:00	8.3	0.0
RN03	2020-12-15 06:47:44	8.6	-0.2
RN03	2020-12-15 06:48:51	8.6	-0.2
RN03	2020-12-15 06:50:47	7.3	-0.2
RN03	2020-12-15 06:54:34	8.4	-0.2
RN03	2020-12-15 06:55:34	8.2	-0.2
RN03	2020-12-29 18:01:05	1.4	-0.9
RN03	2021-01-06 07:55:06	11.3	-0.2
RN03	2021-01-08 05:51:46	3.5	-0.6
RN03	2021-01-13 06:21:30	8.9	-0.4
RN03	2021-01-13 06:27:29	9.8	-0.2
RN03	2021-01-16 06:23:59	8.9	-0.2
RN03	2021-01-20 06:22:32	8.0	-0.4

Appendix C. Continued

Station	Origin Time (UTC)	Distance (mi)	Magnitude
RN03	2021-01-20 06:23:23	8.0	-0.2
RN03	2021-01-20 06:24:29	8.2	-0.2
RN03	2021-01-20 06:25:48	7.4	-0.2
RN03	2021-01-20 06:26:58	8.6	-0.4
RN03	2021-01-22 07:08:55	7.2	0.0
RN03	2021-01-22 07:09:33	8.5	0.0
RN03	2021-01-22 07:10:42	7.4	0.1
RN03	2021-01-22 07:11:49	8.4	-0.4
RN03	2021-01-22 07:12:52	9.8	-0.2
RN03	2021-01-23 06:39:32	8.7	-0.4
RN03	2021-01-23 06:40:33	9.2	-0.2
RN03	2021-01-23 06:41:30	10.9	-0.2
RN03	2021-01-23 06:42:48	11.1	0.1
RN03	2021-01-23 06:44:22	8.2	-0.2
RN03	2021-01-23 06:49:43	9.0	-0.2
RN03	2021-01-25 12:47:47	5.6	-0.6
RN03	2021-01-26 06:58:12	7.0	-0.2
RN03	2021-01-26 06:59:07	8.0	0.0
RN03	2021-01-26 06:59:39	9.1	-0.4
RN03	2021-01-26 07:00:20	9.0	-0.4
RN03	2021-01-26 12:00:24	1.0	-1.5
RN03	2021-01-28 08:12:16	7.9	-0.2
RN03	2021-01-28 08:12:37	9.5	-0.4
RN03	2021-01-28 08:13:35	8.2	-0.2
RN03	2021-01-28 08:16:35	7.9	-0.2
RN03	2021-01-28 08:17:47	8.2	-0.2
RN03	2021-01-28 08:18:48	9.4	-0.4
RN03	2021-01-28 08:19:39	10.7	-0.2
RN03	2021-01-29 00:12:50	2.3	-0.9
RN03	2021-02-05 06:17:02	9.7	0.0
RN03	2021-02-05 06:19:17	8.1	0.0
RN03	2021-02-10 06:27:44	8.8	-0.2
RN03	2021-02-10 06:29:05	8.6	-0.4
RN03	2021-02-10 06:30:15	8.4	-0.4
RN03	2021-02-10 06:30:27	7.4	-0.2
RN03	2021-02-10 06:34:17	6.9	-0.2
RN03	2021-02-10 06:35:18	10.2	-0.4
RN03	2021-02-10 06:36:26	9.7	-0.2
RN03	2021-02-16 06:26:38	9.5	0.1
RN03	2021-02-16 06:27:53	11.1	0.0
RN03	2021-02-16 06:29:15	9.0	-0.2
RN03	2021-02-17 06:40:16	7.8	-0.4
RN03	2021-02-17 06:43:21	7.4	0.0
RN03	2021-02-17 06:44:47	8.4	-0.2
RN03	2021-02-17 06:48:31	9.2	-0.4
RN03	2021-02-18 07:15:48	9.0	-0.2
RN03	2021-02-18 07:15:48	8.9	-0.4
RN03	2021-02-18 07:17:42	9.4	0.0
RN03	2021-02-18 07:18:33	8.7	-0.2
RN03	2021-02-18 07:19:30	9.5	-0.2
RN03	2021-02-18 07:21:22	8.7	-0.2
RN03	2021-02-19 06:36:32	8.8	0.0
RN03	2021-02-19 06:37:27	8.1	-0.4
RN03	2021-02-19 06:38:34	8.2	-0.4
RN03	2021-02-21 13:48:34	9.8	-0.4
RN03	2021-02-23 06:49:37	7.8	-0.2
RN03	2021-02-23 06:50:50	10.4	-0.2
RN03	2021-02-27 06:29:49	8.7	-0.2
RN03	2021-02-27 11:59:42	4.7	-0.9
RN03	2021-03-03 06:47:19	8.5	-0.6

Station	Origin Time (UTC)	Distance (mi)	Magnitude
RN03	2021-03-03 06:49:40	8.6	-0.4
RN03	2021-03-12 07:04:35	8.1	-0.4
RN03	2021-03-12 07:05:48	9.1	-0.2
RN03	2021-03-12 07:07:11	9.2	0.0
RN03	2021-03-13 06:15:48	8.1	0.0
RN03	2021-03-13 06:23:41	7.4	0.1
RN03	2021-03-16 05:32:07	11.6	-0.2
RN03	2021-03-16 05:35:58	8.3	-0.4
RN03	2021-03-16 05:37:23	9.2	-0.4
RN03	2021-03-19 05:40:56	11.0	-0.2
RN03	2021-03-19 05:42:25	12.0	-0.2
RN03	2021-03-19 05:43:49	8.6	-0.4
RN03	2021-03-25 04:13:14	5.4	-0.6
RN03	2021-03-25 05:17:22	9.0	-0.2
RN03	2021-03-26 05:14:43	8.4	0.0
RN03	2021-03-26 05:16:54	8.7	-0.2
RN03	2021-03-31 06:12:56	7.9	-0.2
RN03	2021-03-31 06:14:23	9.1	0.0
RN03	2021-03-31 06:15:37	8.5	-0.2
RN03	2021-03-31 06:16:36	8.6	-0.2
RN03	2021-03-31 06:17:36	7.6	-0.2
RN03	2021-03-31 06:18:27	8.7	-0.2
RN03	2021-04-08 08:02:52	4.4	-0.9
RN03	2021-04-08 08:02:52	3.5	-1.5
RN03	2021-04-08 08:03:33	3.5	-0.9
RN03	2021-04-09 06:25:02	2.5	-0.9
RN03	2021-04-09 06:28:29	10.6	0.0
RN03	2021-04-09 06:29:59	11.4	-0.2
RN03	2021-04-15 05:11:54	8.3	-0.4
RN03	2021-04-15 05:14:57	12.0	-0.4
RN03	2021-04-15 05:17:25	7.8	-0.4
RN03	2021-04-16 06:01:52	11.3	-0.2
RN03	2021-04-16 06:02:01	11.3	-0.4
RN03	2021-04-22 00:29:11	2.8	-0.9
RN03	2021-04-27 02:29:07	4.3	-0.6
RN03	2021-04-30 12:26:16	10.3	-0.2
RN03	2021-05-05 05:26:07	11.1	0.0
RN03	2021-05-11 05:38:21	9.9	-0.2
RN03	2021-05-11 05:39:37	11.5	-0.2
RN03	2021-05-11 05:39:38	10.7	-0.2
RN03	2021-06-03 06:52:59	11.6	-0.2
RN03	2021-06-04 05:57:33	11.8	-0.4
RN03	2021-06-05 16:28:38	3.5	-1.5
RN03	2021-06-06 23:06:54	1.7	-1.5
RN03	2021-06-07 17:14:56	1.8	-1.5
RN03	2021-06-13 01:32:04	2.5	-0.9
RN03	2021-06-16 05:43:42	11.8	0.0
RN03	2021-06-24 09:39:03	3.5	-0.6
RN03	2021-06-24 10:21:42	4.3	-0.2
RN03	2021-06-26 15:19:58	2.4	-1.5
SG02	2020-07-19 06:41:05	7.3	-0.2
SG02	2020-07-19 09:49:38	6.9	-0.4
SG02	2020-09-02 01:27:31	10.3	0.0
SG02	2020-09-17 23:06:22	7.2	-0.4
SG02	2020-10-06 15:59:26	2.2	-1.5
SG02	2020-10-24 20:47:43	8.2	-0.4
SG02	2020-11-30 07:29:49	9.0	0.0
SG02	2020-11-30 07:47:25	9.0	0.0
SG02	2020-11-30 08:52:05	8.8	0.0
SG02	2020-12-07 22:51:19	8.8	-0.2

Appendix C. Continued

Station	Origin Time (UTC)	Distance (mi)	Magnitude
SG02	2021-01-14 08:26:46	11.1	0.3
SG02	2021-01-14 21:11:36	4.2	-0.6
SG02	2021-02-10 05:36:57	6.1	-0.4
SG02	2021-02-11 07:55:03	5.8	-0.6
SG02	2021-02-13 07:58:44	3.0	-0.9
SG02	2021-02-13 08:04:55	2.0	-0.9
SG02	2021-02-13 08:14:55	4.9	-0.9
SG02	2021-02-14 03:40:05	1.6	-1.5
SG02	2021-02-16 07:45:35	10.4	-0.2
SG02	2021-02-25 09:15:29	8.4	0.0
SG02	2021-02-26 03:30:45	10.9	0.3
SG02	2021-02-26 04:46:31	8.9	-0.4

Station	Origin Time (UTC)	Distance (mi)	Magnitude
SG02	2021-03-11 21:41:33	4.4	-0.6
SG02	2021-03-14 17:14:50	3.4	-0.6
SG02	2021-03-14 23:33:43	6.0	-0.4
SG02	2021-03-17 05:02:12	2.8	-0.9
SG02	2021-03-25 11:08:05	3.6	-0.6
SG02	2021-05-16 09:17:26	11.8	0.1
SG02	2021-05-30 17:03:24	11.8	0.0
SG02	2021-06-20 03:37:53	3.2	-0.2

End of table

<u>Appendix D: Literature Review</u>

Diminishing Depth to Water in Cambrian-Ordovician Arbuckle Group Disposal Wells in Kansas

Newell et al. (2020), *Midcontinent Geoscience*
https://doi.org/10.17161/mg.v1i.15525

Key points

- Arbuckle fluid levels and bottomhole pressures measured in Class I wells are rising in south-central and central Kansas
- The Arbuckle may lose its capacity to accept wastewater under gravity flow in parts of Kansas in the next few decades
- Poor correlation between changes in the fluid level and the volume of fluid disposed of in individual Class I wells suggests a regional influence on Arbuckle fluid levels

Summary

Industrial and municipal wastewater and oilfield brines have been disposed of into the Arbuckle Group for decades in Kansas and nearby states in the midcontinent United States. Annual testing of formation pressure and static fluid levels in Class I wells compose a body of data that is useful in monitoring movement of water and fill-up of Arbuckle disposal zones. In parts of southern and southeastern Kansas, the depth to water locally can be less than 100 ft (31 m). Furthermore, most Class I wells indicate Arbuckle fluid levels in central and south-central Kansas are rising ~10 ft (~3 m) annually, suggesting that at current disposal rates, the Arbuckle may lose its capacity to accept wastewater under gravity flow in parts of the state in the next few decades, principally in south-central and southeastern Kansas along the Oklahoma state line. At present in parts of six Kansas counties along the Oklahoma state line, low-density (~1.0 g/cc or slightly greater density) wastewater in a wellbore does not have a sufficient hydrostatic head by gravity alone to force its way into the more dense resident Arbuckle formation water. There is a poor correlation between changes in fluid levels in Class I wells and the volume of fluid disposed of in them annually, thereby indicating that more regional characteristics may control water movement in the Arbuckle.

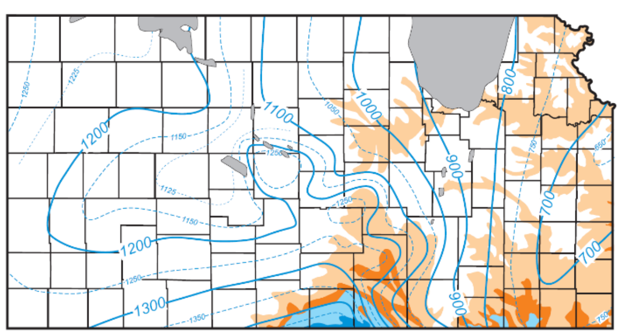

Figure D-1. Arbuckle potentiometric surface for freshwater. Blue-toned regions show where freshwater cannot enter the Arbuckle by gravity alone (modified from Newell et al., 2020).

Comment on "Accelerated Fill-Up of the Arbuckle Group Aquifer and Links to U.S. Midcontinent Seismicity" by Ansari et al. (2019)

Peterie et al. (2020), *Journal of Geophysical Research*
https://doi.org/10.1029/2019JB018348

Key Points

- The spatial relationship of Arbuckle formation pressure changes measured in Kansas Class I wells suggests a regional pressure change
- The pressure change is centered near a group of high-rate saltwater disposal wells at the Kansas-Oklahoma border
- Pressure changes are consistent with onset and progression of earthquakes, suggesting poroelastic stress changes are the primary drivers of the observed seismicity

Summary

Spatial analysis of Arbuckle Group formation pressures provides insight into contributing factors underlying the regional trends in formation pressure identified by Ansari et al. (2019). Based on correlation trends in reported bottomhole pressure and disposal volumes, Ansari et al. (2019) suggested that rising formation pressures were a result of fluid injection within 25 km. Our primary concern is that the correlation trends are most likely an artifact of the method used by Ansari et al. (2019), at least in part. Furthermore, the conclusion that pressure diffusion is limited to within 25 km of the injection point does not necessarily follow from the analysis. We also note that estimated formation pressure depends on the depth of the pressure gauge, which, in some cases, varies from one measurement to the next and should be accounted for to accurately assess measured changes. The spatial relationship of formation pressure changes among wells provides valuable insight into the origin of those changes. For each well, we project pressure to a baseline depth to account for changes in gauge depth and reexamine trends in formation pressure. Spatiotemporal progression suggests post-2011 formation pressure changes originate from a spatially dense group of high-rate saltwater disposal wells near the Kansas-Oklahoma border well beyond 25 km (and as far as 90 km) away.

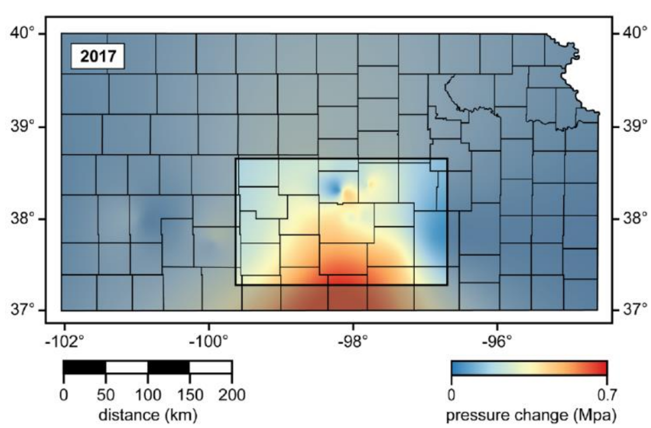

Figure D-2. Change in Arbuckle Group formation pressure in 2017 relative to baseline historic values (modified from Peterie et al., 2020).

Potential factors contributing to induced seismicity near Hutchinson, Kansas

Peterie et al. (2020), *Society of Exploration Geophysicists Expanded Abstracts*
https://doi.org/10.1190/segam2020-3424384.1

Key Points

- Spatial interpolation of formation pressure between Class I wells likely produces an accurate (albeit low-resolution) representation of regional pressure change
- Regional pressure change and seismicity progressed from an area with high-rate disposal near the Kansas-Oklahoma border toward Hutchinson, Kansas
- Historic disposal rates and pressure trends suggest that the Hutchinson earthquakes were likely a result of combined pressure changes from both regional and local disposal

Summary

A persistent earthquake swarm in Hutchinson, Kansas, is a concern for both the public and state regulatory agencies seeking to mitigate seismicity. Near the Hutchinson earthquakes, increases in formation pressure were recorded in the Arbuckle Group, a common disposal interval. In a previous study, formation pressures in a few wells suggested a regional pressure increase as the primary driver of seismicity that migrated into central Kansas. However, the Hutchinson swarm is also in proximity to several high-rate disposal wells. This paper examines the spatial relationship of formation pressures and disposal volumes to evaluate the relative contributions of local and regional disposal practices to inducing earthquakes near Hutchinson. Historic disposal rates and pressure trends suggest that the Hutchinson earthquakes were likely a result of combined pressure changes from both regional and local disposal.

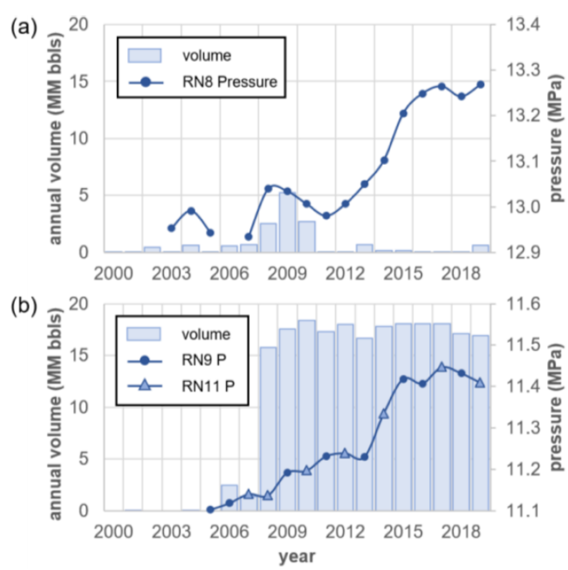

Figure D-3. (a) Formation pressure and annual disposal volume at RN8. (b) Formation pressure and combined annual volume at RN9 and RN11 (from Peterie et al., 2020).

Precambrian crystalline basement properties from pressure history matching and implications for induced seismicity in the US midcontinent

Ansari and Bidgoli (2021), *Geochemistry, Geophysics, Geosystems*
https://doi.org/10.1029/2021GC009660

Key Points

- Pore pressures in the Arbuckle and basement were modeled for reported disposal volumes in Class I and Class II wells in south-central Kansas
- The model only successfully replicates observed pressure changes in one of the three Class I wells used for the simulation
- Conclusions of this study are highly questionable due to the poor match between modeled and observed pressures and limited scope of the model (which excluded key Class I wells just beyond the model boundary

Summary

The authors constructed a 3-D geological model for the Arbuckle and basement, based on data from >400 wells covering south-central Kansas. The model space spanned Harper, Sumner, Sedgwick, and Kingman counties and the southern half of Reno County. Injection and pressures were simulated for more than 300 wells (Class I and Class II). Formation pressures measured in three Class I wells in Harper and Sedgwick counties were used to constrain and update the geological parameters. Simulated and measured pressures matched well in Harper County. However, simulated pressures in Sedgwick County were appreciably lower than measured pressures. The authors discounted the poor match as a result of higher in-well and nearby disposal, which is surprising considering their model included this injection and should account for associated pressure changes. The authors also acknowledged that geologic heterogeneity and disposal in Oklahoma, which were excluded in their model, might influence pressure change and propagation and contribute to the discrepancy between the simulated and measured pressures. Furthermore, numerous studies indicate the importance of long-range poroelastic effects, which were not accounted for in this study. Simulated pressures decreased in 2016, contradicting measured pressures in both the model space and surrounding counties. Therefore, the model and any resulting conclusions should be regarded with caution.

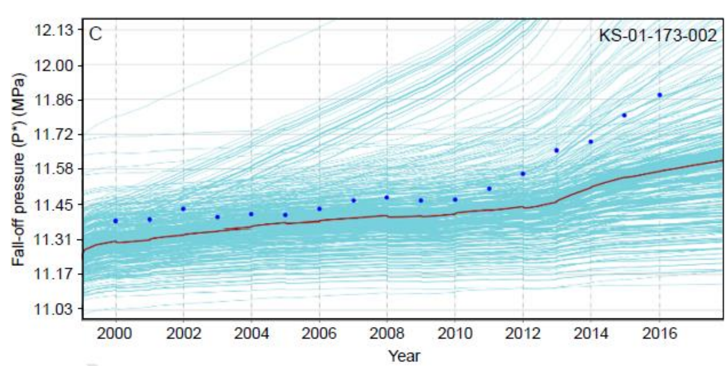

Figure D-4. Simulated (solid red line) and measured (blue dots) Arbuckle formation pressure in Sedgwick County in well KS-01-173-002 (modified from Ansari and Bidgoli, 2021).

Seismic Diffusivity and the Influence of Heterogeneity on Injection-Induced Seismicity

Haggenson and Rajaram (2021), *Journal of Geophysical Research*

Key Points

- Induced seismicity in real and model studies propagates away from disposal wells much more rapidly than expected based on the effective rock permeability and is controlled by high-permeability pathways
- Numerical simulations demonstrate a distinct difference between effective hydraulic diffusivity in fractured rock and observed "seismic diffusivity" (the apparent diffusivity based on earthquake progression, which may be an order of magnitude larger)
- Modeling induced seismicity using effective hydraulic properties in lieu of a more accurate complex model may grossly underestimate the propagation of seismicity and size of the seismically active region.

Summary

Injection-induced seismicity (IIS) is commonly interpreted as propagating in a diffusion-like manner that is characterized by an associated parameter called "diffusivity." In this paper, the authors refer to this as the "seismic diffusivity." Several previous studies equate seismic diffusivity and effective hydraulic diffusivity of the subsurface, which is related to effective permeability and controls the mean pressure field. Seismicity-based approaches for simulations of IIS using homogeneous-equivalent porous media are based on this assumed equivalence. However, seismicity is triggered when pressures exceed the triggering threshold and thus not controlled by the mean pressure field. Numerical simulations in this paper demonstrate that connected pathways of relatively high hydraulic diffusivity in heterogeneous media (particularly in fractured rock) allow the threshold triggering pressure to propagate more rapidly than predicted by the effective hydraulic diffusivity. As a result, the seismic diffusivity is greater than the effective hydraulic diffusivity in heterogeneous porous media, possibly by an order of magnitude or more. One crucial implication is that modeling induced seismicity using effective hydraulic properties in lieu of a more accurate complex model may grossly underestimate the propagation of seismicity and size of the seismically active region.

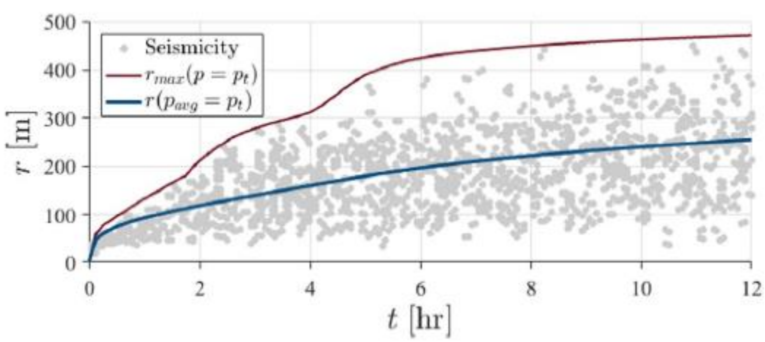

Figure D-5. Scatter plot of earthquakes triggered over time at distance *r* from the well. The red line represents the maximum distance the triggering threshold pressure has reached and, thus, the seismic diffusivity. The blue line represents the average pressure equal to the triggering threshold and, thus, effective hydraulic diffusivity (from Haggenson and Rajaram, 2021).

Response of Induced Seismicity to Injection Rate Reduction: Models of Delay, Decay, Quiescence, Recovery, and Oklahoma

Dempsey and Riffault (2019), *Water Resources Research*
https://doi.org/10.1029/2018WR023587

Key Points

- The induced seismicity rate was modeled for various scenarios to predict possible outcomes of injection rate reductions in Oklahoma
- Because it is possible for earthquake rates to rebound in some scenarios, early estimates of shortly after volume reduction may not represent the expected long-term earthquake rate
- Current mandated volume reduction in western Oklahoma is insufficient for preventing further M 5 events

Summary

The authors quantify how induced seismicity responds to an injection reduction to predict possible outcomes of seismicity within the area of interest for triggered seismicity in western Oklahoma. The delay in seismicity onset and then post-reduction behavior—decay, sometimes quiescence, and recovery of the seismicity rate—depend on the critical triggering pressure and on diffusion, among other parameters. Models were adapted to replicate the timing of onset, peak, and recent pace of decline of seismicity triggered by wastewater injection in western Oklahoma. Fixing the 2018 injection rate, already less than the limit imposed by the state regulator, the authors find a high likelihood of further $M \geq 5$ earthquakes. This suggests that the volume reduction mandate in western Oklahoma is, at present levels, inadequate.

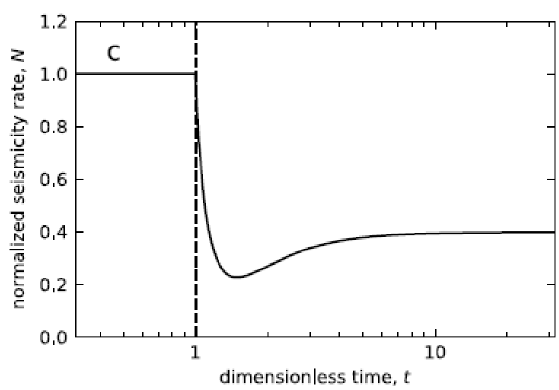

Figure D-6. The theoretical earthquake rate vs. time for a volume reduction for one scenario. The rate drops to about 20% of the initial pre-reduction rate, then eventually rebounds to a long-term rate of 40% (modified from Dempsey and Riffault, 2019).

Leakage and Increasing Fluid Pressure Detected in Oklahoma's Wastewater Disposal Reservoir

Barbour et al. (2019), *Journal of Geophysical Research*
https://doi.org/10.1029/2019JB017327

Key Points

- Arbuckle fluid levels recorded in a Class II well in northern Oklahoma in 2017–2018 are evidence of vertical leakage into adjacent formations
- Despite vertical leakage, Arbuckle fluid levels rose more than a year during a 6-month period in 2018
- Fluid pressure in the Arbuckle is steadily increasing, presumably related to high volume wastewater disposal

Summary

Earthquake scientists generally agree that subsurface fluid pressure changes are the principal cause of the manmade (or "induced") earthquakes occurring in Oklahoma and around the globe. This is because greater fluid pressures reduce the clamping pressure that would otherwise prevent a fault from having an earthquake. The leading cause of pressure changes on faults in Oklahoma is the disposal of wastewater related to production of oil and natural gas. Disposing of wastewater is generally done by pumping fluid down boreholes into deep, highly permeable reservoirs, such as the Arbuckle. One way for scientists to measure water pressure changes is to lower specially designed instruments down unused wastewater disposal wells. This paper presents continuous measurements of fluid pressure at an Arbuckle well located in Osage County, Oklahoma. The authors' findings show an overall trend of fluid pressures increasing over time. The only conceivable source of this increase is the injection of wastewater. Furthermore, their findings show evidence that fluids are leaking out of the reservoir at a significant rate.

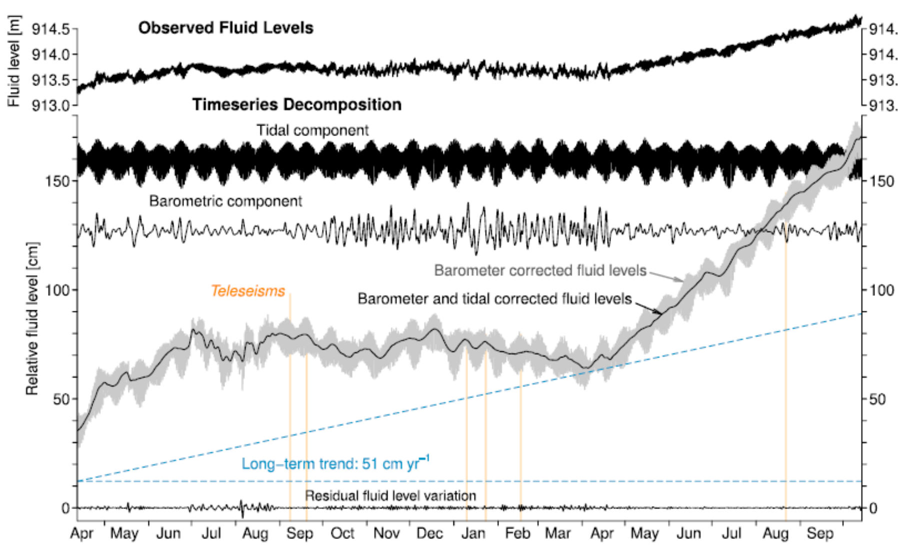

Figure D-7. Arbuckle fluid levels recorded in a well in northern Oklahoma from April 2017 to October 2018 (from Barbour et al., 2019).

Induced Seismicity in the Delaware Basin, Texas

Skoumal et al. (2020), *Journal of Geophysical Research*
https://doi.org/10.1029/2019JB018558

Key Points

- An order of magnitude increase in the earthquake rate in the Delaware Basin is likely induced by wastewater disposal, with ~5% induced by hydraulic fracturing
- Some earthquakes occurred more than 25 km from high-rate disposal wells, suggesting far-field, regional effects
- Geologic structures may act as low-permeability boundaries that influence the occurrence and location of induced seismicity

Summary

The seismicity rate in the Delaware Basin, located in western Texas and southeastern New Mexico, has increased by orders of magnitude within the past ~5 years. Although no seismicity was reported in the southern Delaware Basin during 1980–2014, 37 earthquakes with M > 3 occurred in this area during 2015–2018. The vast majority of the seismicity is most likely associated with wastewater disposal, while at least ~5% of the seismicity was induced directly by hydraulic fracturing. Far-field effects of wastewater disposal likely induced earthquakes over distances >25 km. The spatial limits of seismicity correlate with geologic structures that include the Central Platform and Grisham Fault, suggesting hydrologic compartmentalization by low-permeability boundaries. Given that the seismicity rate increased throughout the duration of the study, if industry operations continue unaltered, it is likely that both the seismicity rate and number of M > 3 earthquakes may continue to increase in the future.

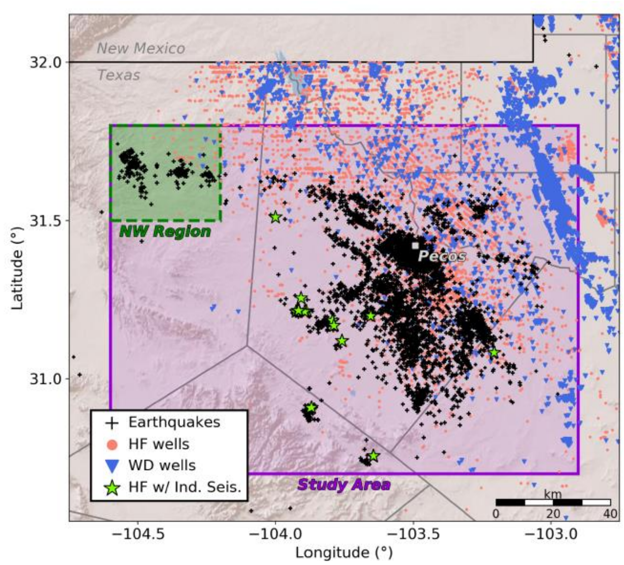

Figure D-8. Map of earthquakes (black), hydraulic fracturing wells (red), and saltwater disposal wells (blue) in the Permian basin in west Texas (from Skoumal et al., 2020).